BioMed Research International

Multitarget Therapeutics for Neurodegenerative Diseases

Lead Guest Editor: Moustafa Gabr
Guest Editors: Mohamed Benchekroun, Samuele Maramai, Manikandan Alagumuthu, and Samir Yahiaoui

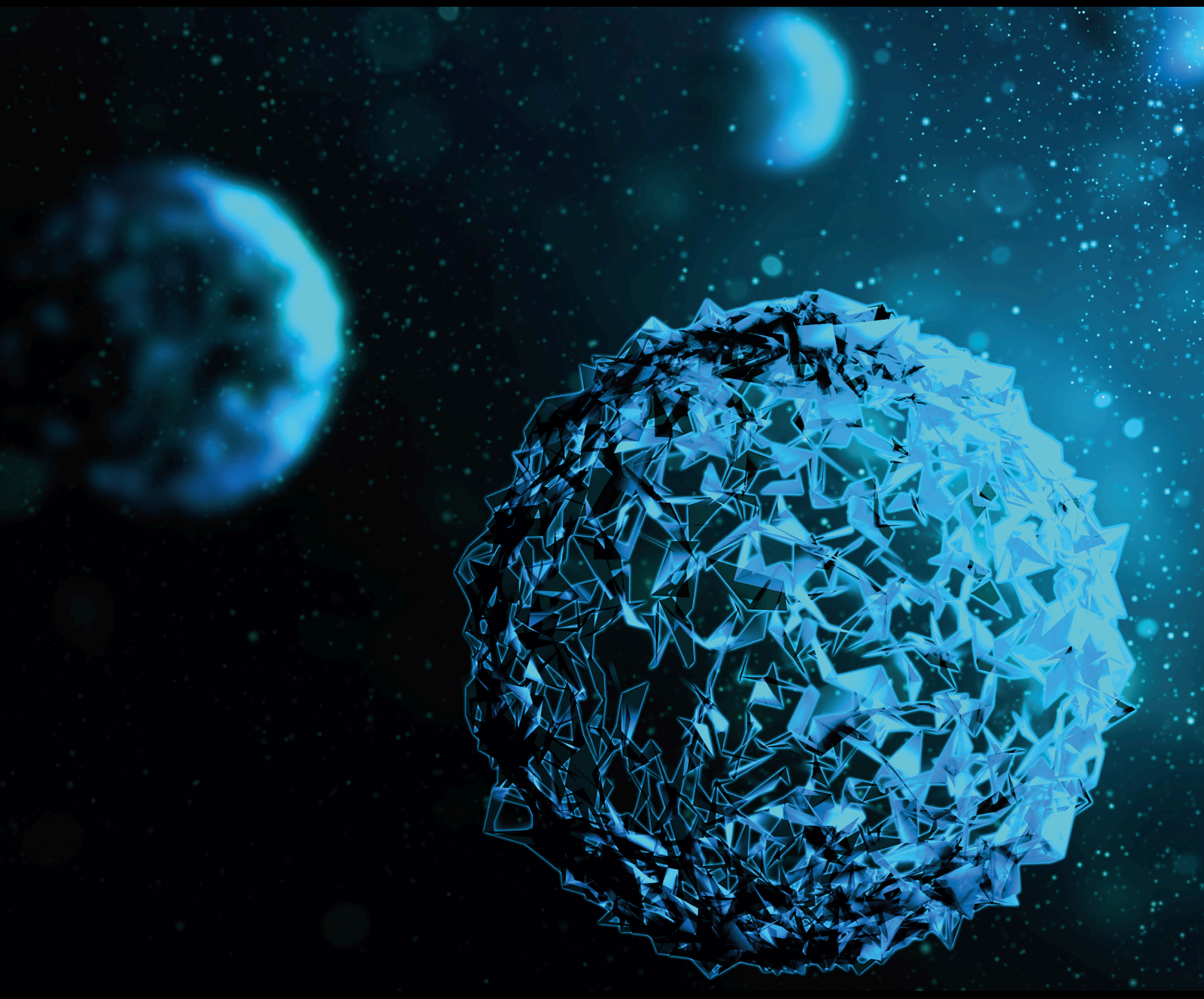

Multitarget Therapeutics for Neurodegenerative Diseases

BioMed Research International

Multitarget Therapeutics for Neurodegenerative Diseases

Lead Guest Editor: Moustafa Gabr
Guest Editors: Mohamed Benchekroun, Samuele Maramai, Manikandan Alagumuthu, and Samir Yahiaoui

Editorial Board

Contents

Hindawi
BioMed Research International
Volume 2020, Article ID 6532827, 2 pages
https://doi.org/10.1155/2020/6532827

Editorial

Multitarget Therapeutics for Neurodegenerative Diseases

Moustafa T. Gabr [1] **and Samir Yahiaoui** [2]

[1] *Department of Radiology, Stanford University School of Medicine, Stanford, CA 94305, USA*
[2] *Department of Drug Design and Optimization, Helmholtz Institute for Pharmaceutical Research Saarland, Campus E8.1, 66123 Saarbrücken, Germany*

Correspondence should be addressed to Moustafa T. Gabr; gabr@stanford.edu

Received 16 November 2019; Accepted 16 November 2019; Published 6 July 2020

Neurodegenerative diseases such as Alzheimer's (AD), Huntington's (HD), and Parkinson's diseases (PD) are a group of progressive disorders that feature degeneration of the structure and function of the human nervous system. Impaired mitochondrial function, excessive oxidative stress in human brain, genetic factors, and malfunction in human brain metabolism contribute to the progression of neurodegenerative diseases [1]. Multitarget therapeutics hold promise in tackling the multifactorial and complex nature of neurodegenerative diseases [2–4]. The use of multitarget directed ligands (MTDLs) emerged in the recent years as a powerful strategy in the development of potential therapeutics for neurological disorders. A major advantage of MTDLs is their ability to act on multiple targets involved in the progression of these diseases in comparison to single target concept. For example, MTDLs have been successfully designed to reduce aggregation of both amyloid peptides and tau proteins which are the major pathological cascades proposed for neurological disorders. This special issue features comprehensive knowledge on recent research efforts in identifying multitargeted therapeutic approaches for neurodegenerative diseases.

We received articles from across the globe featuring interesting research in this area. A case-control study in this special issue demonstrated the potential role of peripheral immune disorders in the pathological progression of late-onset Parkinson's disease (LOPD). Moreover, development of phytomedicines as potential therapeutics for AD is discussed as well. The role of gut microbiota in progression of neurological disorders and approaches for regulation of this effect is featured. In addition, the guest editorial team contributed a detailed review on rational design of MTDLs for neurodegenerative diseases with special focus on Alzheimer's disease. This review explored a large number of promising MTDLs obtained based on different target combinations strategies.

In conclusion, there is a growing interest from researchers from different disciplines to identify efficient multitargeted strategies for neurodegenerative diseases. Comprehension of ongoing efforts in development of multitargeted strategies would enable scientists to identify the most successful approaches in the field and eventually lead to discovery of efficient therapeutics. The multidisciplinary nature of research in this area is evident in this special issue as it features research from various disciplines. The guest editorial team hopes that this special issue will help in featuring the multidisciplinary aspect of this research area and encourage future collaborative efforts.

Conflicts of Interest

The guest editors declare that there are no conflicts of interest regarding the publication of this special issue.

Acknowledgments

We would like to thank all the researchers who contributed to this special issue. We also want to thank the reviewers who made this special issue possible.

Moustafa T. Gabr
Samir Yahiaoui

References

[1] M. T. Lin and M. F. Beal, "Mitochondrial dysfunction and oxidative stress in neurodegenerative diseases," *Nature*, vol. 443, no. 7113, pp. 787–795, 2006.

[2] M. M. Ibrahim and M. T. Gabr, "Multitarget therapeutic strategies for Alzheimer's disease," *Neural Regeneration Research*, vol. 14, no. 3, pp. 437–440, 2019.

[3] A. Hiremathad and L. Piemonese, "Heterocyclic compounds as key structures for the interaction with old and new targets in Alzheimer's disease therapy," *Neural Regeneration Research*, vol. 12, no. 8, pp. 1256–1261, 2017.

[4] L. Kupershmidt, T. Amit, O. Bar-Am, M. B. H. Youdim, and O. Weinreb, "Neuroprotection by the multitarget iron chelator M30 on age-related alterations in mice," *Mechanisms of Ageing and Development*, vol. 133, no. 5, pp. 267–274, 2012.

Hindawi
BioMed Research International
Volume 2020, Article ID 5120230, 27 pages
https://doi.org/10.1155/2020/5120230

Review Article

Multitarget Therapeutic Strategies for Alzheimer's Disease: Review on Emerging Target Combinations

Samuele Maramai,[1] **Mohamed Benchekroun**,[2] **Moustafa T. Gabr**,[3] **and Samir Yahiaoui**[4]

[1]*Department of Biotechnology, Chemistry and Pharmacy, Department of Excellence 2018–2022, University of Siena, Via Aldo Moro 2, 53100 Siena, Italy*
[2]*Conservatoire National des Arts et Métiers, Équipe de Chimie Moléculaire, Laboratoire de Génomique Bioinformatique et Chimie Moléculaire, GBCM, EA7528, 2 Rue Conté 75003 Paris, France*
[3]*Department of Radiology, Stanford University School of Medicine, Stanford, CA 94305, USA*
[4]*Department of Drug Design and Optimization, Helmholtz Institute for Pharmaceutical Research Saarland, Campus E8.1, 66123 Saarbrücken, Germany*

Correspondence should be addressed to Samuele Maramai; maramai@unisi.it and Samir Yahiaoui; yahiaoui.samir.1@gmail.com

Received 22 November 2019; Revised 12 February 2020; Accepted 2 June 2020; Published 3 July 2020

Academic Editor: Stefano Curcio

Neurodegenerative diseases represent nowadays one of the major health problems. Despite the efforts made to unveil the mechanism leading to neurodegeneration, it is still not entirely clear what triggers this phenomenon and what allows its progression. Nevertheless, it is accepted that neurodegeneration is a consequence of several detrimental processes, such as protein aggregation, oxidative stress, and neuroinflammation, finally resulting in the loss of neuronal functions. Starting from these evidences, there has been a wide search for novel agents able to address more than a single event at the same time, the so-called multitarget-directed ligands (MTDLs). These compounds originated from the combination of different pharmacophoric elements which endowed them with the ability to interfere with different enzymatic and/or receptor systems, or to exert neuroprotective effects by modulating proteins and metal homeostasis. MTDLs have been the focus of the latest strategies to discover a new treatment for Alzheimer's disease (AD), which is considered the most common form of dementia characterized by neurodegeneration and cognitive dysfunctions. This review is aimed at collecting the latest and most interesting target combinations for the treatment of AD, with a detailed discussion on new agents with favorable *in vitro* properties and on optimized structures that have already been assessed *in vivo* in animal models of dementia.

1. Introduction

Neurodegeneration is a pathological process that causes the progressive loss of neuronal function and leads to cognitive impairments, memory loss, and several forms of ataxia. This feature is pivotal in illnesses such as Alzheimer's disease (AD), Parkinson's disease (PD), Huntington's disease (HD), or Amyotrophic Lateral Sclerosis (ALS). Neurodegenerative diseases represent a heavy economic and social threat for our societies, especially now in low-to-middle income countries. According to the World Health Organization, around 50 million people—mostly elderly—are affected by dementia with AD representing *ca.* 60-70% of the cases [1]. Given the global increase in life expectancy, prodigious efforts have to be made to find new neuroprotective medicines able to impede, or even reverse, the neurodegeneration.

From a biochemistry perspective, neurodegenerative diseases share between them common pathological processes such as protein misfolding and aggregation, altered levels of neurotransmitters (e.g., acetylcholine and dopamine), metal ion dyshomeostasis [2], mitochondrial malfunction, oxidative stress, and neuroinflammation [3].

For instance, in AD, abnormal histological changes are characterized by the deposition of β-amyloid (Aβ) plaques

formed out of aggregated Aβ fibrils and neurofibrillary tangles (NFTs) made of hyperphosphorylated TAU protein (pTAU) [4]. PD proteopathy is linked to misfolded aggregates of α-synuclein (α-syn) accumulated in Lewis bodies [5]. In ALS, histological studies have shown the presence of aggregates of mutant superoxide dismutase 1 (SOD1), TAR DNA binding protein (TDP-43), fused in sarcoma (FUS), and repeat dipeptides from noncanonical translation of mutant chromosome 9 open reading frame 72 (C9ORF72) [6].

The other main pathological event leading to neurodegeneration is oxidative stress. Even if the human brain constitutes only 2% of the body mass, it consumes 20% of the oxygen brought by the respiratory system [7]. This feature renders the brain more vulnerable towards oxidative stress. Thus, oxidation of the main constituents of neurons (lipids, proteins, and nucleic acids) leads invariably to neurodegeneration [8]. In other words, the constant accumulation of reactive oxygen and nitrogen species (ROS and RNS) leads to the ineluctable damage to neurons. This oxidative stress is caused by various underlying factors such as mitochondrial dysfunction [9, 10], dyshomeostasis of metal ions (e.g., redox-active Fe^{2+}/Fe^{3+} and Cu^{+}/Cu^{2+}) and their role in promoting the deposit of aggregation-prone peptides (e.g., Aβ and α-syn) [11–13], and neuroinflammation [14, 15]. There is a global consensus on the fact that these etiologic mechanisms coexist simultaneously, influencing each other at multiple levels [16]. Consequently, these pathological features are responsible for neuronal cell death and dysfunction in neurotransmission translating into progressive cognitive impairment and/or ataxia. Based on their intertwined roles in the etiology of neurodegenerative diseases, they represent crucial therapeutic targets. Current treatments available in the market for neurodegenerative diseases are mainly palliative and poorly ameliorate the day-to-day life of patients. For instance, the treatments available now in the market for AD consists of three inhibitors of acetylcholinesterase (AChEIs, Figure 1), which maintain the levels of acetylcholine (ACh) and thus the neurotransmission [17]; along with Donepezil, Galantamine, and Rivastigmine (**2**-**4**, Figure 1) approved for mild-to-moderate AD, one NMDA antagonist, Memantine (**5**, Figure 1), has been approved for moderate-to-severe AD [18]. Tacrine (THA, **1**, Figure 1) was the first AChEI to be marketed for AD treatment but was rapidly discontinued due to its hepatotoxicity [19].

Available treatments for PD consist mainly in restoring dopaminergic tone either by administering catecholamines such as L-DOPA and Carbidopa (**6** and **7**, Figure 2) or dopaminergic receptor agonists such as ergot-derived alkaloids (bromocriptine, apomorphine (**8** and **9**, Figure 2), cabergoline, lisuride, and pergolide) and non-ergot-derived small-molecules (pramipexole, ropinirole, and piribedil). Because of the short half-life of L-DOPA, catechol-*O*-methyltransferase (COMT) inhibitors (e.g., Entacapone and Tolcapone (**10** and **11** respectively, Figure 2) are often coadministered with L-DOPA to block COMT-mediated metabolism, thus maintaining a longer dopaminergic tone.

Concerning HD, there is no treatment available to alter the course of the disease. However, there are medications able to lessen movement disorders such as Tetrabenazine (**12**, Figure 3). Antipsychotics, antidepressants, and tranquilizers might be also used. ALS treatments include only palliative drugs such as Riluzole and Edaravone (**13** and **14**, Figure 3) that bring serious side effects such as dizziness and headache, as well as gastrointestinal and liver problems.

Neurodegenerative diseases have a highly intricate etiology where many biological factors concur simultaneously at various levels to induce the neurodegeneration. This critical aspect represents a veritable hurdle for the development of disease-modifying drugs able to target the profound causes of neurodegeneration. The failure of "one drug-one target" drug design strategy and the multifunctional nature of neurodegenerative diseases inspired the scientific community to investigate the effectiveness of another drug design strategy called "designed multiple ligands," "hybrid molecules," or "multitarget-directed ligands" (MTDLs). This emerging strategy is centered on the development of pleiotropic ligands able to interact at least with two therapeutic targets at the same time. The idea of MTDLs has been largely pursued for the discovery of a more efficacious treatment for AD, and a great amount of structures based on this polypharmacology concept have been proposed [20]. Some of the most appealing analogues are the result of molecular hybridization, where the combination of multiple pharmacophores should reproduce the activity of the parent compounds while retaining a certain degree of selectivity towards the selected targets. These hybrid structures can be combined (*i*) by using a linker that spaces and anchors the biologically active moieties, (*ii*) by fusing the active sections together, (*iii*) or simply by merging the functionalities known to be involved in the target engagement [21]. The rational design behind these potential new drugs has been frequently inspired by well-known and/or approved drugs such as THA [22, 23], Donepezil [24, 25], or Rivastigmine, along with different natural bioactive derivatives such as resveratrol or curcumin [26], although other very interesting structural combinations/modifications have been recently identified. Here, we report the most recent and more interesting examples of newly developed MTDLs which are able to interact and modulate different biological systems and represent potential prototypes for a new treatment of AD.

2. Target Combinations in MTDL Design Strategy for AD

The cholinergic deficit represents an undeniable cause of AD. ACh plays a pivotal role in cognitive processes, and disruptions in its neurotransmission can influence all the aspects of cognition and behavior, not only in AD but also in other age-related forms of dementia [27]. Acetylcholinesterase (AChE) rapidly terminates the action of ACh in the synaptic cleft, leaving choline and acetate as the products of its hydrolytic activity. Butyrylcholineterase (BuChE) also plays an important role in cholinergic mediation [28].

Cholinesterases (ChEs) inhibitors can increase the levels of ACh and contribute to upregulate the cholinergic tone in neurons, partially ameliorating cognitive symptoms. AChE is a particularly attractive target to address AD-related

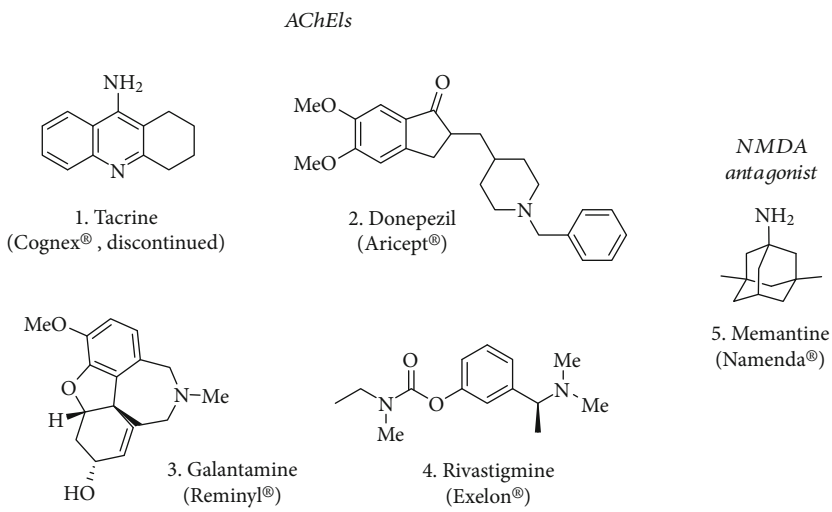

Figure 1: AChE inhibitors marketed for the treatment of AD (1-4) together with the NMDA receptor antagonist Memantine (**5**).

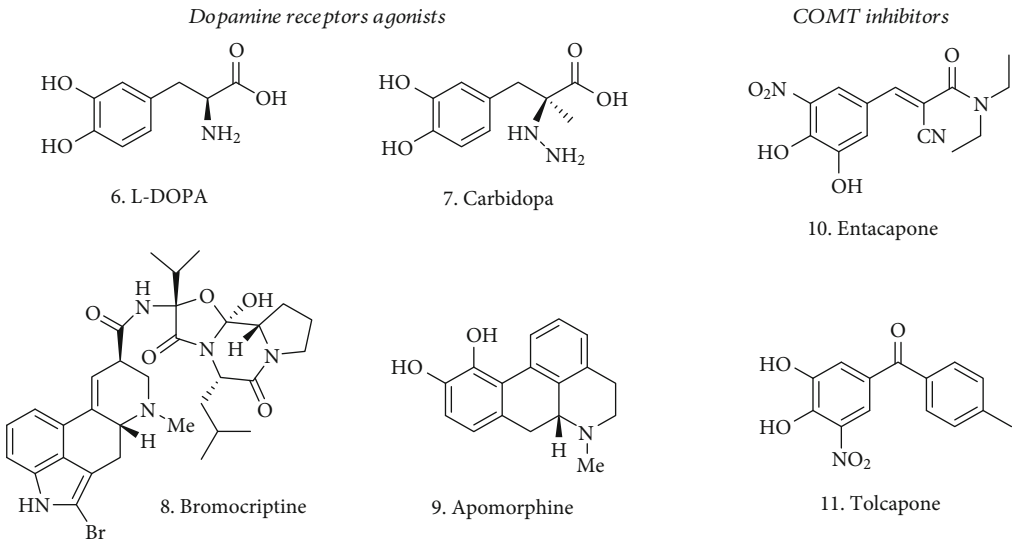

Figure 2: Representative dopamine receptor agonists (**6-9**) and COMT inhibitors (**10** and **11**) for the treatment of PD.

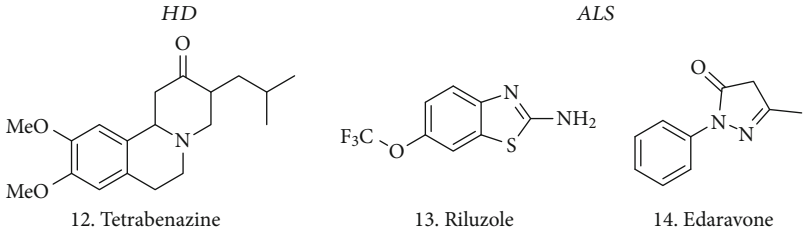

Figure 3: Compounds used in the treatment of hyperkinetic movement disorders related to HD (**12**) and used to slow down the progression of ALS (**13** and **14**).

symptoms, not only for its catalytic functions but also for the effects on Aβ precipitation, plaque formation [29], and inflammation. As discussed before, a few compounds have made their appearance in the market, like Donepezil or Rivastigmine (**2** and **4**, Figure 1), which were approved for the treatment of mild-to-moderate AD symptoms.

In addition to the cholinergic deficit, the presence of extracellular Aβ peptide plaques and NFTs of hyperphosphorylated pTAU represent the other main pathological features. Therefore, the "amyloid cascade hypothesis" is still the main focus for AD treatment. Aβ is generated from the Amyloid Precursor Protein (APP) by sequential cleavages,

involving the β-secretase beta-site APP-cleaving enzyme 1 (BACE-1) in the rate limiting step. Over the years, a great variety of BACE-1 inhibitors have been proposed and have entered clinical trials, highlighting the central role of this protease in AD [30].

The combination of ChEs and/or BACE-1 inhibition with the activity on additional enzymatic/receptor systems and the effects on other AD-related alterations, such as metal dyshomeostasis and oxidative stress (Figure 4), opens up the way for the identification of very interesting MTDLs and represents the preferred approach for the discovery of new treatments.

2.1. Dual ChE/BACE-1 Inhibitors. As mentioned above, ChEs and BACE-1 are pivotal targets for AD. A sensible approach for the discovery of new MTDLs may be represented by the concomitant inhibition of these two enzymatic systems. To this aim, a good variety of structures has been presented.

Gabr and Abdel-Raziq recently explored rigid analogues of Donepezil for their double activity against AChE and BACE-1 (**15** and **16**, Figure 5). Compound **15** [31] is a combination of features from Donepezil and other BACE-1 inhibitors, such as AZD3839 [32] or the simple 2-aminoquinoline ring, which shares with the AZD compound the bidentate interaction in the enzyme active site. The further addition of a double bond to connect the indenone moiety to the rest of the molecule afforded a nanomolar inhibitor of AChE and BACE-1, with $IC_{50} = 14.7$ nM and 13.1 nM, respectively. Kinetic studies on AChE revealed a concentration-dependent mixed-type inhibition of this enzyme, while the improved activity on BACE-1 confirmed the pivotal role played by the aminoquinoline group. The viability of SH-SY5Y neuroblastoma cells was not affected by concentrations of up to 50 μM. Moreover, the compound 15 had the potential to be brain penetrant, showing high permeability in the PAMPA-BBB assay, and had considerable metabolic stability in rat liver microsomes.

Another interesting series of analogues typified by structure **16** [33] possessed a favorable combination of groups, resulting in a dual AChE/BACE-1 inhibitor potentially endowed with chelating ability, thanks to the amidic portions. As a matter of fact, compound **16** was a low nanomolar inhibitor of the two target enzymes (IC_{50}, AChE = 4.11 nM, BACE − 1 = 18.3 nM). No cytotoxic effect was detected in SH-SY5Y cells up to 50 μM, while the balanced lipophilicity, coupled with high membrane permeability, allowed predicting a good brain penetration and metabolic stability. Moreover, the title compound was able to chelate Cu^{2+}, thus having an impact on the concentration of these metal ions and their promoted neurodegeneration.

Structurally related to Donepezil on the benzylpiperidine side, compounds with general structure **17** (Figure 5) represent another recent example of MTDL, where the properties of the parent compound on AChE have been retained and then extended to BACE-1 with the introduction of properly decorated aryl groups, linked via aminic- or iminic bonds [34]. When this aryl group is represented by a 4-CF_3 substituted ring, both the amine and the imine resulted in submicromolar inhibitors of the human enzyme isoforms and were selected for further characterization. The 4-CF_3 substituent added higher potential to permeate through membranes, as confirmed with the PAMPA-BBB assay. The amine-based compound had also a significant effect in displacing propridium iodide from PAS-AChE, hence being more interesting for further progression. Probably due to its capacity to bind PAS-AChE, 5-20 μM concentrations of this compound had antiaggregation properties not only on self-induced Aβ aggregation but also on the AChE-induced one (50% and 89%, respectively). AFM studies confirmed the reduction of Aβ aggregates after the incubation with this agent. No neurotoxic effect was observed in concentrations of up to 80 μM in SH-SY5Y cells, and the effects on cognition were tested in a scopolamine-induced amnesia animal model at the maximum dose of 10 mg/kg. Both the elevated plus maze and Y-maze experiments confirmed the potential for this compound to improve spatial and immediate memory, thus having an impact on cognitive impairment. *Ex vivo* analysis evidenced attenuated levels of malondialdehyde (MDA) and increased levels of superoxide dismutase (SOD) in compound-treated animals compared to the scopolamine-treated group, suggesting antioxidant properties. A robust improvement in cognitive and memory function was also observed when the compound was evaluated in the Morris water maze experiment with an $A\beta_{1\text{-}42}$-induced ICV rat model.

These dual AChE/BACE-1 inhibitors confirmed once again the importance of these enzymes in the pathology of AD and how the combined action against them still represent a valuable approach to address cognitive impairment and Aβ-related dysfunctions.

2.2. Dual ChE and GSK-3β Inhibitors. Glycogen synthase kinase-3β (GSK-3β) is a multitasking serine/threonine kinase largely expressed in the CNS. It is involved in several cellular processes and signaling pathways and its dysregulation occurs in the development of different disorders [35]. GSK-3β is also related to the pTAU phosphorylation process [36], and an increase in its activity correlates with Aβ production by interfering with APP-cleaving enzymes [37], leading to neuronal toxicity. Moreover, the overexpression of GSK-3β in transgenic mice is responsible for the development of cognitive deficits, thus making it a validated target in AD pathology [38]. Over the past decade, GSK-3β has been intensively targeted and its concomitant inhibition with AChE represents a well-consolidated and efficient approach to address the multifactorial nature of AD, influencing plaque deposition and pTAU hyperphosphorylation.

From the combination of a known GSK-3β inhibitor [39] and the THA moiety as AChE binder, some thiazole-based compounds were synthesized (**18**, Figure 6) with the potential to be a novel class of dual GSK-3β/AChE [40]. An amidic bond served to link the two pharmacophoric elements, spaced by a 2- or 3-C chain, and a few substitutions on the THA aromatic ring were also assessed. The introduction of the THA moiety did not affect the potency of GSK-3β inhibition, and the new compounds displayed nanomolar activity against this latter enzyme and *h*AChE, with almost all of them being also selective over *h*BuChE. However, the series

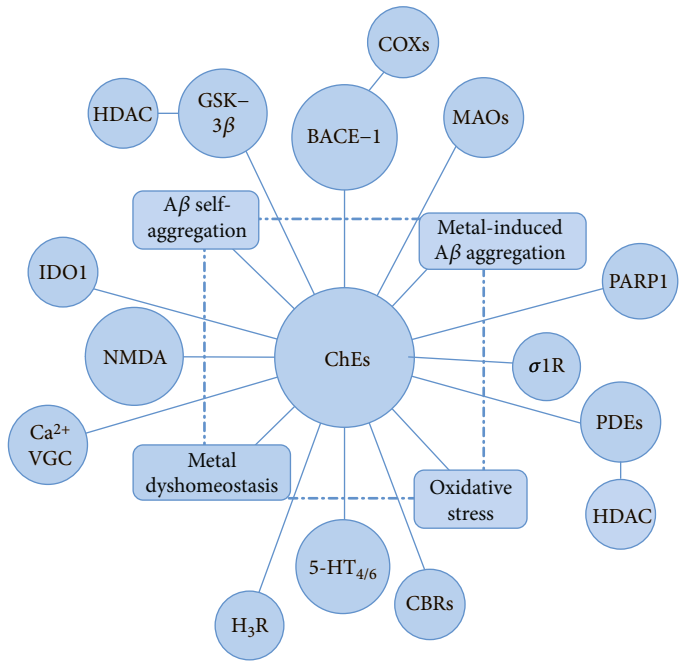

Figure 4: Schematic representation of some recent and interesting combinations regarding ChEs and BACE-1 inhibitors and/or other targets involved in AD. Beside the dual action on the selected systems, most of the newly developed analogues have the potential to affect Aβ peptide aggregation along with oxidative stress and metal dyshomeostasis.

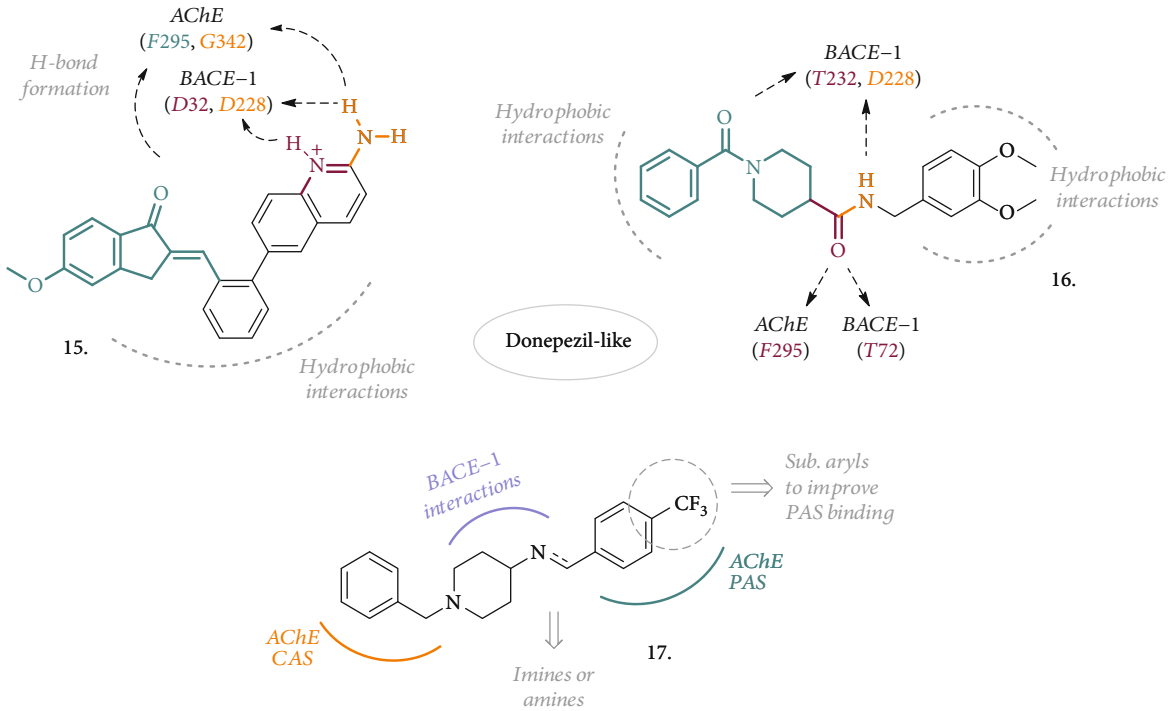

Figure 5: Structures of inspired- or rigid analogues of Donepezil as dual AChE and BACE-1 inhibitors. Highlighted are the main interactions with the two enzyme residues, mainly represented by H-bonds and hydrophobic interactions.

showed remarkable antiproliferative effects on SH-SY5Y cells and only the analogue with the unsubstituted THA moiety and a 3C-linker progressed, having an IC_{50} of 30 μM against the neuroblastoma cell line and being safe in hepatocytes, with low impact on these latter cells' viability at the same concentration. This compound also showed a moderate activity against Aβ self-oligomerization. It was then tested in mouse neuroblastoma N2a-TAU cells at increasing

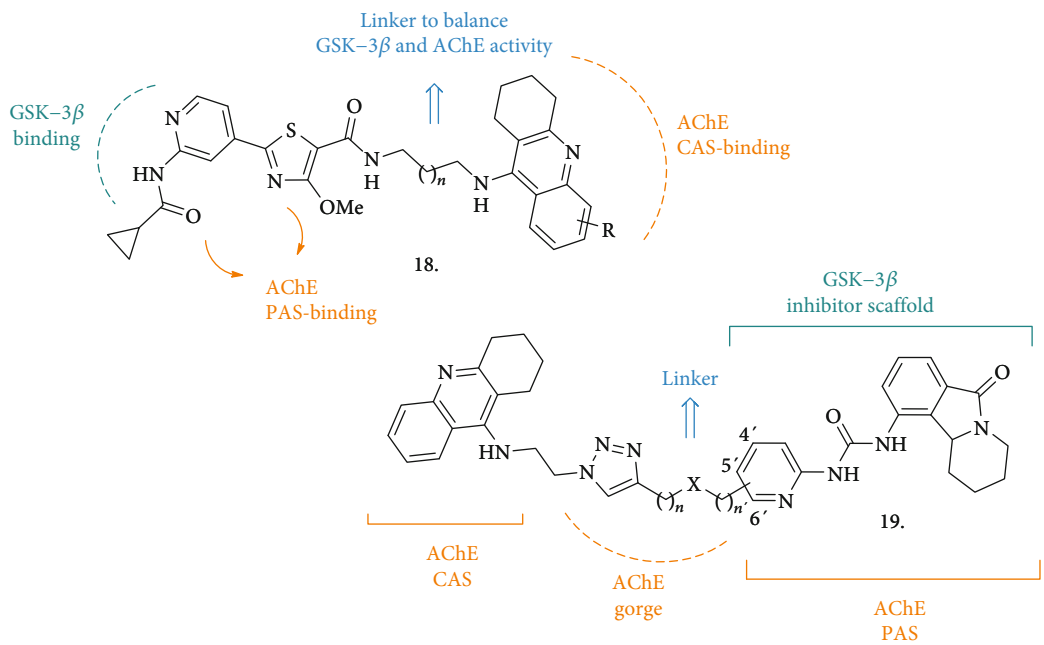

Figure 6: Dual AChE/GSK-3β inhibitors **18** and **19** and their relative pharmacophoric elements for the interaction with key enzyme residues.

concentrations to assess its effect on pTAU hyperphosphorylation, where it displayed a significant inhibition of this process. In the animal model of cognition impairment induced by scopolamine, the compound-treated mice displayed a significant ameliorated memory performance in the Morris water maze test, confirming the compound *in vivo* activity.

Another new series of compounds as dual inhibitors of ChEs and GSK-3β (**19**, Figure 6) was recently reported [41]. Here, the structure of THA (the ChE inhibitor side) and the scaffold of Valmerin (isoindolone, GSK-3β inhibitor side) were hybridized. The analysis of the crystal structures of the new MTDLs in complex with *Tc*AChE, combined with molecular docking studies, allowed the identification of the 1,2,3-triazole group as the best linker to retain or increase the inhibitory potency amongst both of the enzymatic systems. Together with the final hybrid compounds, the THA- and isoindolone-based fragments have also been tested for their ability to inhibit the enzymes, to give further information on the contribution of the single parts on each enzyme inhibition. The best performing compounds were able to inhibit both human AChE and GSK-3α/β in the nanomolar range, and the triazole ring undoubtedly played a pivotal role in enhancing the inhibitory potency towards the GSKs, even though the compounds were not displaying high selectivity over other kinases. Interestingly, the new analogues were less cytotoxic than the corresponding THA and isoindolone fragments in several cell lines (including the liver HuH7 cell line); however, when tested at concentrations of up to 100 μM in SH-SY5Y cells, a reduction in cell viability was observed after 24 h. The viability of MDCK-MDR1 cells was not affected in the same way, so the MDCK-MDR1 cell line expressing P-gp was used as a BBB model to predict brain penetration. The new compounds displayed good permeability through this system and showed no interaction with P-gp.

All the *in vitro* and *in vivo* biological properties shown by these classes of compounds highlight a very interesting potential for the treatment of AD. Even if there is still the need of improving selectivity and lowering cytotoxicity, these hybrid structures are once again proving how different pharmacophoric elements, joined by an appropriate and specifically designed linker, represent a valuable starting point that deserves to be progressed as MTDL drugs.

2.3. Dual ChE and MAO Inhibitors. Another combination for a multitarget purpose arises from the dual inhibition of ChEs and Monoamino Oxidases (MAOs). In the CNS, MAOs terminate the action of several monoamine neurotransmitters, such as dopamine and serotonin, and MAO-B, the predominant isoform in the human brain, is already a validated target for neurodegenerative diseases, with its inhibitor Rasagiline being approved to treat PD symptoms [42]. The expression of MAO-B is also increased in AD patients, where a correlation between its activity and intracellular Aβ levels has been observed, possibly due to interactions with γ-secretase [43]. Although the role of MAO-B in AD pathogenesis remains unclear, its inhibitors have shown neuroprotective effects, thus making this enzyme an appealing target in AD [44].

Sang et al. reported a series of chalcone-*O*-carbamate derivatives (**20**, Figure 7) potentially able to behave as ChEs and MAO-A/MAO-B inhibitors and endowed with antioxidant activities, anti Aβ_{42} aggregation and metal-chelating properties, and neuroprotective effects against H_2O_2-induced PC12 cell injury [45]. The new compounds are designed to combine the interesting biological activities of chalcones [46] with the well-known AChE and BuChE inhibitory

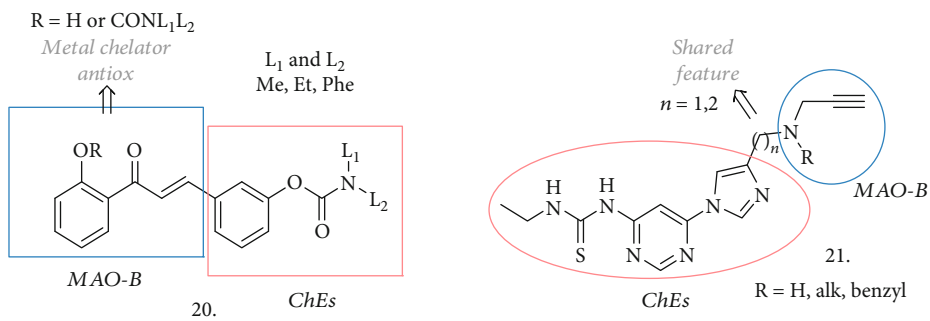

Figure 7: Novel ChE/MAO-B dual inhibitors and relative pharmacophoric elements. The new analogues are also endowed with structural elements which confer the ability to chelate metals and to protect against oxidative stress.

activity of Rivastigmine. The addition of a hydroxyl group adjacent to the chalcone carbonyl group confers the potential to be metal-chelating agents. The combination of L1=Me and L2=Et with R=H or N(Me)Et as substituents gave the best results in terms of expected properties. The compounds were selective BuChE and MAO-B inhibitors, active in the μM range for both of the enzymes, and they could inhibit the self-induced aggregation of Aβ_{42} with values higher than 50% (63.9% for the most active). A potent antioxidant activity in the Oxygen Radicals Absorbance Capacity by Fluorescence (ORAC-FL) method was observed, with the compound bearing the hydroxyl group (R=H) being more potent than its carbamate counterpart. The same hydroxyl analogue was also a selective metal chelator that could chelate Cu^{2+} and Al^{3+}. Thus, its capability on Cu^{2+}-induced Aβ_{42} aggregation was evaluated, displaying higher inhibition values, higher than curcumin as a reference. The two compounds were further progressed to assess their neuroprotective potential against H_2O_2-induced PC12 cell injury using MTT assays, where they were demonstrated to increase cell viability in correlation with their ability to capture hydroxyl radicals. Being also permeable through artificial membranes in the PAMPA-BBB assay, the compounds were finally tested *in vivo* in the scopolamine-induced cognitive impairment assay. The hydroxyl-derivative was effective in improving short-term working memory in mice, even though at the highest dose (23.4 mg/kg) it showed some neurotoxic effect.

Xu et al. have also presented a nice example of propargylamine-modified scaffolds (**21**, Figure 7) as ChE and MAO inhibitors [47]. In more detail, they combined the imidazole-substituted pyrimidinylthiourea moiety (AChE inhibitor pharmacophore) with the propargylamine group of Selegiline (MAO-B inhibitor pharmacophore), spaced by different linkers. All the compounds resulted in submicromolar inhibitors of AChE with negligible activity on BuChE, and the R=H or Me substitutions were the most appropriate for an efficient inhibition, especially when coupled with a single carbon atom linker ($n = 1$). Following these encouraging preliminary results, MAO inhibition was tested, revealing that the abovementioned compounds efficiently inhibited the enzymes in the micromolar range, and with the R=Me compound being selective for MAO-B. It also showed good antioxidant activity in the ORAC-FL assay, and the thiourea fragment worked as the metal-chelating part, resulting in a selective chelation for Cu^{2+} and inhibition of the ROS produced by Cu(II)-related redox. This compound had no effect on the Aβ self-aggregation but could efficiently inhibit Cu-mediated Aβ aggregation, as expected. It was safely tolerated on rat primary cortical neurons at concentrations of up to 30 μM, showing mild neurotoxicity at 100 μM, and it could protect neuronal cells from Cu-induced Aβ toxic damage, increasing cell viability. The PAMPA assay indicated a good potential to cross the BBB, and the *in vivo* effect in the scopolamine-induced cognitive deficit in mice was evaluated. The HCl salt was dosed orally at 30 mg/kg, and it could ameliorated learning and memory deficits, with the treated mice showing shorter escape latency and less frequent errors compared to the scopolamine group.

These data demonstrated a promising profile for these dual ChE/MAO inhibitors, and together with other described series of compounds, they are worth of further development and analysis in additional analysis in animal models of dementia associated to neurodegenerative conditions.

2.4. ChE Inhibitors and Other Enzymatic Systems. The simultaneous inhibition of ChEs and indoleamine 2,3-dioxygenase 1 (IDO1) resulted in another target combination endowed with beneficial effects in AD. IDO is an intracellular cytosolic heme-containing enzyme that regulates the degradation of Tryptophan (Trp) to N-formylkynurenine in the kynurenine pathway (KP), acting as a first-step rate controller [48]. KP is unbalanced in some neurodegenerative disorders and, as a result, Trp catabolism leads to neurotoxic metabolites such as 3-hydroxykunurenine. IDO1 is essential for this pathway, and its activation has been linked with Aβ-related inflammation in AD [49], making it the focus of various researches on neurodegenerative diseases treatment [50–51]. Lu et al. have identified a novel structure endowed with double activity on BuChE and IDO1 [52]. The selective activity on BuChE is of particular interest, as its levels rise up in the advanced stages of AD, replacing AChE deficiency in the hydrolysis of Ch, thus becoming an even more important target. Compounds with general structure **22** (Figure 8) are prototypes based on the antifungal drug Miconazole, which had already shown activity as an IDO1 inhibitor [53] and was tested in vivo as a reference compound. The 3-OMe or 4-OMe-substituted analogues showed the weakest activity on AChE and the best inhibitory IC_{50} values on BuChE and IDO1 (8.3 and 2.8 μM

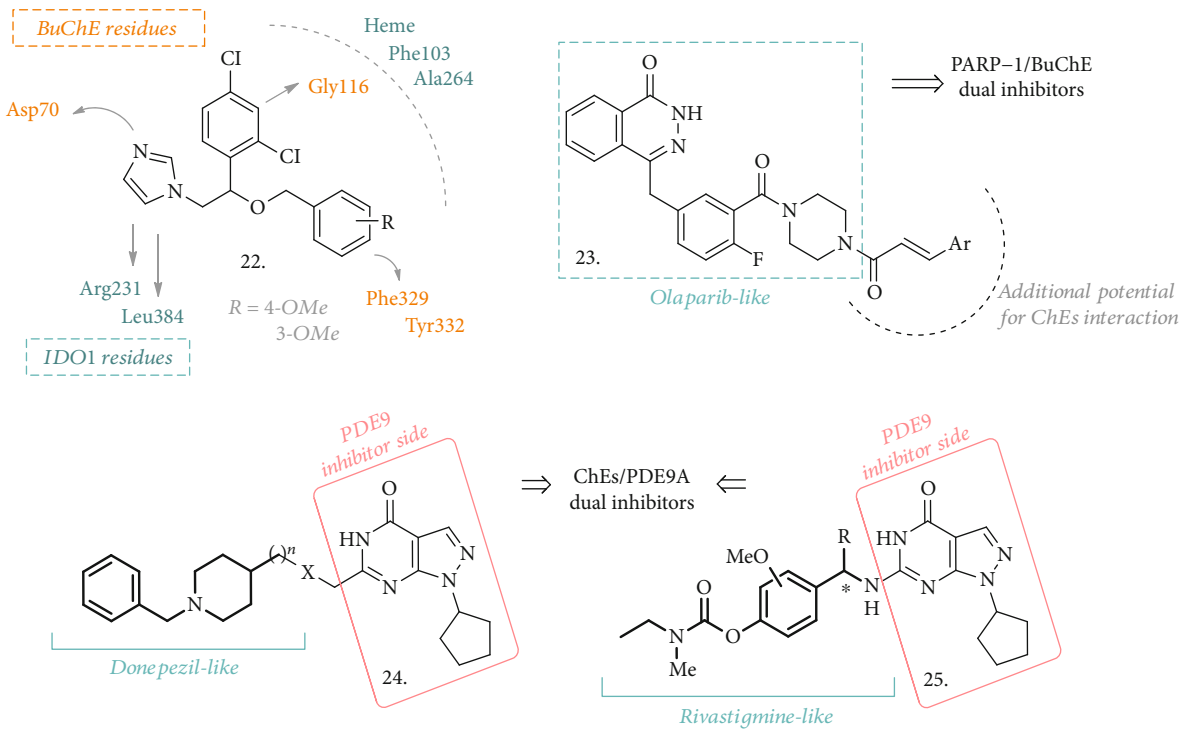

Figure 8: Structures of dual BuChE/IDO1, ChE/PARP-1, and ChE/PDE inhibitors. While structure **22** is inspired by Miconazole, Olaparib has been taken as the reference structure in the synthesis of MTDL **23**, while Donepezil and Rivastigmine, coupled with the pyrazolopyrimidinone structure of a known PDE9A inhibitor led to the identification of compounds with general structures **24** and **25**.

for the 3-OMe and 16.5 and 1.0 μM for the 4-OMe, respectively), being more potent than Miconazole. Their effect on spatial memory was assessed in the scopolamine-induced impairment in mice, where they displayed better performances than the control group treated with THA. Moreover, no acute hepatotoxic damage was observed. Taken together, all these characteristics highlight the favorable potential for these structures to combine interesting activities on innovative AD-related targets.

Another interesting approach in the search for MTDLs comes from Gao et al., who presented dual ChE and Poly(ADP-ribose) Polymerase-1 (PARP-1) inhibitors [54]. PARP-1 inhibitors have been extensively studied for their anticancer activity [55], but they may also serve as potential therapeutics for neurodegenerative diseases, with particular attention to AD and PD [56]. The role of PARP-1 has not yet been fully elucidated, but there are emerging evidences for the neuroprotective effect of its inhibitors. To merge the PARP-1 inhibition with that on ChEs, the structure of the known PARP-1 inhibitor Olaparib has been selected and modified with the introduction of substituted aryl vinyl groups in the place of the cyclopropane one (**23**, Figure 8). This combination should guarantee the dual activity on PARP-1 and ChEs, since it led to the formation of 3-aromatic-α,β-unsaturated carbonyl moieties, which are recurring groups in several natural ChE inhibitors and bioactive/neuroprotective compounds. The *in vitro* test revealed that all the analogues of the series were low micromolar inhibitors of PARP-1, even though none of them was more potent than the parent compound Olaparib. However, they showed moderate micromolar activity against AChE and BuChE, being more potent inhibitors of this latter enzyme. When Ar was a 3- or 4-nitrosubstituted phenyl ring, the highest inhibitory potency against BuChE was achieved, with an IC_{50} of 9.2 and 5.9 μM, respectively, even greater than Neostigmine as the reference. The abovementioned analysis confirmed the dual activity of these analogues and, although they may not be potent enough for *in vivo* analysis, molecular docking studies have already helped find a way to improve their activity. Thus, another interesting class of MTDLs may arise from the combination of these pharmacophoric elements leading to dual ChE and PARP-1 inhibition.

Phosphodiesterases have recently gained interest for their potential to ameliorate cognitive functions in AD patients. These enzymes can be involved in the regulation of cAMP and cGMP levels [57], and their inhibition can offer a valuable tool to increase the levels of the two second messengers in the hippocampus and cerebral cortex, with a consequent improvement in the memory and learning processes. Phosphodiesterase-9 (PDE9), which exerts its hydrolytic activity against cGMP, is now being studied as a potential target for CNS disorders [58], including AD, and the recently developed inhibitor PF-04447943 [59] has been tested in Phase II clinical trials for AD treatment (NCT00930059).

To assess the effects of dual PDE9A/AChE inhibitors, Hu et al. [60] exploited the benzylpiperidine moiety of Donepezil in combination with the pyrazolopyrimidinone structure (**24**, Figure 8) of a reported PDE9A inhibitor [61]. Although

different amidic or (cyclic)amine chains were explored as linkers for the two pharmacophores, the best results were obtained with 4-member ethereal or carbon tethers, resulting in compounds with submicromolar inhibitory activity against PDE9A and AChE. The type and length of the linkage played a pivotal role in the inhibition of PDE9A and was also responsible for the mixed type of inhibition of AChE, allowing the binding to both catalytic anionic site (CAS) and peripheral anionic site (PAS) of the enzyme. No effect was observed on SH-SY5Y cell viability at concentrations between 10 and 20 μM, demonstrating a limited neurotoxic potential. All the compounds were tested in the PAMPA assay, where the results showed that they were also potentially able to cross the BBB. Despite the moderate metabolic stability, acute toxicity was evaluated and, following the lack of detrimental adverse events, the compounds were tested *in vivo* in the scopolamine-induced mice model of cognitive and learning deficits. These analogues could significantly improve spatial memory and cognition in the Morris water maze tests; thus, they were also investigated in a mice model of spatial learning and memory deficits produced by an ICV injection of Aβ_{25-35}. Once again, there was a partial amelioration of the deficits induced by the treatment with the best performing compounds of the series.

Following a similar approach, hybridization of the pyrazolopyrimidinone skeleton with Rivastigmine led to the identification of another series of promising MTDLs (**25**, Figure 8) [62]. Even if various groups were used to replace the carbamate functionality of Rivastigmine and different chains were employed to create the linkage between the two pharmacophoric elements, compounds with general structure **25** resulted as the most promising and efficacious analogues of the series. Interestingly, these agents were behaving as selective inhibitors of BuChE, with IC_{50} values ranging from 0.96 to 18.8 μM, and were also potent PDE9A inhibitors in the nanomolar range. A little study on the selectivity over the PDE superfamily was also reported, confirming a good degree of selectivity for the PDE9A enzyme. Nevertheless, carbamate compounds were not active as antioxidants, and only the replacement of this functionality with hydroxyl groups restored the antioxidant potential. In addition, some of the tested compounds were not cytotoxic in SH-SY5Y cells in concentrations of up to 100 μM and were able to inhibit Aβ self-aggregation to some extent at a concentration of 50 μM.

All these data pointed out that the combination of the pyrazolopyrimidinone with other pharmacophores of ChE inhibitors is an optimal strategy to develop novel candidates for the treatment of AD.

2.5. ChE Inhibitors and NMDA Receptor Antagonists or Ca^{2+} Channel Blockers. The simultaneous inhibition of ChEs and the antagonistic effect on *N*-methyl-*D*-aspartate receptors (NMDARs) is definitely one of the most promising strategies towards the identification of new MTDLs. NMDA ionotropic receptors are activated by the excitatory neurotransmitter glutamate, and they are permeable to different positive ions, including Ca^{2+}, thus contributing not only to synaptic plasticity and long-term changes but also to the excitotoxicity process [63]. When the concentration of intracellular Ca^{2+} reaches pathological levels, there is a loss of synaptic functions and neuronal cell death, with a progressive cognitive decline. Recently, the activation of NMDARs has been linked to AD-related synaptic dysfunctions [64] and the NMDAR noncompetitive antagonist Memantine has been approved as symptomatologic treatment for moderate to severe AD [65]. The combination of NMDAR antagonism with the inhibitory activity on ChEs may have beneficial or synergic effects on AD symptomatology, as already proven in animal models of AD [66, 67]. Moreover, a fixed-dose combination of Donepezil and Memantine (known as the drug Namzaric®) is now used to treat moderate to severe dementia stages associated with AD [68].

In line with this hypothesis, a new series of benzohomoadamantane-chlorotacrine hybrids has been proposed as novel ChE inhibitors and brain penetrant antagonists for NMDARs. Following their previous knowledge in the development of THA-based AChE and BuChE inhibitors and polycyclic amines as antagonists of NMDA receptors, the authors exploited different linkers, varying their lengths and linkage positions, to connect the benzohomoadamantane motif with a 6-chlorotacrine (**26** and **27**, Figure 9) [69]. In particular, the two linkage positions were represented by the bridgehead amino group on the benzene ring of the benzohomoadamantane core (**26**) or by an additional amino group on the same system (**27**). This resulted in the identification of novel MTDLs, potentially able not only to inhibit ChEs and to antagonize NMDA receptors but also to interfere with BACE-1 activity and Aβ_{42} and pTAU aggregation, as already reported for the two separate pharmacophoric elements.

In both of the series, the new compounds retained the activities of the parent analogues on the primary targets, being AChE and BuChE inhibitors in the subnanomolar and submicromolar ranges, respectively, and binding to NMDA receptors in the micromolar range. Nevertheless, there was no activity on other proteins or targets associated with AD, as it was originally expected for the association of the two moieties. However, the increased potencies of some agents compared to the reference compounds represent a valid reason for a more in-depth evaluation in the anti-AD drug discovery field.

Another remarkable step forward for the discovery of new MTDLs took into account the possibility of creating structures that could merge the ChE inhibitory activity with the calcium channel blockade ability, thus limiting the entrance of Ca^{2+} through voltage-gated channels (VGC) and preventing neuronal damage [70]. To this aim, a series of tacripyrimidines have been proposed (**28**, Figure 9) [71], whose structures arise from the hybridization of THA with 3,4-dihydropyrimidin-2(1H)-thiones, known to be efficient calcium channel blockers. The 3-Br substituted analogue resulted as the most potent and selective *h*AChE inhibitor with $IC_{50} = 0.037$ μM, although the 3-methoxyphenyl derivative also showed good μM activity. The selectivity over BuChE was generally high, with the 4-(halo)-substituted compounds being slightly more potent against this enzyme. The 4-Cl derivative showed a reverted trend and was more

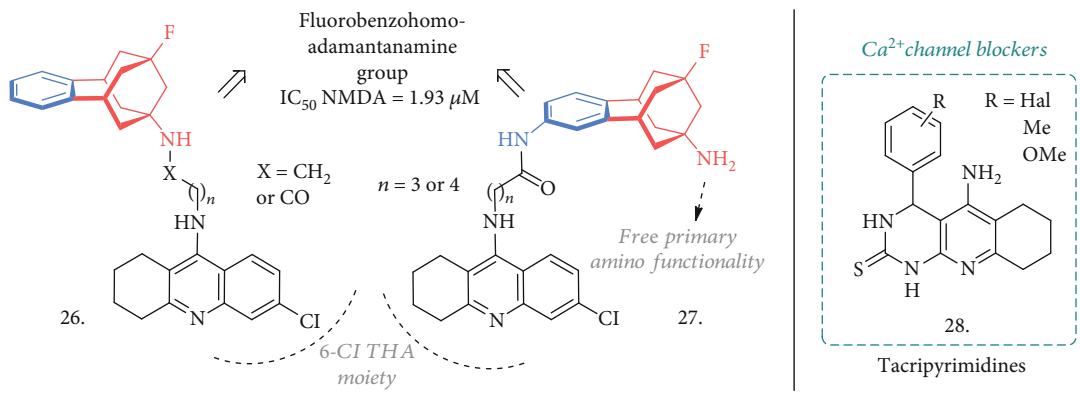

Figure 9: The novel THA-adamantanamines **26** and **27** acting as ChE inhibitors and NMDAR antagonists. Also, tacripyrimidines with general structure **28** are here represented as agents influencing Ca^{2+} influx and intracellular concentration by blocking voltage-gated Ca^{2+} channels.

potent on BuChE, while the 3-OMe-substituted compound was equipotent on the two enzymes. Further analysis revealed a noncompetitive type of inhibition, and molecular docking studies helped establish the key interactions of these compounds in the enzyme's CAS and PAS, pointing out the halogens as important substitutions for the activity and selectivity over the ChEs. The Ca^{2+}-channel blockade was investigated in SH-SY5Y cells by measuring the Ca^{2+} influx induced by K^+ depolarization. All the tacripyrimidines inhibited Ca^{2+} influx, with the most promising and potent inhibitors of AChE showing blockade activity similar to the reference Nomodipine. The compounds were relatively safe on HepG2 cells up to 100 μM, even if some derivatives showed higher hepatotoxicity than THA at higher concentrations. There was no significant effect on self-induced Aβ aggregation, as expected, but predicted ADMET properties showed a favorable potential for this candidate to be evaluated *in vivo*. The best performing tacripyrimidine of the series had a balanced activity over the selected targets and good ADME properties coupled with a lower toxicity than THA, thus making it an attractive structure deserving further investigation and development as an MTDL in AD.

2.6. ChE Inhibitors and Serotonin Receptor Modulators (5-HT$_4$ and 5-HT$_6$). Serotonin and its receptors (5-HTRs) have been conferred notable attention during the past decades, especially for their peculiar distribution in brain areas connected to memory and learning and thus for the role played by this system in cognition [72]. Hence, the modulation of specific 5-HTR subtypes could represent a major therapeutic strategy in the fight against AD [73]. Selective ligands for 5-HT$_4$R and 5-HT$_6$R have been the principal focus of the latest researches, and the effects of 5-HT$_4$R agonists and 5-HT$_6$R antagonists (or a combination of these efficacies) have been evaluated [74].

5-HT$_4$Rs belong to the G-protein-coupled receptor family and are localized both in peripheral areas and in the CNS, with a high density in the substantia nigra, striatum, and hippocampus. Here, they act as modulators of hippocampal synaptic responsiveness and plasticity, thus playing a central role in information storage and cognition [75]. Therefore, 5-HT$_4$R agonists have the potential to be therapeutically useful in AD not only for the effects on memory and behavioral performances, but also because 5-HT$_4$Rs influence the cholinergic system and ACh release, and are linked to APP activity and Aβ production [76]. 5-HT$_6$Rs are also G-protein-coupled receptors whose expression is restricted to the CNS. Although the information regarding their pharmacology is still limited, the presence of 5-HT$_6$R in brain areas responsible for cognitive functions, memory, and learning (such as hippocampus and cerebral cortex) made them another interesting target in AD [77]. Antagonists of these receptors become attractive therapeutics to address some of the AD-related dysfunctions [78], also in correlation with their procholinergic effect which is enhanced by the combination with approved AChE inhibitors.

With the aim of merging the anti-ChE activity and the modulation of 5-HT$_4$/5-HT$_6$ receptors, different structural combinations have been explored. Recently, the same group that discovered Donecopride (**30**, Figure 10) was able to develop a novel class of MTDL able to inhibit AChE, activate 5-HT$_4$R, and block 5-HT$_6$R. Donecopride [79] is an AChE inhibitor with partial 5-HT$_4$R agonist activity inspired by the 5-HT$_4$R agonist RS67333 (**29**, Figure 10), which showed *in vivo* procognitive and antiamnesic effects in NMRI mice and promoted sAPPα release in C57BL/6 mice [80]. Through minor structural modifications of the benzyl analogue of Donecopride, a few derivatives were obtained with very promising *in vitro* triple effects (**31**, Figure 10) [81] with R=3-Me substitution (as a fumarate salt), the compound possessed an interesting profile with $Ki_{(5\text{–HT4R})} = 210$ nM and $Ki_{(5\text{–HT6R})} = 219$ nM and IC_{50} on AChE = 33.7 nM, acting as a partial agonist towards *h*5-HT$_4$R (similar to Donecopride) and as an inverse agonist towards *h*5-HT$_6$R. Moreover, *in vivo* evaluation on an NMRI mice model demonstrated an antiamnesic effect at a dose of 0.3 mg/kg, with no detrimental effects at concentrations higher than 100 mg/kg, thus representing a quite promising MTDL candidate for AD treatment.

Further structural modifications of Donecopride allowed the discovery of other interesting compounds endowed with a multitarget profile, such as a dual 5-HT$_4$R partial agonist and 5-HT$_6$R antagonist, with no activity on AChE (**32**,

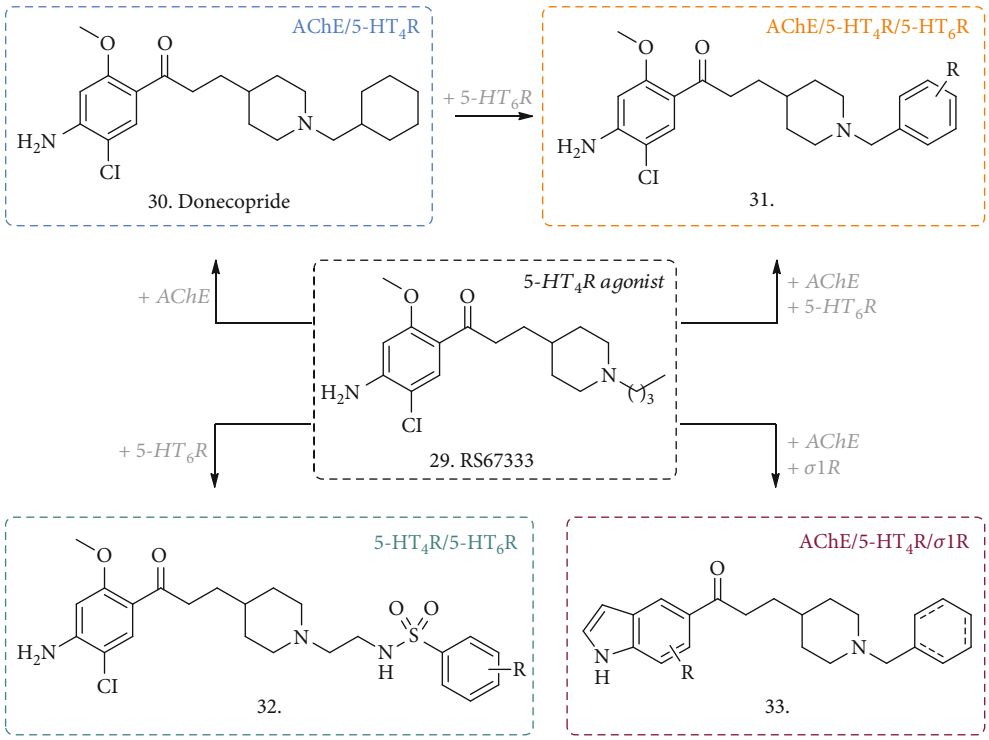

Figure 10: The discovery of Donecopride (**30**) inspired by the 5-HT_4R agonist RS67333 (**29**) and the structurally related MTDLs acting as ChE inhibitors and/or serotonin 5-HT_4 and 5-HT_6 receptor modulators (**31** and **32**). The general structure **33** has been added as a further modification of the scaffold of RS67333 and Donecopride, although its activity shifted from 5-HTRs to σ1R.

Figure 10) [82] useful to study the serotoninergic role in AD, or a dual inhibitor of AChE and modulator of σ1 receptor (σ1R) (**33**, Figure 10), that will be subject of discussion in the following paragraph as a more recent combination to address AD-related dysfunctions.

Another series of compounds reported by Marcinkowska et al. merged an *N*-benzylindole-piperazine skeleton with phthalimide- [83] or THA-moieties [84] (**34** and **35**, Figure 11), using carbon tethers with different lengths as linkers. While the indole-piperazine section brought the potential antagonism for 5-HT_6R [85], indole alone may have antioxidant properties and the phthalimide or THA groups could contribute to ChEs inhibition, thus creating hybrid compounds with a multifaceted activity. In the phthalimide subseries (**34**), the new compounds displayed affinity for 5-HT_6R with *K*i ranging from 21 to 252 nM and a clear correlation of the binding potency with the length of the linkers with phthalimide. Cell functional studies confirmed the antagonistic activity of these derivatives. Moreover, they were micromolar inhibitors of BuChE, with no or slight activity on AChE, and once again shorter linkers performed better than the longer ones, with R=H unsubstituted analogues being slightly more potent than the halogenated counterparts. The antioxidant activity was determined by FRAP assay, where all the compounds showed antioxidant potential starting from 10 μM, and some of them had even better activity than the reference ascorbic acid.

When the THA moiety (**35**) was in the place of the phthalimide one, the R=H compounds showed a higher nanomolar activity against AChE and, to the same extent, on BuChE, becoming nonselective and noncompetitive ChE inhibitors, but still deserving further development for AD treatment. The antagonist activity on 5-HT_6R was also conserved, and the 5-C atom chain gave the best *K*i value of 72 nM. The thioflavin-T (ThT) assay on Aβ self-aggregation revealed equal or better inhibitory potency (over 92%) than resveratrol used as a reference, and PAMPA-BBB prediction determined a favorable potential to diffuse across the membranes.

Another combination of the THA moiety with a tolylamino fragment, known to be a 5-HT_6R antagonist [86], and spaced by the same linkers (**36**, Figure 11) displayed similar activities on the abovementioned systems [77]. In this case, *K*i values on AChE and BuChE were even higher in comparison with the previous structures (reaching 10 nM and 22 nM for the best analogue, respectively) and still showing potent binding and antagonism towards 5-HT_6R. Together with the positive effects on Aβ self-aggregation and a good predicted permeability across membranes, the *in vitro* metabolic stability of these analogues in human liver microsomes highlighted a of 120 min with none of the known THA-related hepatotoxic metabolites identified.

Even if these compounds have not been tested *in vivo* in animal models of cognitive disorders, their *in vitro* analysis revealed a high potential to be useful MTDLs deserving further evaluation in AD.

2.7. ChE Inhibitors and H_3R Antagonists or σ1R Agonists. Besides the more classical couplings of ChE inhibitors with the previously described receptor families, other appealing

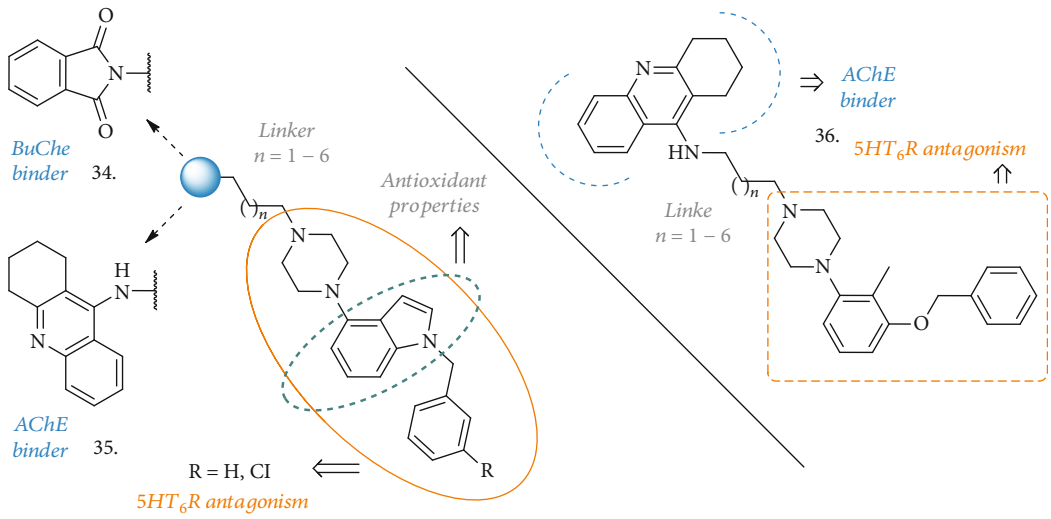

Figure 11: General structures of recent ChE inhibitors/5-HT_6R antagonists. The pharmacophoric elements for the dual activity are highlighted for each structure. Together with the multiple activity, some of these agents are also endowed with antioxidant activity and effects on Aβ aggregation.

combinations have been recently explored. So far, the histamine H3 receptor (H_3R) has been the focus of numerous researches for the treatment of cognitive disorders [87]. H_3R are mainly expressed in the cortex, hippocampus, caudate, and putamen [88], and their activation influences the release of different neurotransmitters (including AChE), thus having an impact on brain disorders like AD. For this reason, antagonists of H_3R have been investigated for their potential role in cognitive dysfunctions related to AD [89]. As mentioned above, σ1Rs also found their place in the context of neurodegenerative disorders [90]. These receptors are mainly situated in the endoplasmic reticulum where they normally exert prosurvival and antiapoptotic effects, but they can be found in other organelles influencing lipid, protein, and ion trafficking [91]. Changes in the function or expression of this multifunctional protein have been linked to various diseases, including AD [92] and HD. Here is why some examples of ChE inhibitors in combination with H_3R antagonist or σ1R agonist activities have been proposed.

Wang et al. presented some novel isoflavone derivatives bearing amino or THA groups linked to the 7-position of the isoflavone core by different chains, along with some diamino-substituted analogues inspired by known H_3R antagonists (**37** and **38**, Figure 12) [93]. A preliminary analysis of the H_3R antagonist profile made on isoflavone-based compounds with known AChE inhibitory activity guided the identification of the appropriate linkers and amines for SAR studies. Even if the monoamino substituted derivatives (**37**) showed good activities on the selected targets, the analogues bearing a second amino functionality (**38**) resulted as the more potent low micromolar antagonists of H_3R. They also displayed pronounced dual AChE and BuChE inhibition at the low- or submicromolar level, with the best inhibitor having IC_{50} values of 0.08 μM and 2.9 μM, respectively. These compounds also showed antioxidant activity in the ORAC-FL test and possessed an anti-inflammatory effect in LPS-stimulated BV-2 microglia cells, suppressing the production of IL-6 and TNF-α without affecting cell viability. Moreover, they were not cytotoxic in SH-SY5Y cells in concentrations of up to 100 μM, and in the SH-SY5Y-APPsw cell line (overexpressing the Swedish mutant form of human APP), they significantly prevented copper-induced Aβ aggregate toxicity, increasing cell viability. Acute toxicity was assessed in mice, resulting in the toleration of up to 1000 mg/kg, and the favorable PK parameters and drug-like properties prompted the authors to test the compounds in animal models of cognitive deficits. In mice, there was a significant prolongation of the scopolamine-induced latency of step-down in a dose-dependent manner (10 to 30 mg/kg) and an increase in brain cholinergic activity, ameliorating cognitive deficit. All together, these results highlighted an exquisite multitarget profile for these compounds and the *in vivo* analysis suggested an interesting potential for the treatment of AD.

Starting from the structure of the previously described Donecopride (**30**, Figure 10) [79], Lalut et al. focused their research on novel ligands endowed with AChE inhibitory activity and σ1R affinity [94]. Modifications to the aromatic region of the reference compound with the introduction of a substituted indole ring (**33**, Figure 12) afforded a different receptor affinity profile, where the activity on 5-HT_4R was partially lost while the interaction with σ1R become the pivotal feature for the new analogues. Together with the binding affinity for σ1R, the indole scaffold was also increasing the interactions with the peripheral anionic site (PAS) of AChE.

All the compounds were evaluated for their ability to inhibit *h*AChE and to bind to guinea pig (gp) 5-HT_4R. They showed an overall decrease in 5-HT_4R affinity, with the *N*-benzylpiperidines being the weakest ones, although some analogues changed their functional activity on the receptor, acting as an antagonist instead of a partial agonist, as

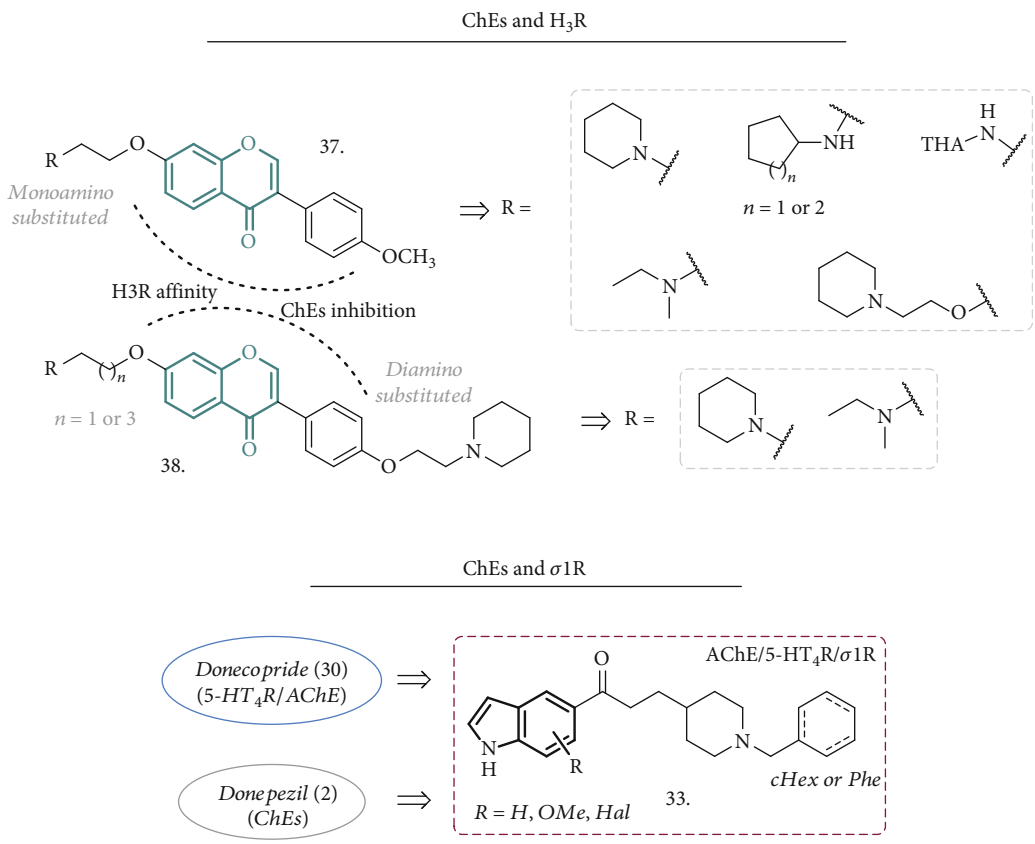

Figure 12: General structures of novel combinations for the discovery of dual ChE inhibitors with H_3R antagonist (**37** and **38**) or σ1R agonist (**33**) activities.

Donecopride was. They all displayed a potent inhibition of AChE, with the *N*-benzyl groups on piperidines enhancing this activity, behaving as noncompetitive inhibitors, suggesting a possible interaction with the PAS and the subanionic site of the active site. These interactions were subsequently confirmed by the X-ray analysis of the crystal structures of selected compounds with the enzyme. Regarding the σ1R affinity, most of the compounds of the series were very potent ligands of this receptor, and the presence of the indole ring was crucial for the activity. One of the best compounds (IC_{50} (AChE) = 28.8 nM, Ki (5 − HT_4R) = 37.5 nM, and Ki (σ1R) = 5.1 nM) was also evaluated *in vivo* in a dizocilpine-induced amnesia model, showing a protecting effect in the passive avoidance test that correlates with its *in vitro* potent σ1R affinity. For all these reasons, this new series of compounds has a great potential to be useful in the treatment of AD and deserves further investigation.

2.8. The Effects of Dual ChE Inhibitors and Modulators of the Endocannabinoid System. Another innovative approach in the search for MTDLs envisages the possibility to act on ChEs or BACE-1 and to couple this activity with the modulation of the endocannabinoid system (ECS). The ECS is composed of endogenous lipid-signaling molecules defined as endocannabinoids (ECBs) and their cellular targets, the G-protein-coupled cannabinoid receptors (type-1 and type-2 CBRs), along with the transporters and enzymes responsible for ECB biosynthesis and metabolism. *N*-Arachidonoylethanolamine (anandamide (AEA)) and 2-arachidonoylglycerol (2-AG) are two members of the ECB signaling molecules, and they activate CBRs to modulate a wide range of responses and processes including pain, inflammation, and thermoregulation [95]. The actions of these signaling lipids are rapidly terminated by cellular reuptake and subsequent hydrolysis operated by a number of enzymes. Amongst the latter, the Fatty Acid Amide Hydrolase (FAAH) was originally identified as the enzyme responsible for AEA hydrolysis [96] while the Monoacylglycerol Lipase (MGL) plays a pivotal role in the regulation of 2-AG levels [97]. ECB signaling has been found altered in some neurodegenerative diseases. Evidences pointed out to how decreased levels of AEA, for example, correlate with an inverse trend to those of Aβ [98]. In addition, CB2R, which is associated with immune system and microglia activation during neuroinflammation, is selectively expressed in areas of neuritic plaques, suggesting a potential role for this receptor in the inflammation associated with AD [99]. These findings suggested that the modulation of ECS may have a profound impact on AD.

ECS can be modulated either by direct stimulation of CBRs or by inhibition of the ECB catabolic enzymes, leading to increased levels of ECBs [100–104]. For this latter purpose, Montanari et al. have recently proposed some compounds, here represented by **39** (Figure 13), endowed with inhibitory

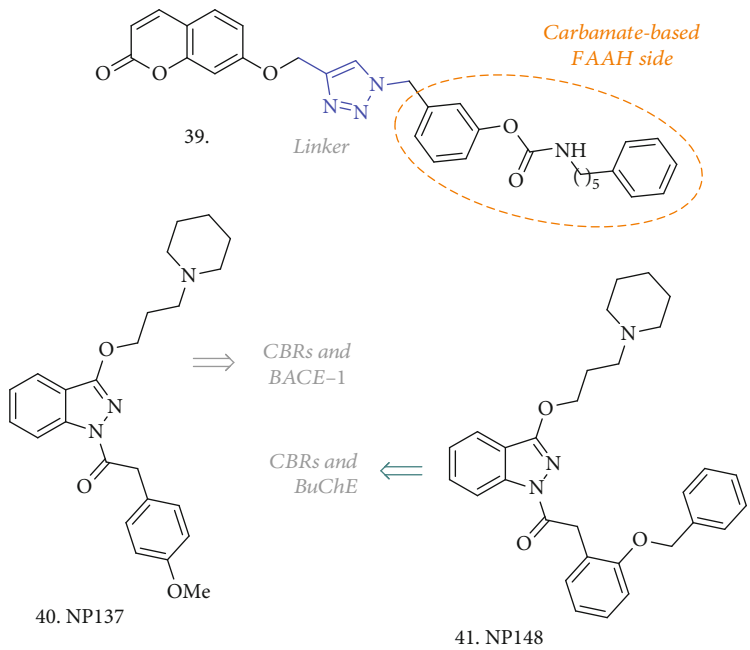

Figure 13: Structures of the novel compounds acting on ChEs (and BACE-1) and able to modulate the ECS via direct interaction with CBRs (**40** and **41**) or by increasing the ECBs' tone through the inhibition of the AEA-metabolizing enzyme FAAH.

activity towards FAAH, AChE, and BuChE [105]. They evaluated several structures where the triazole linker of **39** was replaced by a more flexible *N*-methylalkyl chain, some of which were able to inhibit both AChE and BuChE to a similar extent, and to retain a good activity towards the FAAH enzyme. However, a more balanced profile was achieved with **39**, having an IC_{50} against *r*FAAH, *h*AChE, and *h*BuChE of 922, 42.7, and 27.9 nM, respectively, and thus displaying good selectivity for BuChE. Cytotoxicity evaluation on SH-SY5Y cells up to 50 μM showed no acute toxicity and, although no in vivo evaluation was performed, these compounds are worth further investigation for AD treatment.

With the aim of discovering MTDLs for AD treatment able to modulate ECS via direct CBR stimulation, Nuñez-Borque et al. have identified two CBR agonists which also act as BACE-1 and/or BuChE inhibitors [106]. No *K*i values were reported for CBRs, but functional experiments confirmed the agonist profile for **40** and **41** (Figure 13), and while **40** had a 60% inhibition of BACE-1 at 10 μM, compound **41** had a 38% inhibition at the same concentration and an IC_{50} on BuChE of 2.5 nM. In rat primary cortical neuronal cultures, both compounds efficiently attenuated Aβ-induced cell death, increasing cell viability, while only **40** was able to improve performances in an animal model of AD, namely TgAPP transgenic mice. Moreover, this compound was able to restore abnormal features of the AD lymphoblast, thus having an impact on nonneuronal cell cycle alterations, considered systemic manifestation of the disease. This was achieved either by preventing the enhanced serum stimulation of cell proliferation or by sensitizing cells to apoptosis in conditions of higher resistance to serum deprivation-induced cell death. More detailed studies are needed to completely understand the effects and mechanisms behind these MTDLs, but they represent a nice way to address AD from a different perspective.

2.9. ChE Inhibitors with Multiple Effects on Aβ-Aggregation, Metal-Induced Toxicity, and Oxidative Stress. Even when not coupled with other enzymatic activities, ChE inhibitors may have a multitarget profile if considering (*i*) their possible action against Aβ aggregation, (*ii*) their disaggregation effect on preformed Aβ fibrils, and (*iii*) the metal-chelating properties, affecting metal dyshomeostasis and oxidation processes. This combination often resulted in compounds with the potential to be neuroprotective MTDLs.

In the search for ChE inhibitors with additional neuroprotective and antioxidant properties, Patel et al. reproposed the exploitation of the indole ring to build up novel multiactive structures, guided by the observation that melatonin, based on the same indole moiety, is endowed with free radical scavenging ability and neuroprotection against Aβ-induced toxicity [107]. They merged this ring with the 1,2,4-triazine scaffold, which is also a common feature for several drugs, and then explored the effects of thio- and amino-linked aryl/benzyl/aminoalkyl side chains (typified by **42**, Figure 14). All the compounds showed micromolar to submicromolar activity towards AChE and BuChE. Some of the most active analogues ($IC_{50} < 5\,\mu$M) showed antioxidant activity in the 1,1-diphenyl-2-picrylhydrazyl (DPPH) assay at concentrations ranging from 10 to 20 μM, with moderate to good free radical scavenging activity (54.9-64.3%) compared to ascorbic acid. No cytotoxicity was observed in the SH-SY5Y cell line (up to 80 μM) and in H_2O_2- and Aβ-induced toxicity studies; compound **42** exerted a substantial protection against the toxic insult in a concentration-dependent manner. Besides a very detailed computational

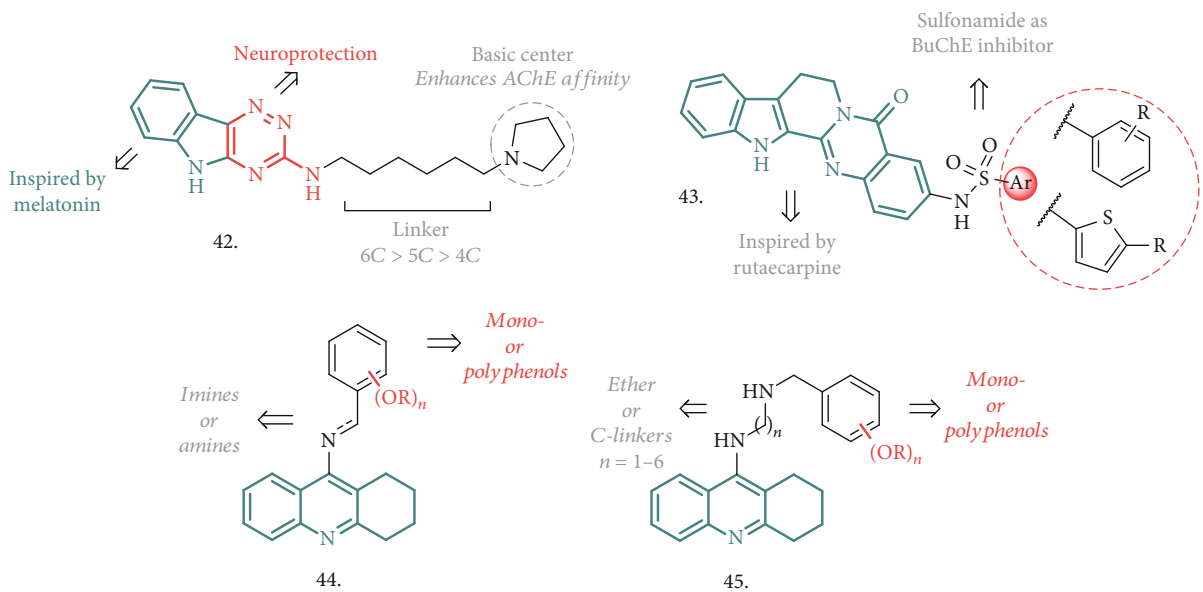

Figure 14: Some of the most recent compounds which combine ChE inhibition with the neuroprotective effects, acting on the classical hallmarks of AD, such as Aβ aggregation/disaggregation, metal-induced toxicity, and oxidative stress.

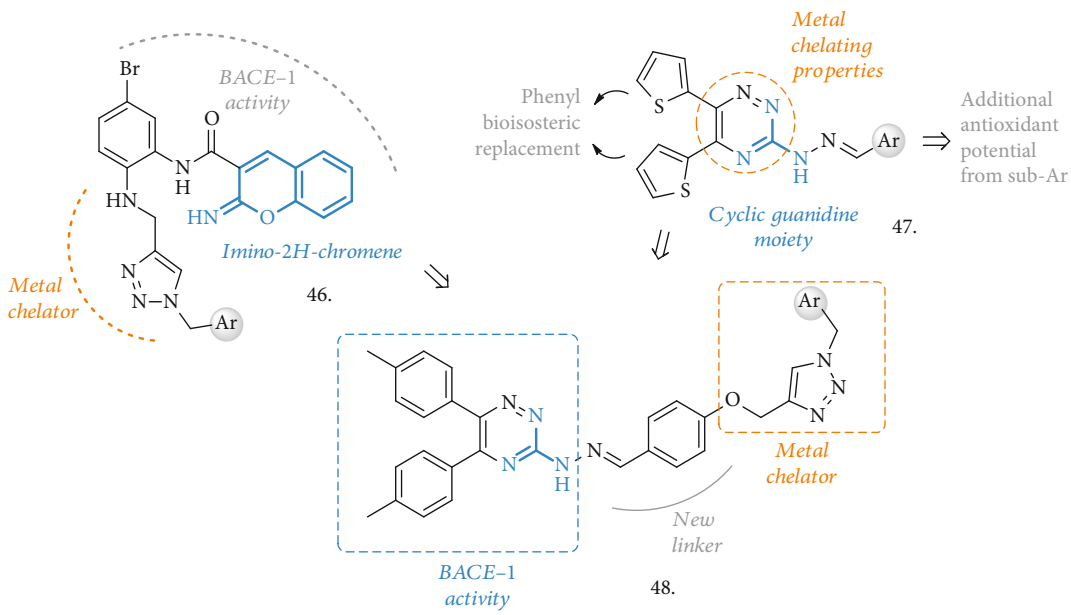

Figure 15: BACE-1 inhibitors with metal-chelating properties and radical scavenging potential.

analysis to establish the essential interactions and features required for the multitarget activity, confirming the key role of the triazinoindole core and the enhancement brought by the introduction of a basic center in the chain, the compound was tested for its cognitive improvement effect in animal models of AD. In scopolamine-induced amnesia in rodents, it showed spatial memory improvement in the Morris water maze learning test at doses of 5 and 10 mg/kg p.o. Moreover, in the Aβ-induced AD model, the lowered spontaneous alternations induced by Aβ_{1-42} were significantly reversed at the same doses. The neurochemical analysis carried out on the scopolamine- and compound-treated animals contributed to confirm the ability of **42** to reverse the reference and working memory deficit as well to manage the oxidative stress-induced dementia. If coupled with the notable *in silico* ADMET properties, all these analyses highlighted the favorable potential for this analogue to be a useful treatment for AD-related deficiencies.

The combination of a sulphonamide moiety with the core structure of Rutaecarpine, a well-known pentacyclic indolo-pyridoquinazolinone alkaloid from Chinese medicine, has been proposed by Wu et al. as a promising MTDL (**43**, Figure 14) [108]. All these analogues had good to moderate concentration-dependent activity against BuChE in the μM

range, being more potent than the parent compound but not as efficient as THA. They also resulted to be selective inhibitors of the abovementioned enzyme, with almost a null effect on AChE. At a concentration of 100 μM, there was a significant effect in the DPPH free radical scavenger assay, with ascorbic acid and Donepezil used as reference antioxidants, underlying a mild scavenging activity. There was also a robust effect against intracellular ROS generation in H_2O_2-treated SH-SY5Y and PC12 cells, where the compound treatment restored the ROS levels almost to the blank group, highlighting a neuroantioxidant potential. The same models and cell lines were used to assess neurotoxicity by measuring cell viability after incubation with increasing concentrations of the title compounds. In both of the cases, survival rate increased in a dose-dependent manner. Coincubation of Aβ_{42} with the best performing analogue of the series resulted into interference with the peptide self-assembly process, and TEM analysis confirmed an antiaggregation effect comparable or superior to that of Donepezil at concentrations of 100 μM. The presence of the carbonyl and sulfonamide groups in the compounds may have conferred chelating properties, and differences in the UV absorption at a peculiar wavelength indicated the capability to chelate Cu^{2+} in a 1 : 1 stoichiometry. The newly introduced features in the Rutaecarpine scaffold led to a combination of interesting activities, placing this core and its analogues under the spotlight for further development as MTDLs against AD.

Another recent research work evaluated the possibility of using different tethers to combine the THA motif with (poly)phenolic or methoxy-substituted rings, generating novel MTDLs potentially useful for AD treatment (general structures **44** and **45**, Figure 14) [109]. In more detail, the new analogues were designed to overcome classical THA-derived side effects and to provide access to other significant therapeutic targets, such as neuronal redox status, deposition of amyloid plaque, leading to neuroprotection. The linkage strategy, guided by molecular docking analysis, envisaged the formation of imino-, amino- (**44**), or ethereal (**45**) bonds, coupled with the variation of the tether length by increasing the number of carbon atoms. The best performing analogue of series **44**, bearing a 9-atom ether-type chain and a dimethoxy-substituted ring, behaved as an extremely potent (subnanomolar range) and selective BuChE inhibitor, with an 85-fold increase of activity compared to THA, and displayed a good ability to interfere with Aβ self-aggregation, lacking neurotoxicity at concentrations of up to 5 μM. Its neuroprotective properties were assessed in primary rat neurons, inducing neuronal damage by serum and K^+-deprivation, where it showed neuroprotection at concentrations of up to 10 μM. All these activities, combined with a low hepatotoxicity and good stability under physiological conditions, pointed out to this lead compound as a promising pharmacophore combination deserving further analysis and progression in the list of AD treatment.

2.10. BACE-1 Inhibitors and Their Combinations into MTDLs. As already discussed in the previous sections, BACE-1 represents another key enzyme targeted in AD and the importance and effects of dual ChE/BACE-1 inhibitors have been reported (Section 2.1). In the search for MTDLs, other interesting combinations may arise from the exploration of novel BACE-1 inhibitors endowed with neuroprotective and anti-inflammatory effects.

Inspired by coumarine, acylguanidine, and cyclic guanidine moieties, different series of compounds have been identified as BACE1 inhibitors, also endowed with antioxidant and metal-chelating activities (**46-48**, Figure 15). Some of them arise from the combination of the phenylimino-2H-chromen core with an aminomethylene-1,2,3-triazole ring (**46**), while the use of the 3-hydrazynyl-1,2,4-triazine structure led to the identification of compounds **47** and **48**. The latter also prompted the authors to evaluate the contribution of the 1,2,4-triazine and the 1,2,3-triazole moieties in chelating metals. Compounds with general structure **46** [110] were moderate inhibitors of the BACE-1 enzyme, with the most active compound having a phthalimide pendant and anIC_{50} = 2.2 μM. They showed some potential as neuroprotective agents, increasing the % of PC12 cell viability treated with A$\beta_{25\text{-}35}$ and displaying no cytotoxic effect. The 4-bromophenyl-substituted analogue also had an acceptable ability to chelate Fe^{2+} with a 3 : 2 complex formation with the metal.

In the series of triazine-based compounds [111], an interesting set of analogues was reported, bearing di-(thiophene-2-yl) substitutions and different aryl hydrazone moieties (**47**, Figure 15). Inspired by other previously reported cyclic guanidine MTDLs, the authors exploited the use of the thiophene rings to modulate the lipophilic characteristics of the compounds and to increase the interactions within the BACE-1 active site, while varying the aryl pendants linked to the hydrazone functionality in the search for antioxidant and radical scavenging potential. The series had good to moderate inhibitory activity against BACE-1, and after a nice evaluation of the SAR around the aryl pendants, the 2-indole-substituted analogue resulted in the most potent inhibitor with an IC_{50} = 0.69 μM. Also the hydroxylphenyl-substituted compounds were of interest, especially for the higher scavenging potential displayed in the DPPH assay (IC_{50} = 7 μM, compared to quercetin, whose IC_{50} value is 4.6 μM). The abovementioned 2-indole-substituted analogue resulted to be noncytotoxic in the PC12 neuronal cells in concentrations of up to 10 μM and was selected for testing the metal-chelating activity, showing the ability to chelate Zn^{2+}, $Fe^{2+/3+}$, and Cu^{2+}in different stoichiometries.

As additional modifications to the triazine core, compounds with general structure **48** (Figure 15) were reported [112]. Here, the introduction of the aryl phenoxymethyl-1,2,3-triazole moiety added further potential to display metal-chelating and antioxidant effects. In these hybrids, substituted phenyl groups replaced the two thiophene rings and the pendant aryl attached to the hydrazone functionality was also O-linked to the 1,2,3-triazole group. The compounds were tested for their ability to inhibit BACE-1, and when the Ar group was a propylisoindoline fragment, the highest potency was achieved, corresponding to an IC_{50} of 18 μM (67.09% inhibition at 30 μM). These tool compounds were evaluated in the DPPH and MTT assays, showing only

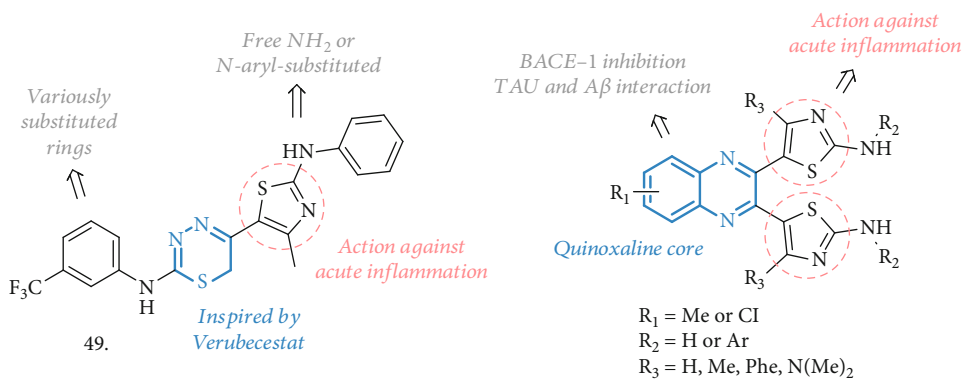

Figure 16: BACE-1 inhibitors with anti-inflammatory activity related to COX interaction.

mild activity as antioxidants and a moderate neuroprotective activity in PC12 cells treated with $A\beta_{25\text{-}35}$. However, the compound containing a pendant 4-nitrobenzyl group showed a higher antioxidant effect and was also able to chelate Fe^{2+} and Zn^{2+} in a 1 : 1 stoichiometry.

These interesting series of compounds, combining different pharmacophoric elements, need to undergo further optimization but are certainly of interest as MTDLs able to address some of the most common hallmarks of AD.

BACE-1 inhibitors able to interfere with the inflammation process arose from a thiazolyl-thiadiazine scaffold, which Sagar et al. used to embark with the synthesis of novel MTDLs for AD (**49**, Figure 16) [113]. They were inspired by Verubecestat [114] and other thiadiazine-1,1-dioxide scaffolds acting as BACE-1 inhibitors, along with thiazole-based compounds useful in reducing acute inflammation status, thus potentially able to interfere with COX activity.

The prototypic compound **49** (bearing the CF_3 substituent) was the most potent BACE-1 inhibitor of the series, with an IC_{50} of 9 μM, and it was also evaluated in animal models of carrageenan-induced acute inflammation. There was a high percentage of edema inhibition (70%), comparable to the treatment with Diclofenac, while the effects were slightly less marked on chronic inflammation induced by Formalin (58%), compared to Celecoxib as the reference. The memory-enhancing effect was assessed in an $AlCl_3$-induced AD rat model, where a significant and robust improvement in behavioral tests, such as the elevated plus maze or the Y-maze was observed. $AlCl_3$-treated animals also showed a significant increase in MDA levels, a marker for lipid peroxidation and oxidative stress. Notably, MDA levels were reduced in treated rats while SOD activity was increased, thus suggesting an antioxidant ability of the compound. No detrimental effects were observed on hematological parameters, and the healthy hippocampus region was the most convincing proof of the protection from neuronal cell degeneration induced by the treatment. Moreover, no hemorrhagic damage or lesion was reported in the stomach and intestine of the animals, demonstrating high gastrointestinal safety. This compound represents a valuable example of how the BACE-1 inhibition and anti-inflammatory activity combined together could serve as efficient agents against AD.

Another nice example of quinoxaline-based molecules acting as BACE-1 inhibitors and useful to modulate inflammation has been reported by the same authors (**50**, Figure 16) [115]. The new compounds were rationally designed to interact with BACE-1 over BACE-2 and to increase binding affinity for COX-1 and COX-2 enzymes, thanks to the introduction of thiazole rings that could establish H-bonds with these enzymes' residues. All the analogues inhibited BACE-1 in the micromolar range, especially those with the unsubstituted amino functionality (R_2=H). The acute and chronic anti-inflammatory effects were evaluated in carrageenan- and formalin-induced rat paw edema studies, respectively. At doses of 50 mg/kg, the best performing compound showed an inhibition of the edema up to 69% and 55% in the two animal models, even though no *in vitro* inhibition of COX-1 or COX-2 was measured. Having the required activity profile, the compounds were evaluated *in vivo* in behavioral tests, such as the Y-maze, conditioned avoidance response, and elevated plus maze. In all the tests, there were significant effects with reduction of the amnesic effect aroused from $AlCl_3$ injections, significant decrease in conditioned avoidance response, and improvement in spatial working memory. Additional antioxidant activity and a promising free radical scavenging effect were confirmed by lipid peroxidase (LPO) and SOD assays in rat brains, with a reduction in MDA levels compared to the control. For their potential as COX inhibitors, the safety on the gastrointestinal tract was checked, evidencing no damages but a minimal lesion in the gastric section. Merged together, BACE-1 inhibition and anti-inflammatory activity can promote beneficial effects on AD and the concomitant antioxidant and antiamyloid potentials observed *in vivo* made these structures interesting MTDLs.

2.11. The Multitarget Effect on AD Not Related to ChE or BACE-1 Inhibition. A slightly different approach, aimed at targeting $A\beta$-mediated toxicity and self- and metal-induced aggregation, together with oxidative stress and no enzymatic activity against any of the common AD-related systems, may offer a great opportunity for the discovery of neuroprotective MTDLs.

Histone deacetylases (HDACs) have attracted attention for their roles in AD brains. HDACs are a class of enzymes

that catalyzes the removal of acetyl groups from the lysine residues of both histone and nonhistone proteins [116]. The 18 existing isoforms can use either a zinc- or a NAD^+-dependent mechanism to accomplish the deacetylation process. Classes I (isoforms 1, 2, 3, and 8), IIa (isoforms 4, 5, 7, and 9), IIb (isoforms 6 and 10), and IV (isoform 11) are zinc-dependent metalloamidases, while Class III HDACs (sirtuine) are the NAD-dependent enzymes. Several inhibitors of selected isoforms have already been successfully tested as promising anticancer agents [117–118]. Nevertheless, the inhibition of HDACs can also provide neuroprotection and enhance synaptic plasticity as well as learning and memory, thus representing a valuable approach for AD treatment [119]. In particular, HDAC2 and HDAC3 have a critical role in controlling memory-related genes [120], while dampening HDAC6 activity enhances pTAU and Aβ clearance [121–122]. Moreover, HDAC2 and HDAC6 seem to be overexpressed in the cortex and hippocampus of AD patients [123].

With the aim of combining the effect on HDACs and other AD-related proteins, Cuadrado-Tejedor et al. have explored the effect of a concomitant inhibitor of HDAC6 and PDE5, namely compound **51** (CM-414, Figure 17) [124]. Previously, a cocktail of two different drugs acting on these two enzymes (Vorinostat and Tadalafil) gave *in vivo* positive effects, by alleviating cognitive deficits in AD mice and by reversing the reduced density of hippocampal neurons [125]. In this case, a single compound is responsible for the dual activity, with a moderate class I HDAC activity and a potent inhibition of HDAC6 and PDE5. Compound **51** is a pyrazolopyrimidinone that was inspired by known HDAC and PDE5 inhibitors and bears some key elements endowing it with the essential pharmacophoric features. It also possesses favorable ADME properties and a safe profile in terms of toxicity and cardiovascular safety. CM-414 has IC_{50} against HDAC1-3, HDAC6, and PDE5 of 310, 490, 322, 91, and 60 nM, respectively, with the hydroxamic acid moiety being responsible for the HDAC activity. The synergic effect of HDAC/PDE5 inhibition is responsible for an increase of histone 3 lysine 9 (AcH3K9) acetylation in WT neurons at 10 nM, which correlates with the same effect on SH-SY5Y starting from 64 nM. In Tg2576 neurons, similar effects were observed at 100 nM, where also the effect on hAPP processing and pTAU were evaluated, highlighting a decrease in $A\beta_{42}$ precursors and pTAU levels. When preincubated with hippocampal slices (200 nM), compound **51** rescued the synaptic plasticity impairment in APP/PS1 AD mice, with synaptic potentiation. After the evaluation of PK parameters, toxicity, and BBB penetration in the in vitro PAMPA assay, this analogue was tested in Tg2576 mice, choosing the dose of 40 mg/kg as the optimal one for having acceptable brain concentration and half-life. After 2 weeks of treatment, compound **51** was able to rescue the memory impairment in the fear conditioning (FC) test, with a freezing response similar to WT mice, while a 3-week treatment followed by the Morris water maze test demonstrated a positive effect on spatial memory. To further explain these activities, the authors found that soluble $A\beta_{42}$ and pTAU levels decreased in treated mice (but not in WT ones), paralleled by an increase of the inactive form of GSK-3β. Moreover, **51** increased the spine density on apical CA1 dendrites, upregulated markers of synaptic plasticity, and induced the restoration of some of the downregulated genes in Tg2576. A 4-week treatment also led to an enrichment of gene expression and related synaptic transmission in the hippocampal region, and these changes were triggered by an epigenetic mode of action. Overall, compound **51** represents an optimal starting point in the discovery of novel HDACs and PDE5 inhibitors as novel and promising agents to treat AD-related dysfunctions.

To a similar extent, De Simone et al. have recently proposed a series of HDAC/GSK-3β inhibitors here represented by compound **52** (Figure 17) [126]. As already mentioned, GSK-3β plays a central role in the pathogenic mechanisms of AD through the phosphorylation of pTAU, and the close connection between the latter and HDACs has already emerged. For instance, the neurotoxicity induced by HDAC1 has already been linked to GSK-3β activity [127], while the enhanced phosphorylation of HDAC6 by GSK-3β has been connected with an increase in the activity of this HDAC and pTAU phosphorylation [128]. Compound **52** is a combination of pharmacophoric elements where the HDAC-interacting part is once again represented by hydroxamic acid while the phthalimide-like scaffold served as the binder for the ATP-site of GSK-3β. This analogue is able to inhibit HDAC1, HDAC6, and GSK-3β in the low micromolar range of concentration (12.78, 3.19, and 2.69 μM, respectively). SH-SY5Y cells were used to determine the effect of this compound *in vitro*, by analyzing the level of acetylation of tubulin and histone H3 at lysins 9 and 14, and the phosphorylation of pTAU. Treated cells showed hyperacetylated α-tubulin, while no effect was observed on AcH3K9 or K14, highlighting a preferential action through HDAC6; pTAU hyperphosphorylation induced by copper was counteracted by 10 μM concentrations of **52**. Despite the fact that HDAC inhibitors are used as anticancer agents, the molecule was safe in this cell line up to 100 μM, and it was also able to efficiently contrast H_2O_2-induced oxidative stress, with an effect also on the levels of p53 expression. Moreover, compound **52** was able to promote neurogenesis, as confirmed by the induced expression of recognized markers of neurogenesis such as GAP43, N-myc, and MAP-2, and it had an immunomodulatory activity on microglia, producing a shift from neurotoxic to neuroprotective phenotype. Starting from 50 μM, a clear effect on zebrafish development was also observed and correlated to the inhibition of GSK-3β. Although additional studies have to be assessed, the profile of compound **52**, coupled with its low MW and high solubility, make it a promising hit compound for the development of innovative AD-modifying agents.

Kaur et al. identified two series of triazole-based compounds (**53** and **54**, Figure 17) which are able to address four of the major AD hallmarks, including Aβ aggregation, metal-induced Aβ aggregation, metal dyshomeostasis, and oxidative stress [129, 130]. These analogues resulted from the combination of a hydrophobic part, namely the substituted phenyl rings, which are responsible for the contacts with the Aβ peptide and the antiaggregation effect, and a metal chelator part, involving the ditriazole moiety, able to

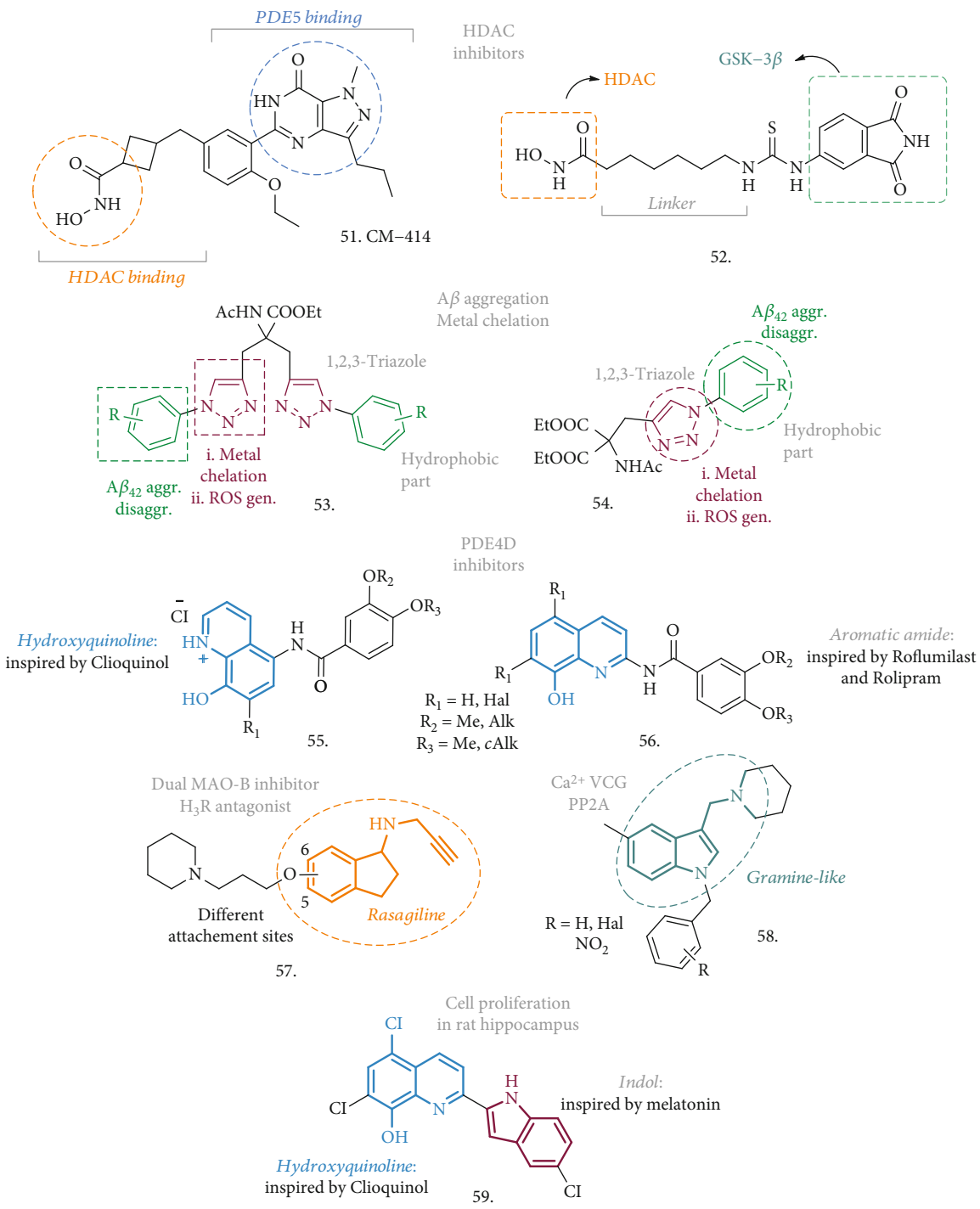

Figure 17: General structures of novel MTDLs to treat AD whose actions are not related to their activities on ChEs or BACE-1 enzymes.

modulate copper-mediated Aβ_{42} aggregation and reduce the oxidative stress.

Amongst the triazole-bearing compounds with general structure **53**, the R=*o*-CF_3 substituted analogue was the best performer of the series and displayed the most potent inhibitory activity against self-mediated Aβ_{42} aggregation in the ThT fluorescence binding assay, with an IC_{50} of 8.065 μM (even better than the reference curcumin). The significantly reduced formation of Aβ_{42} fibrils was also confirmed by TEM assay. Moreover, the coincubation of preformed fibrils with a 40 μM solution of this agent for 24 h had the capability of reducing the amount of Aβ fibrils in the TEM assay, highlighting a disruptive effect on preformed Aβ_{42} fibrils. The compound also showed metal-chelating ability, as assessed by UV-Vis spectroscopy, thus inhibiting Cu^{2+}-induced Aβ_{42} aggregation and promoting the disaggregation of Cu^{2+}-induced Aβ_{42} fibrils at a concentration of 40 μM. Furthermore, the multifunctional ligand influenced the

generation of ROS by preventing the copper redox cycle in a Cu-ascorbate redox system. The compound was not cytotoxic and did not influence the viability in SH-SY5Y cells in concentrations of up to 50 μM. Noteworthy, it was also able to inhibit the toxicity induced by Aβ_{42} aggregates in the same neuronal cell line. Taken together, all these activities make this compound a promising neuroprotective candidate, worthy of further *in vitro*/*in vivo* investigation.

The use of diethyl acetamidomalonate to build up a 1,2,3-triazole core (the metal-chelating part), *N*-linked to the substituted phenyl groups (the hydrophobic part), led to compounds with general structure **54**, which were meant to interact with the hydrophobic pocket of Aβ aggregates. The 2-iodophenyl group was the best performing in the ThT assay, inhibiting Aβ_{42} self-aggregation by 78% with an IC_{50} = 4.6 μM, as also confirmed by TEM analysis. In addition, this analogue was able to disaggregate preformed fibrils at a concentration of 20 μM. When tested for its metal-chelating characteristic, it resulted in being able to complex Cu^{2+} in a 2 : 1 stoichiometry and this maintained the metal in a redox-inert state preventing the production of ROS. Also the effect on Cu-mediated Aβ aggregation was evaluated, and while the presence of Cu alone increased the formation of Aβ_{42} fibrils, the treatment with the selected compound was followed by its drastic decrease. The same disruptive effect was observed on preformed fibrils whose precipitation was induced by the presence of the metal. The compound had no effect on SH-SY5Y neuronal cell viability whilst it could increase the same viability by up to 78% at 50 μM after Aβ-induced toxic insult. Hence, there is plenty of evidences to state that these structures could substantially contribute to the discovery of novel MTDLs, acting on the principal hallmarks of AD and thus endowed with neuroprotective effects.

A nice example of PDE inhibitors coupled with a multifaceted activity against Aβ-induced toxicity and metal-chelating/antioxidant properties came from the work of Hu et al. (**55** and **56**, Figure 17) [131]. They proposed hybrid compounds merging the metal ion chelating framework of chloroquine and the key binding site fragments of the known PDE4 inhibitors Rolipram and Roflumilast, already tested in preclinical models of AD [132] (see also NCT01433666 and NCT02051335). The result was a series of novel (halo)-hydroxyquinolines linked via an amidic bond to di-alkoxy-substituted aryls, which resulted to be a μM inhibitor of PDE4D. Differently from the reference compounds, these analogues exerted a good antioxidant activity in the ORAC assay (comparable to Clioquinol) and showed the ability to chelate metals, including Cu^{2+}, Zn^{2+}, and $Fe^{2+/3+}$, with a stoichiometry of 2 : 1 ligand : metal in the case of Cu^{2+}. The PAMPA test assessed the potential of these analogues to be brain penetrant and cross the BBB, thus prompting the author to perform further analysis. In the Cu^{2+}-ascorbate system, no significant production of ROS was observed after coincubation with the compounds, preventing Cu redox by metal chelation. A similar effect was observed in SH-SY5Y cells where besides the lack of a cytotoxic effect, there was a concentration-dependent protective effect against BuOOH-induced intracellular oxidative stress. The effects on metal-induced Aβ aggregation were evaluated, and both the ThT and TEM analysis confirmed that title compounds influenced Cu-induced aggregation. Being safe up to 2000 mg/kg dose and relatively stable in liver microsomes, some compounds were also tested *in vivo* in the Morris water maze test, performed with mice affected by A$\beta_{25\text{-}35}$-induced cognitive dysfunction. Compared to the reference PDE inhibitors, the results indicated an enhancement in cognitive spatial memory and behavioral performances, in addition to a protecting effect on hippocampal neurons. Clearly, these structures represent promising candidates for the development of a novel class of anti-AD agents.

As already discussed, the combination of the cholinesterase inhibitory activity with the MAO inhibition may represent an attractive approach to treat some neurodegenerative diseases, such as PD or AD. In a similar manner, the combination of MAO inhibitors with histamine receptor H_3R antagonists may open up the way for the development of interesting MTDLs [133]. To this extent, two compounds arising from the combination of the 3-piperidinopropyloxy moiety with Rasagiline (MAO inhibitor) have been proposed by Stark et al. (**57**, Figure 17), with the only structural difference represented by the anchoring point on the aminoindane skeleton. The two analogues showed low nanomolar affinity for H_3R, and only the 5-linked one had inhibitory activity on MAO-B in the nanomolar range, thus demonstrating a preference for linear vs. branched structures. This compound had also a preference for H_3R over H_1R and H_4R and dopamine D2 and D3 receptor subtypes. Moreover, both of the structures showed low cytotoxicity in neuroblastoma cells and were optimal candidates endowed with drug-like properties. No further evaluations were performed, not even regarding the chiral nature of the compounds and the possible separation of the two enantiomers. However, there is a relevant perspective for these analogues to serve as lead structures for the design of MTDLs useful in the treatment of neurodegenerative diseases.

In the search for agents targeting AD-inducing processes, a new class of compounds acting on Ca^{2+} VGC and preventing the inhibition of phosphatase 2A (PP2A) has been reported (**58**, Figure 17) [134]. As already observed, Ca^{2+} overload due to an altered VGC opening is common in several neurodegenerative diseases [70], but PP2A downregulation has also been linked to the progression of AD [135], since this enzyme plays a role in the phosphorylation of pTAU. Inspired by the structure of natural alkaloid Gramine, whose derivatives have already been evaluated as a potential treatment for neurodegenerative disease [136], Gonzales et al. used the indole core to create a new series of *N*-benzyl-substituted compounds able to prevent PP2A inhibition and Ca^{2+} overload. The preincubation of these analogues with SH-SY5Y cells subjected to high K^+ concentration prevented the cytosolic increase of Ca^{2+}, proving the blockade effect on cell depolarization and VGC opening, and showing IC_{50} values ranging from 1.8 to 4.8 μM. A mild antagonist effect was also reported on NMDA receptors in rat cortical embryonic neurons, even if this may be ascribed

to an indirect interaction with PP2A. In fact, this latter can form stable complexes with NMDA receptors [137], leading to receptor dephosphorylation and desensitization, with a lower influx of Ca^{2+}. To demonstrate this hypothesis, PP2A activity in SH-SY5Y cells treated with okadaic acid (a known PP2A inhibitor) was evaluated, as this represent a common AD model to study PP2A dysfunction and to assess the effects of the new compounds on restoring the enzyme activity. The loss in PP2A activity was prevented by pre- and coincubation with most of the compounds at 0.1 μM, confirming their ability to act as PP2A-activating drugs. At the same time, okadaic acid had a detrimental effect on cell viability and the treatment with these agents increased SH-SY5Y cell viability up to an extent of 70%, resulting nontoxic *per se* at concentrations 30-fold higher than the one necessary to induce neuroprotection. All these results confirmed how this pharmacological combination could represent a valuable tool to address AD-related dementia.

A very detailed research involving several quinoline-indole-based derivatives pointed out the ability of these compounds in promoting cell proliferation in the adult murine hippocampus, as a result of their neuroprotective effect against Aβ-related toxicity and oxidative stress [138]. Although there would be more than one analogue that may be worthy of investigation, the optimized compound **59** (Figure 17) has been identified as the most promising candidate of the series and arose from the combination of the Clioquinol structure with the substituted indole fragment. The ORAC-FL test revealed that the compound had higher antioxidant efficacy (ORAC value = 5.0) compared to Clioquinol, and the PAMPA assay confirmed the potential to be BBB penetrant by passive diffusion. In the ThT assay for $A\beta_{1\text{-}42}$ self-induced aggregation, it showed higher inhibitory activity than parent and reference compounds and it had a significant effect in disaggregating preformed fibrils. The new derivative was able to chelate Cu^{2+}, Zn^{2+}, Fe^{2+}, and Fe^{3+} generating Cu^{2+}/compound complexes in a 1 : 2 stoichiometry. Following this chelating potential, the effect on metal-induced Aβ aggregation was also evaluated, demonstrating a substantial rate of inhibition for Cu^{2+}-associated Aβ-aggregation and disaggregation of Cu^{2+}-promoted preformed fibrils. The compound had no neurotoxicity in the PC12 cell line in concentrations of up to 50 μM, but rather revealed the ability to increase the number of cells, possibly via a MAPK-dependent mechanism. There was also a clear effect in reducing the production of ROS in SH-SY5Y stimulated cells. The HCl salt formulation displayed a considerable metabolic stability in liver microsomes ($T_{1/2}$ = 116 min), and no acute toxicity or significant alteration was observed in adult C57BL/6 mice (up to 2000 mg/kg). In the same animal model, following ICV injection of the hydrochloride salt, there was a clear effect in inducing hippocampal cell proliferation from the reservoirs of neuronal stem cells in the subgranular zone, and from the neural precursor in other hippocampus regions, as confirmed by immunohistochemical analysis of the mice brains. Double transgenic APP/PS1 mice (a model of AD) were used to assess the cognitive and memory strengthening effect in the Morris water maze test, where the treatment with the compound demonstrated a significant amelioration of memory impairment and cognitive dysfunctions. Daily doses of 30 mg/kg were safe and well tolerated, and the chronic oral treatment also lead to a remarkable reduction in Aβ plaque deposition, in correlation with the positive effects on learning and memory. In conclusion, this analogue is a nice example of an MTDL with optimal *in vitro* properties and proven *in vivo* activity which makes it an attractive agent to be further pursued for AD treatment.

2.12. The Role of Synthetic Peptides in AD. Although the use of small molecules as MTDLs is the most common approach towards the discovery of new treatments for AD, it may be interesting to spend a few words on the role of synthetic peptides as novel agents against AD. Aβ oligomers, protofibrils, and prefibrillar aggregates are pivotal players in the toxic insult leading to brain damage. Other neurodegenerative disorders, such as ALS, prior disease, or HD, are characterized by the aggregation of misfolded proteins. Synthetic peptides offer the possibility to modulate this process by interacting with endogenous peptides or interfering with protein aggregation. In the past decades, the use of peptide-based drugs has emerged as a valuable tool to treat different pathologies [139–141] and increasing interest has been paid to their effects as disease-modifying tools. They can also serve as probes and diagnostic tools for an early diagnosis or discovery of neurodegeneration [142]. Potential targets for peptide-based therapies could be the cognitive impairment (e.g., neuroprotective effect of insulin) or the modulation of Aβ formation and aggregation through protein-protein-like interactions. These peptides can be either natural or modified Aβ derivatives, capable of interfering with the Aβ structure and aggregates, and/or bearing nonnatural amino acids, which have already proven their ability of inhibiting Aβ aggregation and attenuating mild cognitive impairments [143]. Nevertheless, these agents have to penetrate in the brain; thus, they have to be evaluated for their ability to cross BBB and reach their targets. Interestingly, some oligopeptides have already shown significant effects in animal models of dementia [144] and an even narrowed set has been progressed into clinical studies [143]. Despite the fact that they may not perfectly fall under the definition of MTDLs, synthetic peptides have the potential to hit or modulate multiple targets associated with AD dysfunctions, and thanks to their versatility, they can also serve as disease-modifying agents, giving new perspectives and opportunities in the search for novel AD treatments.

3. Conclusions

The multifaceted and complex nature of AD has triggered tremendous research efforts towards developing multitarget therapeutic strategies. These strategies are mainly developed to target multiple factors involved in the progression of AD such as mitochondrial dysfunction, deposition of amyloid aggregates in the brain, oxidative stress, and altered brain glucose metabolism. This review focused on the development of small molecules that were rationally designed to interact with multiple targets directly related to the etiology of AD.

In addition, structural modification of the lead compounds enabled introduction of key features such as metal chelation and antioxidant and anti-inflammatory activities which have proven to be beneficial properties in the identification of potential therapeutics of AD. The design of dual inhibitors of enzymes involved in the progression of AD is one of the most common strategies implicated in the development of MTDLs. Inhibitors of ChEs have been widely used in the design of dual enzyme inhibitors mainly through molecular hybridization. The majority of research in this area focused on using scaffolds of AD drugs such as THA and Donepezil with reported ChE inhibitory activity. Hybridization with scaffolds with known inhibitory activities against GSK-3β, MAOs, PARP-1, and PDEs have resulted in multiple examples of MTDLs. Similarly, hybridization of ChEs with NMDA receptor antagonists as well as 5-HT_6R antagonists evolved as a promising approach for the development of MTDLs. BACE-1-centered MTDLs have received growing attention from researchers in the previous years. Numerous MTDLs have been reported that combine BACE-1 inhibition with anti-inflammatory and antioxidant properties.

The unfavorable pharmacokinetic properties of reported MTDLs remain to be the main barrier for further clinical translation of these compounds. Thus, efforts focusing on optimizing oral bioavailability, metabolic clearance, and CNS permeation of lead compounds would be critical in advancing more MTDLs into clinical trials. Moreover, MTDLs that are designed to target different pathological cascades of AD are more likely to be efficient against multifactorial AD in comparison to MTDLs designed against a single pathway of AD progression.

Conflicts of Interest

The authors declare that they have no conflicts of interest.

References

[1] "Dementia," Sep-2019 https://www.who.int/news-room/fact-sheets/detail/dementia.

[2] M. G. Savelieff, S. Lee, Y. Liu, and M. H. Lim, "Untangling amyloid-β, tau, and metals in Alzheimer's disease," *ACS Chemical Biology*, vol. 8, no. 5, pp. 856–865, 2013.

[3] H. Braak and K. Del Tredici, "Alzheimer's disease: pathogenesis and prevention," *Alzheimer's & Dementia*, vol. 8, no. 3, pp. 227–233, 2012.

[4] P. Sweeney, H. Park, M. Baumann et al., "Protein misfolding in neurodegenerative diseases: implications and strategies," *Translational Neurodegeneation*, vol. 6, no. 1, 2017.

[5] L. V. Kalia and A. E. Lang, "Parkinson's disease," *The Lancet*, vol. 386, no. 9996, pp. 896–912, 2015.

[6] R. H. Brown and A. Al-Chalabi, "Amyotrophic lateral sclerosis," *The New England Journal of Medicine*, vol. 377, no. 2, pp. 162–172, 2017.

[7] L. Sokoloff, "Energetics of functional activation in neural tissues," *Neurochemical Research*, vol. 24, no. 2, pp. 321–329, 1999.

[8] D. Praticò, "Oxidative stress hypothesis in Alzheimer's disease: a reappraisal," *Trends in Pharmacological Sciences*, vol. 29, no. 12, pp. 609–615, 2008.

[9] A. Federico, E. Cardaioli, P. Da Pozzo, P. Formichi, G. N. Gallus, and E. Radi, "Mitochondria, oxidative stress and neurodegeneration," *Journal of the Neurological Sciences*, vol. 322, no. 1-2, pp. 254–262, 2012.

[10] M. H. Yan, X. Wang, and X. Zhu, "Mitochondrial defects and oxidative stress in Alzheimer disease and Parkinson disease," *Free Radical Biology & Medicine*, vol. 62, pp. 90–101, 2013.

[11] R. von Bernhardi and J. Eugenín, "Alzheimer's disease: redox dysregulation as a common denominator for diverse pathogenic mechanisms," *Antioxidants & Redox Signaling*, vol. 16, no. 9, pp. 974–1031, 2012.

[12] M. A. Greenough, J. Camakaris, and A. I. Bush, "Metal dyshomeostasis and oxidative stress in Alzheimer's disease," *Neurochemistry International*, vol. 62, no. 5, pp. 540–555, 2013.

[13] L. Breydo, J. W. Wu, and V. N. Uversky, "α-Synuclein misfolding and Parkinson's disease," *Biochimica et Biophysica Acta (BBA) - Molecular Basis of Disease*, vol. 1822, no. 2, pp. 261–285, 2012.

[14] G. Candore, M. Bulati, C. Caruso et al., "Inflammation, cytokines, immune response, apolipoprotein E, cholesterol, and oxidative stress in Alzheimer disease: therapeutic implications," *Rejuvenation Research*, vol. 13, no. 2-3, pp. 301–313, 2010.

[15] Y.-J. Lee, S. B. Han, S.-Y. Nam, K.-W. Oh, and J. T. Hong, "Inflammation and Alzheimer's disease," *Archives of Pharmacal Research*, vol. 33, no. 10, pp. 1539–1556, 2010.

[16] M. Rosini, E. Simoni, A. Milelli, A. Minarini, and C. Melchiorre, "Oxidative stress in Alzheimer's disease: are we connecting the dots?," *Journal of Medicinal Chemistry*, vol. 57, no. 7, pp. 2821–2831, 2014.

[17] B. Ibach and E. Haen, "Acetylcholinesterase inhibition in Alzheimer's disease," *Current Pharmaceutical Design*, vol. 10, no. 3, pp. 231–251, 2004.

[18] M. Bond, G. Rogers, J. Peters et al., "The effectiveness and cost-effectiveness of Donepezil, Galantamine, Rivastigmine and Memantine for the treatment of Alzheimer's disease (review of technology appraisal no. 111): a systematic review and economic model," *Health Technology Assessment*, vol. 16, no. 21, pp. 1–470, 2012.

[19] D. J. Ames, P. S. Bhathal, B. M. Davies, and J. R. E. Fraser, "HEPATOTOXICITY OF TETRAHYDROACRIDINE," *Lancet*, vol. 331, no. 8590, p. 887, 1988.

[20] R. E. Hughes, K. Nikolic, and R. R. Ramsay, "One for all? Hitting multiple Alzheimer's disease targets with one drug," *Frontiers in Neuroscience*, vol. 10, 2016.

[21] F. Mesiti, D. Chavarria, A. Gaspar, S. Alcaro, and F. Borges, "The chemistry toolbox of multitarget-directed ligands for Alzheimer's disease," *European Journal of Medicinal Chemistry*, vol. 181, article 111572, 2019.

[22] S. Butini, M. Brindisi, S. Brogi et al., "Multifunctional cholinesterase and amyloid beta fibrillization modulators. Synthesis and biological investigation," *ACS Medicinal Chemistry Letters*, vol. 4, no. 12, pp. 1178–1182, 2013.

[23] S. Brogi, S. Butini, S. Maramai et al., "Disease-modifying anti-Alzheimer's drugs: inhibitors of human cholinesterases interfering with β-amyloid aggregation," *CNS Neuroscience and Therapeutics*, vol. 20, no. 7, pp. 624–632, 2014.

[24] L. Ismaili, B. Refouvelet, M. Benchekroun et al., "Multitarget compounds bearing tacrine- and donepezil-like structural and functional motifs for the potential treatment of

Alzheimer's disease," *Progress in Neurobiology*, vol. 151, pp. 4–34, 2017.

[25] M. Unzeta, G. Esteban, I. Bolea et al., "Multi-target directed donepezil-like ligands for Alzheimer's disease," *Frontiers in Neuroscience*, vol. 10, 2016.

[26] G. Mazzanti and S. Di Giacomo, "Curcumin and resveratrol in the management of cognitive disorder: what is the clinical evidence?," *Molecules*, vol. 21, no. 9, p. 1243, 2016.

[27] T. H. Ferreira-Vieira, I. M. Guimaraes, F. R. Silva, and F. M. Ribeiro, "Alzheimer's disease: targeting the cholinergic system," *Current Neuropharmacology*, vol. 14, no. 1, pp. 101–115, 2016.

[28] G. A. Reid, N. Chilukuri, and S. Darvesh, "Butyrylcholinesterase and the cholinergic system," *Neuroscience*, vol. 234, pp. 53–68, 2013.

[29] N. C. Inestrosa, M. C. Dinamarca, and A. Alvarez, "Amyloid-cholinesterase interactions," *FEBS Journal*, vol. 275, no. 4, pp. 625–632, 2008.

[30] J. R. M. Coimbra, D. F. F. Marques, S. J. Baptista et al., "Highlights in BACE1 inhibitors for Alzheimer's disease treatment," *Frontiers in Chemistry*, vol. 6, 2018.

[31] M. T. Gabr and M. S. Abdel-Raziq, "Structure-based design, synthesis, and evaluation of structurally rigid donepezil analogues as dual AChE and BACE-1 inhibitors," *Bioorganic & Medicinal Chemistry Letters*, vol. 28, no. 17, pp. 2910–2913, 2018.

[32] F. Jeppsson, S. Eketjäll, J. Janson et al., "Discovery of AZD3839, a potent and selective BACE1 inhibitor clinical candidate for the treatment of Alzheimer disease," *The Journal of Biological Chemistry*, vol. 287, no. 49, pp. 41245–41257, 2012.

[33] M. T. Gabr and M. S. Abdel-Raziq, "Design and synthesis of donepezil analogues as dual AChE and BACE-1 inhibitors," *Bioorganic Chemistry*, vol. 80, pp. 245–252, 2018.

[34] P. Sharma, A. Tripathi, P. N. Tripathi et al., "Design and development of multitarget-directed _N_ -Benzylpiperidine analogs as potential candidates for the treatment of Alzheimer's disease," *European Journal of Medicinal Chemistry*, vol. 167, pp. 510–524, 2019.

[35] E. Beurel, S. F. Grieco, and R. S. Jope, "Glycogen synthase kinase-3 (GSK3): regulation, actions, and diseases," *Pharmacology & Therapeutics*, vol. 148, pp. 114–131, 2015.

[36] J. Avila, F. Wandosell, and F. Hernández, "Role of glycogen synthase kinase-3 in Alzheimer's disease pathogenesis and glycogen synthase kinase-3 inhibitors," *Expert Review of Neurotherapeutics*, vol. 10, no. 5, pp. 703–710, 2014.

[37] Z. Cai, Y. Zhao, and B. Zhao, "Roles of glycogen synthase kinase 3 in Alzheimer's disease," *Current Alzheimer Research*, vol. 9, no. 7, pp. 864–879, 2012.

[38] M. Llorens-Martín, J. Jurado, F. Hernández, and J. Avila, "GSK-3Î², a pivotal kinase in Alzheimer disease," *Frontiers in Molecular Neuroscience*, vol. 7, 2014.

[39] P. Sivaprakasam, X. Han, R. L. Civiello et al., "Discovery of new acylaminopyridines as GSK-3 inhibitors by a structure guided in-depth exploration of chemical space around a pyrrolopyridinone core," *Bioorganic & Medicinal Chemistry Letters*, vol. 25, no. 9, pp. 1856–1863, 2015.

[40] X. Y. Jiang, T. K. Chen, J. T. Zhou et al., "Dual GSK-3β/AChE inhibitors as a new strategy for multitargeting anti-Alzheimer's disease drug discovery," *ACS Medicinal Chemistry Letters*, vol. 9, no. 3, pp. 171–176, 2018.

[41] K. Oukoloff, N. Coquelle, M. Bartolini et al., "Design, biological evaluation and X-ray crystallography of nanomolar multifunctional ligands targeting simultaneously acetylcholinesterase and glycogen synthase kinase-3," *European Journal of Medicinal Chemistry*, vol. 168, pp. 58–77, 2019.

[42] L. Dezsi and L. Vecsei, "Monoamine oxidase B inhibitors in Parkinson's disease," *CNS & Neurological Disorders Drug Targets*, vol. 16, no. 4, pp. 425–439, 2017.

[43] S. Schedin-Weiss, M. Inoue, L. Hromadkova et al., "Monoamine oxidase B is elevated in Alzheimer disease neurons, is associated with γ-secretase and regulates neuronal amyloid β-peptide levels," *Alzheimers Research & Therapy*, vol. 9, no. 1, p. 57, 2017.

[44] E. Borroni, B. Bohrmann, F. Grueninger et al., "Sembragiline: a novel, selective monoamine oxidase type B inhibitor for the treatment of Alzheimer's disease," *The Journal of Pharmacology and Experimental Therapeutics*, vol. 362, no. 3, pp. 413–423, 2017.

[45] Z. Sang, K. Wang, J. Shi, W. Liu, and Z. Tan, "Design, synthesis, in-silico and biological evaluation of novel chalcone- _O_ -carbamate derivatives as multifunctional agents for the treatment of Alzheimer's disease," *European Journal of Medicinal Chemistry*, vol. 178, pp. 726–739, 2019.

[46] X. Zhang, K. P. Rakesh, S. N. A. Bukhari, M. Balakrishna, H. M. Manukumar, and H. L. Qin, "Multi-targetable chalcone analogs to treat deadly Alzheimer's disease: Current view and upcoming advice," *Bioorganic Chemistry*, vol. 80, pp. 86–93, 2018.

[47] Y.-x. Xu, H. Wang, X.-k. Li et al., "Discovery of novel propargylamine-modified 4-aminoalkyl imidazole substituted pyrimidinylthiourea derivatives as multifunctional agents for the treatment of Alzheimer's disease," *European Journal of Medicinal Chemistry*, vol. 143, pp. 33–47, 2018.

[48] C. Bilir and C. Sarisozen, "Indoleamine 2,3-dioxygenase (IDO): only an enzyme or a checkpoint controller?," *Journal of Oncological Sciences*, vol. 3, no. 2, pp. 52–56, 2017.

[49] L. C. Souza, C. R. Jesse, M. S. Antunes et al., "Indoleamine-2,3-dioxygenase mediates neurobehavioral alterations induced by an intracerebroventricular injection of amyloid-$\beta_{1\text{-}42}$ peptide in mice," *Brain, Behavior, and Immunity*, vol. 56, pp. 363–377, 2016.

[50] G. Mazarei and B. R. Leavitt, "Indoleamine 2,3 dioxygenase as a potential therapeutic target in Huntington's disease," *Journal Huntington's Disease*, vol. 4, no. 2, pp. 109–118, 2015.

[51] D. J. Bonda, M. Mailankot, J. G. Stone et al., "Indoleamine 2,3-dioxygenase and 3-hydroxykynurenine modifications are found in the neuropathology of Alzheimer's disease," *Redox Report*, vol. 15, no. 4, pp. 161–168, 2013.

[52] X. Lu, S. He, Q. Li et al., "Investigation of multi-target-directed ligands (MTDLs) with butyrylcholinesterase (BuChE) and indoleamine 2,3-dioxygenase 1 (IDO1) inhibition: The design, synthesis of miconazole analogues targeting Alzheimer's disease," *Bioorganic & Medicinal Chemistry*, vol. 26, no. 8, pp. 1665–1674, 2018.

[53] U. F. Rohrig, S. R. Majjigapu, M. Chambon et al., "Detailed analysis and follow-up studies of a high-throughput screening for indoleamine 2,3-dioxygenase 1 (IDO1) inhibitors," *European Journal of Medicinal Chemistry*, vol. 84, pp. 284–301, 2014.

[54] C. Z. Gao, W. Dong, Z. W. Cui et al., "Synthesis, preliminarily biological evaluation and molecular docking study of new

Olaparib analogues as multifunctional PARP-1 and cholinesterase inhibitors," *Journal of Enzyme Inhibition and Medicinal Chemistry*, vol. 34, no. 1, pp. 150–162, 2019.

[55] Y. Q. Wang, P. Y. Wang, Y. T. Wang, G. F. Yang, A. Zhang, and Z. H. Miao, "An update on poly(ADP-ribose)polymerase-1 (PARP-1) inhibitors: opportunities and challenges in cancer therapy," *Journal of Medicinal Chemistry*, vol. 59, no. 21, pp. 9575–9598, 2016.

[56] S. Martire, L. Mosca, and M. d'Erme, "PARP-1 involvement in neurodegeneration: A focus on Alzheimer's and Parkinson's diseases," *Mechanisms of Ageing and Development*, vol. 146-148, pp. 53–64, 2015.

[57] R. Scott Bitner, "Cyclic AMP response element-binding protein (CREB) phosphorylation: a mechanistic marker in the development of memory enhancing Alzheimer's disease therapeutics," *Biochemical Pharmacology*, vol. 83, no. 6, pp. 705–714, 2012.

[58] K. S. Kroker, C. Mathis, A. Marti, J. C. Cassel, H. Rosenbrock, and C. Dorner-Ciossek, "PDE9A inhibition rescues amyloid beta-induced deficits in synaptic plasticity and cognition," *Neurobiology of Aging*, vol. 35, no. 9, pp. 2072–2078, 2014.

[59] P. H. Hutson, E. N. Finger, B. C. Magliaro et al., "The selective phosphodiesterase 9 (PDE9) inhibitor PF-04447943 (6-[(3S,4S)-4-methyl-1-(pyrimidin-2-ylmethyl)pyrrolidin-3-yl]-1-(tetrahydro-2H-pyran-4-yl)-1,5-dihydro-4H-pyrazolo[3,4-d]pyrimidin-4-one) enhances synaptic plasticity and cognitive function in rodents," *Neuropharmacology*, vol. 61, no. 4, pp. 665–676, 2011.

[60] J. Hu, Y. D. Huang, T. Pan et al., "Design, synthesis, and biological evaluation of dual-target inhibitors of acetylcholinesterase (AChE) and phosphodiesterase 9A (PDE9A) for the treatment of Alzheimer's disease," *ACS Chemical Neuroscience*, vol. 10, no. 1, pp. 537–551, 2018.

[61] M. Huang, Y. Shao, J. Hou et al., "Structural asymmetry of phosphodiesterase-9A and a unique pocket for selective binding of a potent enantiomeric inhibitor," *Molecular Pharmacology*, vol. 88, no. 5, pp. 836–845, 2015.

[62] Y. F. Yu, Y. D. Huang, C. Zhang et al., "Discovery of novel pyrazolopyrimidinone derivatives as phosphodiesterase 9A inhibitors capable of inhibiting butyrylcholinesterase for treatment of Alzheimer's disease," *ACS Chemical Neuroscience*, vol. 8, no. 11, pp. 2522–2534, 2017.

[63] K. B. Hansen, F. Yi, R. E. Perszyk et al., "Structure, function, and allosteric modulation of NMDA receptors," *The Journal of General Physiology*, vol. 150, no. 8, pp. 1081–1105, 2018.

[64] E. J. Kodis, S. Choi, E. Swanson, G. Ferreira, and G. S. Bloom, "N-Methyl-D-aspartate receptor-mediated calcium influx connects amyloid-β oligomers to ectopic neuronal cell cycle reentry in Alzheimer's disease," *Alzheimer's & Dementia*, vol. 14, no. 10, pp. 1302–1312, 2018.

[65] R. Wang and P. H. Reddy, "Role of glutamate and NMDA receptors in Alzheimer's disease," *Journal of Alzheimer's Disease*, vol. 57, no. 4, pp. 1041–1048, 2017.

[66] Y. Yabuki, K. Matsuo, K. Hirano, Y. Shinoda, S. Moriguchi, and K. Fukunaga, "Combined memantine and donepezil treatment improves behavioral and psychological symptoms of dementia-like behaviors in olfactory bulbectomized mice," *Pharmacology*, vol. 99, no. 3-4, pp. 160–171, 2017.

[67] P. T. Francis, C. G. Parsons, and R. W. Jones, "Rationale for combining glutamatergic and cholinergic approaches in the symptomatic treatment of Alzheimer's disease," *Expert Review of Neurotherapeutics*, vol. 12, no. 11, pp. 1351–1365, 2014.

[68] S. L. Greig, "Memantine ER/donepezil: a review in Alzheimer's disease," *CNS Drugs*, vol. 29, no. 11, pp. 963–970, 2015.

[69] F. J. Pérez-Areales, A. L. Turcu, M. Barniol-Xicota et al., "A novel class of multitarget anti-Alzheimer benzohomoadamantane–chlorotacrine hybrids modulating cholinesterases and glutamate NMDA receptors," *European Journal of Medicinal Chemistry*, vol. 180, pp. 613–626, 2019.

[70] V. Nimmrich and A. Eckert, "Calcium channel blockers and dementia," *British Journal of Pharmacology*, vol. 169, no. 6, pp. 1203–1210, 2013.

[71] M. Chioua, E. Buzzi, I. Moraleda et al., "Tacripyrimidines, the first tacrine-dihydropyrimidine hybrids, as multi-target-directed ligands for Alzheimer's disease," *European Journal of Medicinal Chemistry*, vol. 155, pp. 839–846, 2018.

[72] D. Švob Štrac, N. Pivac, and D. Mück-Šeler, "The serotonergic system and cognitive function," *Translational Neuroscience*, vol. 7, no. 1, pp. 35–49, 2016.

[73] W. J. Geldenhuys and C. J. Van der Schyf, "Role of serotonin in Alzheimer's disease: a new therapeutic target?," *CNS Drugs*, vol. 25, no. 9, pp. 765–781, 2011.

[74] S. Claeysen, J. Bockaert, and P. Giannoni, "Serotonin: a new hope in Alzheimer's disease?," *ACS Chemical Neuroscience*, vol. 6, no. 7, pp. 940–943, 2015.

[75] H. Hagena and D. Manahan-Vaughan, "The serotonergic 5-HT4 receptor: a unique modulator of hippocampal synaptic information processing and cognition," *Neurobiology of Learning and Memory*, vol. 138, pp. 145–153, 2017.

[76] F. Lezoualc'h, "5-HT_4 receptor and Alzheimer's disease: The amyloid connection," *Experimental Neurology*, vol. 205, no. 2, pp. 325–329, 2007.

[77] M. J. Ramírez, "5-HT6 receptors and Alzheimer's disease," *Alzheimers Research & Therapy*, vol. 5, no. 2, p. 15, 2013.

[78] M. Andrews, B. Tousi, and M. N. Sabbagh, "5HT6 antagonists in the treatment of Alzheimer's dementia: current progress," *Neurology & Therapy*, vol. 7, no. 1, pp. 51–58, 2018.

[79] C. Lecoutey, D. Hedou, T. Freret et al., "Design of donecopride, a dual serotonin subtype 4 receptor agonist/acetylcholinesterase inhibitor with potential interest for Alzheimer's disease treatment," *Proceedings of the National. Academy of Sciences*, vol. 111, no. 36, pp. E3825–E3830, 2014.

[80] C. Rochais, C. Lecoutey, F. Gaven et al., "Novel multitarget-directed ligands (MTDLs) with acetylcholinesterase (AChE) inhibitory and serotonergic subtype 4 receptor (5-HT4R) agonist activities as potential agents against Alzheimer's disease: the design of donecopride," *Journal of Medicinal Chemistry*, vol. 58, no. 7, pp. 3172–3187, 2015.

[81] B. Hatat, S. Yahiaoui, C. Lecoutey et al., "A novel in vivo anti-amnesic agent, specially designed to express both acetylcholinesterase (AChE) inhibitory, serotonergic subtype 4 receptor (5-HT4R) agonist and serotonergic subtype 6 receptor (5-HT6R) inverse agonist activities, With a Potential Interest Against Alzheimer's Disease," *Frontiers in Aging Neuroscience*, vol. 11, 2019.

[82] S. Yahiaoui, K. Hamidouche, C. Ballandonne et al., "Design, synthesis, and pharmacological evaluation of multitarget-directed ligands with both serotonergic subtype 4 receptor (5-HT4R) partial agonist and 5-HT6R antagonist activities, as potential treatment of Alzheimer's disease," *European Journal of Medicinal Chemistry*, vol. 121, pp. 283–293, 2016.

[83] M. Marcinkowska, A. Bucki, D. Panek et al., "Anti-Alzheimer's multitarget-directed ligands with serotonin 5-HT6antagonist, butyrylcholinesterase inhibitory, and antioxidant activity," *Archiv der Pharmazie*, vol. 352, no. 7, article 1900041, 2019.

[84] A. Więckowska, T. Wichur, J. Godyń et al., "Novel multitarget-directed ligands aiming at symptoms and causes of Alzheimer's disease," *ACS Chemical Neuroscience*, vol. 9, no. 5, pp. 1195–1214, 2018.

[85] M. Kołaczkowski, M. Marcinkowska, A. Bucki et al., "Novel 5-HT_6 receptor antagonists/D_2 receptor partial agonists targeting behavioral and psychological symptoms of dementia," *European Journal of Medicinal Chemistry*, vol. 92, pp. 221–235, 2015.

[86] J. M. Singer, M. W. Wilson, P. D. Johnson et al., "Synthesis and SAR of tolylamine 5-HT_6 antagonists," *Bioorganic & Medicinal Chemistry Letters*, vol. 19, no. 9, pp. 2409–2412, 2009.

[87] T. A. Esbenshade, K. E. Browman, R. S. Bitner, M. Strakhova, M. D. Cowart, and J. D. Brioni, "The histamine H3 receptor: an attractive target for the treatment of cognitive disorders," *British Journal of Pharmacology*, vol. 154, no. 6, pp. 1166–1181, 2008.

[88] G. Nieto-Alamilla, R. Márquez-Gómez, A. M. García-Gálvez, G. E. Morales-Figueroa, and J. A. Arias-Montaño, "The histamine H3 receptor: structure, pharmacology, and function," *Molecular Pharmacology*, vol. 90, no. 5, pp. 649–673, 2016.

[89] J. D. Brioni, T. A. Esbenshade, T. R. Garrison, S. R. Bitner, and M. D. Cowart, "Discovery of Histamine H3Antagonists for the Treatment of Cognitive Disorders and Alzheimer's Disease," *The Journal of Pharmacology and Experimental Therapeutics*, vol. 336, no. 1, pp. 38–46, 2010.

[90] L. Nguyen, B. P. Lucke-Wold, S. Mookerjee, N. Kaushal, and R. R. Matsumoto, "Sigma-1 receptors and neurodegenerative diseases: towards a hypothesis of sigma-1 receptors as amplifiers of neurodegeneration and neuroprotection," *Advances in Experimental Medicine and Biology*, vol. 964, pp. 133–152, 2017.

[91] D. A. Ryskamp, S. Korban, V. Zhemkov, N. Kraskovskaya, and I. Bezprozvanny, "Neuronal sigma-1 receptors: signaling functions and protective roles in neurodegenerative diseases," *Frontiers in Neuroscience*, vol. 13, p. 862, 2019.

[92] J. L. Jin, M. Fang, Y. X. Zhao, and X. Y. Liu, "Roles of sigma-1 receptors in Alzheimer's disease," *International Journal of Clinical and Experimental Medicine*, vol. 8, no. 4, pp. 4808–4820, 2015.

[93] D. Wang, M. Hu, X. Li et al., "Design, synthesis, and evaluation of isoflavone analogs as multifunctional agents for the treatment of Alzheimer's disease," *European Journal of Medicinal Chemistry*, vol. 168, pp. 207–220, 2019.

[94] J. Lalut, G. Santoni, D. Karila et al., "Novel multitarget-directed ligands targeting acetylcholinesterase and σ_1 receptors as lead compounds for treatment of Alzheimer's disease: Synthesis, evaluation, and structural characterization of their complexes with acetylcholinesterase," *European Journal of Medicinal Chemistry*, vol. 162, pp. 234–248, 2019.

[95] N. Battista, M. Di Tommaso, M. Bari, and M. Maccarrone, "The endocannabinoid system: an overview," *Frontiers in Behavioral Neuroscience*, vol. 6, 2012.

[96] B. F. Cravatt, D. K. Giang, S. P. Mayfield, D. L. Boger, R. A. Lerner, and N. B. Gilula, "Molecular characterization of an enzyme that degrades neuromodulatory fatty- acid amides," *Nature*, vol. 384, no. 6604, pp. 83–87, 1996.

[97] G. Labar, C. Bauvois, F. Borel, J. L. Ferrer, J. Wouters, and D. M. Lambert, "Crystal structure of the human monoacylglycerol lipase, a key actor in endocannabinoid signaling," *Chembiochem*, vol. 11, no. 2, pp. 218–227, 2010.

[98] K. M. Jung, G. Astarita, S. Yasar et al., "An amyloid β_{42}-dependent deficit in anandamide mobilization is associated with cognitive dysfunction in Alzheimer's disease," *Neurobiology of Aging*, vol. 33, no. 8, pp. 1522–1532, 2012.

[99] C. Benito, E. Núñez, R. M. Tolón et al., "Cannabinoid CB2 receptors and fatty acid amide hydrolase are selectively overexpressed in neuritic plaque-associated glia in Alzheimer's disease brains," *The Journal of Neuroscience*, vol. 23, no. 35, pp. 11136–11141, 2003.

[100] S. Butini, M. Brindisi, S. Gemma et al., "Discovery of potent inhibitors of human and mouse fatty acid amide hydrolases," *Journal of Medicinal Chemistry*, vol. 55, no. 15, pp. 6898–6915, 2012.

[101] S. Butini, S. Gemma, M. Brindisi et al., "Identification of a novel arylpiperazine scaffold for fatty acid amide hydrolase inhibition with improved drug disposition properties," *Bioorganic & Medicinal Chemistry Letters*, vol. 23, no. 2, pp. 492–495, 2013.

[102] M. Brindisi, S. Brogi, S. Maramai et al., "Harnessing the pyrroloquinoxaline scaffold for FAAH and MAGL interaction: definition of the structural determinants for enzyme inhibition," *RSC Advances*, vol. 6, no. 69, pp. 64651–64664, 2016.

[103] M. Brindisi, G. Borrelli, S. Brogi et al., "Development of potent inhibitors of fatty acid amide hydrolase useful for the treatment of neuropathic pain," *ChemMedChem*, vol. 13, no. 19, pp. 2090–2103, 2018.

[104] V. Di Marzo and S. Petrosino, "Endocannabinoids and the regulation of their levels in health and disease," *Current Opinion in Lipidology*, vol. 18, no. 2, pp. 129–140, 2007.

[105] S. Montanari, L. Scalvini, M. Bartolini et al., "Fatty acid amide hydrolase (FAAH), acetylcholinesterase (AChE), and butyrylcholinesterase (BuChE): networked targets for the development of carbamates as potential anti-Alzheimer's disease agents," *Journal of Medicinal Chemistry*, vol. 59, no. 13, pp. 6387–6406, 2016.

[106] E. Nuñez-Borque, P. González-Naranjo, F. Bartolomé et al., "Targeting cannabinoid receptor activation and BACE-1 activity counteracts TgAPP mice memory impairment and Alzheimer's disease lymphoblast alterations," *Molecular Neurobiology*, vol. 57, no. 4, pp. 1938–1951, 2020.

[107] D. V. Patel, N. R. Patel, A. M. Kanhed et al., "Novel multitarget directed triazinoindole derivatives as anti-Alzheimer agents," *ACS Chemical Neuroscience*, vol. 10, no. 8, pp. 3635–3661, 2019.

[108] M. Wu, J. Ma, L. Ji, M. Wang, J. Han, and Z. Li, "Design, synthesis, and biological evaluation of rutacecarpine derivatives as multitarget-directed ligands for the treatment of Alzheimer's disease," *European Journal of Medicinal Chemistry*, vol. 177, pp. 198–211, 2019.

[109] J. M. Roldán-Peña, V. Romero-Real, J. Hicke et al., "Tacrine-_O_ -protected phenolics heterodimers as multitarget-directed ligands against Alzheimer's disease: Selective subnanomolar BuChE inhibitors," *European Journal of Medicinal Chemistry*, vol. 181, p. 111550, 2019.

[110] A. Iraji, O. Firuzi, M. Khoshneviszadeh et al., "Multifunctional iminochromene-2H-carboxamide derivatives containing different aminomethylene triazole with BACE1 inhibitory, neuroprotective and metal chelating properties targeting Alzheimer's disease," *European Journal of Medicinal Chemistry*, vol. 141, pp. 690–702, 2017.

[111] A. Iraji, O. Firuzi, M. Khoshneviszadeh, H. Nadri, N. Edraki, and R. Miri, "Synthesis and structure-activity relationship study of multi-target triazine derivatives as innovative candidates for treatment of Alzheimer's disease," *Bioorganic Chemistry*, vol. 77, pp. 223–235, 2018.

[112] M. Yazdani, N. Edraki, R. Badri, M. Khoshneviszadeh, A. Iraji, and O. Firuzi, "Multi-target inhibitors against Alzheimer disease derived from 3-hydrazinyl 1,2,4-triazine scaffold containing pendant phenoxy methyl-1,2,3-triazole: design, synthesis and biological evaluation," *Bioorganic Chemistry*, vol. 84, pp. 363–371, 2019.

[113] S. R. Sagar, D. P. Singh, N. B. Panchal et al., "Thiazolyl-thiadiazines as beta site amyloid precursor protein cleaving enzyme-1 (BACE-1) inhibitors and anti-inflammatory agents: multitarget-directed ligands for the efficient management of Alzheimer's disease," *ACS Chemical Neuroscience*, vol. 9, no. 7, pp. 1663–1679, 2018.

[114] J. D. Scott, S. W. Li, A. P. J. Brunskill et al., "Discovery of the 3-imino-1,2,4-thiadiazinane 1,1-dioxide derivative verubecestat (MK-8931)-a β-site amyloid precursor protein cleaving enzyme 1 inhibitor for the treatment of Alzheimer's disease," *Journal of Medicinal Chemistry*, vol. 59, no. 23, pp. 10435–10450, 2016.

[115] S. R. Sagar, D. P. Singh, R. D. Das et al., "Pharmacological investigation of quinoxaline-bisthiazoles as multitarget-directed ligands for the treatment of Alzheimer's disease," *Bioorganic Chemistry*, vol. 89, p. 102992, 2019.

[116] E. Seto and M. Yoshida, "Erasers of histone acetylation: the histone deacetylase enzymes," *Cold Spring Harbor Perspectives in Biology*, vol. 6, no. 4, 2014.

[117] M. Brindisi, C. Cavella, S. Brogi et al., "Phenylpyrrole-based HDAC inhibitors: synthesis, molecular modeling and biological studies," *Future Medicinal Chemistry*, vol. 8, no. 13, pp. 1573–1587, 2016.

[118] T. Eckschlager, J. Plch, M. Stiborova, and J. Hrabeta, "Histone deacetylase inhibitors as anticancer drugs," *International Journal of Molecular Sciences*, vol. 18, no. 7, p. 1414, 2017.

[119] K. Xu, X. L. Dai, H. C. Huang, and Z. F. Jiang, "Targeting HDACs: A Promising Therapy for Alzheimer's Disease," *Oxidative Medicine and Cellular Longevity*, vol. 2011, 5 pages, 2011.

[120] J.-S. Guan, S. J. Haggarty, E. Giacometti et al., "HDAC2 negatively regulates memory formation and synaptic plasticity," *Nature*, vol. 459, no. 7243, pp. 55–60, 2009.

[121] C. Cook, T. F. Gendron, K. Scheffel et al., "Loss of HDAC6, a novel CHIP substrate, alleviates abnormal tau accumulation," *Human Molecular Genetics*, vol. 21, no. 13, pp. 2936–2945, 2012.

[122] L. Zhang, C. Liu, J. Wu et al., "Tubastatin A/ACY-1215 improves cognition in Alzheimer's disease transgenic mice," *Journal of Alzheimer's Disease*, vol. 41, no. 4, pp. 1193–1205, 2014.

[123] J. Gräff, D. Rei, J. S. Guan et al., "An epigenetic blockade of cognitive functions in the neurodegenerating brain," *Nature*, vol. 483, no. 7388, pp. 222–226, 2012.

[124] M. Cuadrado-Tejedor, C. Garcia-Barroso, J. A. Sánchez-Arias et al., "A First-in-Class Small-Molecule that Acts as a Dual Inhibitor of HDAC and PDE5 and that Rescues Hippocampal Synaptic Impairment in Alzheimer's Disease Mice," *Neuropsychopharmacology*, vol. 42, no. 2, pp. 524–539, 2017.

[125] M. Cuadrado-Tejedor, C. Garcia-Barroso, J. Sanzhez-Arias et al., "Concomitant histone deacetylase and phosphodiesterase 5 inhibition synergistically prevents the disruption in synaptic plasticity and it reverses cognitive impairment in a mouse model of Alzheimer's disease," *Clinical Epigenetics*, vol. 7, no. 1, 2015.

[126] A. De Simone, V. La Pietra, N. Betari et al., "Discovery of the first-in-class GSK-3β/HDAC dual inhibitor as disease-modifying agent to combat Alzheimer's disease," *ACS Medicinal Chemistry Letters*, vol. 10, no. 4, pp. 469–474, 2019.

[127] F. H. Bardai, V. Price, M. Zaayman, L. Wang, and S. R. D'Mello, "Histone Deacetylase-1 (HDAC1) is a molecular switch between neuronal survival and death," *The Journal of Biological Chemistry*, vol. 287, no. 42, pp. 35444–35453, 2012.

[128] C. Cook, J. N. Stankowski, Y. Carlomagno, C. Stetler, and L. Petrucelli, "Acetylation: a new key to unlock tau's role in neurodegeneration," *Alzheimer's Research & Therapy*, vol. 6, no. 3, p. 29, 2014.

[129] A. Kaur, S. Mann, A. Kaur et al., "Multi-target-directed triazole derivatives as promising agents for the treatment of Alzheimer's disease," *Bioorganic Chemestry*, vol. 87, pp. 572–584, 2019.

[130] A. Kaur, S. S. Narang, A. Kaur et al., "Multifunctional monotriazole derivatives inhibit Aβ_{42} aggregation and Cu^{2+}-mediated Aβ42 aggregation and protect against Aβ42-induced cytotoxicity," *Chemical Research in Toxicology*, vol. 32, no. 9, pp. 1824–1839, 2019.

[131] J. Hu, T. Pan, B. An, Z. Li, X. Li, and L. Huang, "Synthesis and evaluation of clioquinol-rolipram/roflumilast hybrids as multitarget-directed ligands for the treatment of Alzheimer's disease," *European Journal of Medicinal Chemistry*, vol. 163, pp. 512–526, 2019.

[132] B. Gong, O. V. Vitolo, F. Trinchese, S. Liu, M. Shelanski, and O. Arancio, "Persistent improvement in synaptic and cognitive functions in an Alzheimer mouse model after rolipram treatment," *The Journal of Clinical Investigation*, vol. 114, no. 11, pp. 1624–1634, 2004.

[133] K. Lutsenko, S. Hagenow, A. Affini, D. Reiner, and H. Stark, "Rasagiline derivatives combined with histamine H3 receptor properties," *Bioorganic & Medicinal Chemistry Letters*, vol. 29, no. 19, p. 126612, 2019.

[134] D. Gonzalez, R. L. Arribas, L. Viejo, R. Lajarin-Cuesta, and C. de Los Rios, "Substituent effect of N-benzylated gramine derivatives that prevent the PP2A inhibition and dissipate the neuronal Ca^{2+} overload, as a multitarget strategy for the treatment of Alzheimer's disease," *Bioorganic & Medicinal Chemistry*, vol. 26, no. 9, pp. 2551–2560, 2018.

[135] V. Theendakara, D. E. Bredesen, and R. V. Rao, "Downregulation of protein phosphatase 2A by apolipoprotein E: Implications for Alzheimer's disease," *Molecular and Cellular Neurosciences*, vol. 83, pp. 83–91, 2017.

[136] R. Lajarín-Cuesta, C. Nanclares, J.-A. Arranz-Tagarro et al., "Gramine derivatives targeting Ca(2+) channels and Ser/Thr phosphatases: a new dual strategy for the treatment of neurodegenerative diseases," *Journal of Medicinal Chemistry*, vol. 59, no. 13, pp. 6265–6280, 2016.

[137] S. F. Chan and N. J. Sucher, "An NMDA receptor signaling complex with protein phosphatase 2A," *The Journal of Neuroscience*, vol. 21, no. 20, pp. 7985–7992, 2001.

[138] Z. Wang, J. Hu, X. Yang et al., "Design, synthesis, and evaluation of orally bioavailable quinoline-indole derivatives as innovative multitarget-directed ligands: promotion of cell proliferation in the adult murine hippocampus for the treatment of Alzheimer's disease," *Journal of Medicinal Chemistry*, vol. 61, no. 5, pp. 1871–1894, 2018.

[139] S. Brogi, S. Maramai, M. Brindisi et al., "Activation of the Wnt pathway by small peptides: rational design, synthesis and biological evaluation," *ChemMedChem*, vol. 12, no. 24, pp. 2074–2085, 2017.

[140] M. Brindisi, S. Maramai, S. Brogi et al., "Development of novel cyclic peptides as pro-apoptotic agents," *European Journal of Medicinal Chemistry*, vol. 117, pp. 301–320, 2016.

[141] J. L. Lau and M. K. Dunn, "Therapeutic peptides: historical perspectives, current development trends, and future directions," *Bioorganic & Medicinal Chemistry*, vol. 26, no. 10, pp. 2700–2707, 2018.

[142] M. H. Baig, K. Ahmad, G. Rabbani, and I. Choi, "Use of peptides for the management of Alzheimer's disease: diagnosis and inhibition," *Frontiers in Aging Neuroscience*, vol. 10, p. 21, 2018.

[143] S. Ribarič, "Peptides as potential therapeutics for Alzheimer's disease," *Molecules*, vol. 23, no. 2, p. 283, 2018.

[144] R. Soudy, R. Kimura, A. Patel et al., "Short amylin receptor antagonist peptides improve memory deficits in Alzheimer's disease mouse model," *Scientific Reports*, vol. 9, no. 1, p. 10942, 2019.

Hindawi
BioMed Research International
Volume 2020, Article ID 2546365, 10 pages
https://doi.org/10.1155/2020/2546365

Research Article

The Cataleptic, Asymmetric, Analgesic, and Brain Biochemical Effects of Parkinson's Disease Can Be Affected by *Toxoplasma gondii* Infection

Mahnaz Taherianfard,[1] Moslem Riyahi,[1] Mostafa Razavi,[2] Zahedeh Bavandi,[1] Narges Eskandari Roozbahani,[3] and Mohammad Mehdi Namavari[4]

[1]*Physiology Division, Department of Basic Science, School of Veterinary Medicine, Shiraz University, Shiraz, Iran*
[2]*Department of Pathobiology, School of Veterinary Medicine, Shiraz University, Shiraz, Iran*
[3]*Pharmacology Division, Department of Basic Sciences, School of Veterinary Medicine, Shiraz University, Shiraz, Iran*
[4]*Razi Vaccine and Serum Research Institute, Shiraz, Iran*

Correspondence should be addressed to Mahnaz Taherianfard; taherian@shirazu.ac.ir

Received 1 September 2019; Accepted 18 March 2020; Published 5 May 2020

Guest Editor: Moustafa Gabr

Purpose. Parkinson's disease (PD) is a neurodegenerative disorder with progressive motor defects. Therefore, the aim of the present investigation was to examine whether catalepsy, asymmetry, and nociceptive behaviors; the Nissl-body and neuron distribution; brain-derived neurotrophic factor (BDNF); malondialdehyde (MDA); total antioxidant capacity (TAC) levels; and the percentage of dopamine depletion of striatal neurons in the rat model of Parkinson's disease (PD) can be affected by *Toxoplasma gondii* (TG) infection. *Methods*. Fifty rats were divided into five groups: control (intact rats), sham (rats which received an intrastriatal injection of artificial cerebrospinal fluid (ACSF)), PD control (induction of PD without TG infection), TG control (rats infected by TG without PD induction), and PD infected (third week after PD induction, infection by TG was done). PD was induced by the unilateral intrastriatal microinjection of 6-hydroxydopamine (6-OHDA) and ELISA quantified dopamine, BDNF, MDA, and TAC in the striatum tissue. Cataleptic, asymmetrical, nociceptive, and histological alterations were determined by bar test, elevated body swing test, formalin test, and Nissl-body and neuron counting in the striatal neurons. *Results*. The results demonstrated that PD could significantly increase the number of biased swings, descent latency time, and nociceptive behavior and decrease the distribution of Nissl-stained neurons compared to the control and sham groups. TG infection significantly improved biased swing, descent latency time, nociceptive behavior, and the Nissl-body distribution in striatal neurons in comparison to the PD control group. The striatal level of BDNF in the PD-infected and TG control groups significantly increased relative to the PD control group. The striatal MDA was significantly higher in the PD control than other groups, while striatal TAC was significantly lower in the PD control than other groups. *Conclusions*. The current study indicates that TG infection could improve the cataleptic, asymmetric, nociceptive and behaviors; the level of striatal dopamine release; BDNF levels; TAC; and MDA in PD rats.

1. Introduction

Parkinson's disease (PD) is one of the most widespread neurodegenerative diseases, with a prevalence of approximately 1% of individuals with an age above 65 years [1]. It determined by the chronic and slowly progressive injury and depletion of dopaminergic neurons in the substantia nigra that may led to motor disturbances, including bradykinesia, akinesia, rest tremor, and postural instability. Likewise, patients may suffer from nonmotor symptoms, including depression, anxiety, rapid eye movement (REM) disorder, and pain [2, 3]. Catalepsy, the impairment of movement initiation, is an extrapyramidal dysfunction known as a prominent motor symptom of PD, which is related to the striatal

dopamine reduction. Cataleptic behavior in the PD rodent has been employed as a standard model of bradykinesia and rigidity in human PD [4]. Pain is an important nonmotor symptom in PD patients that overshadow the quality of PD's life. Forty to 85 percentages of PD patients have painful sensations [3] in five different manners: musculoskeletal (related to parkinsonian rigidity and akinesia), neuropathic (related to neural lesion), dystonia-related, akathisia, and central neuropathic pain [5]. Although some genetic mutations identified have been associated with PD, the exact causes of PD remain unknown. Nevertheless, the crucial roles of oxidative stress and neuroinflammation in its pathogenesis have been well documented [6]. Even though the underlying cause of idiopathic PD remains unknown, the role of an increase in the oxidative stress, inflammatory responses, and mitochondrial dysfunction of dopamine neurons and a decrease in the availability of brain-derived neurotrophic factor (BDNF) have been well documented as pathophysiologic mechanisms [7].

Toxoplasma gondii (TG), a member of the phylum *Apicomplexa*, is an obligate intracellular parasite with high worldwide distribution which has infected one-third of the world population [8]. Tachyzoites, the invasive form of TG, infect neural cells. Afterward, in rodents, they differentiate into bradyzoites, which form the intracellular brain cysts. TG infection is considered asymptomatic in adults, but it can cause problems such as encephalitis, blindness, and mental retardation in immunocompromised individuals and congenitally infected children [8]. It has been observed that brain biochemistry is affected by the host immune system responses against TG infection [9]. On the other hand, TG protects itself and host cells against the immune response through some strategies, such as increasing the levels of antioxidant activity [10], brain-derived neurotrophic factor)BDNF([11], dopamine concentration [12], and antiapoptotic activity [13]. IFN-γ production is increased by TG infection through tyrosine hydroxylase activity 1 (TH1) immune response [14]. Torres et al. found that TG reduces the expression of N-methyl-D-aspartate (NMDA) receptor via IFN-γ stimulation [15]. Moreover, TG activates the astrocytes that synthesize some metabolites to modulate NMDA receptor function [16]. The dopamine levels can be changed by TG in the brain [12]. The behavioral changes observed in infected rodents are attributed to its ability to change the neurotransmitter levels [12]. Dopamine depletion in PD decreases the inhibitory control of the corticostriatal glutamatergic pathway [17]. Moreover, PD causes hypofunction of the output pathways from the substantia nigra and medial globus pallidus, which leads to the increase in the excitatory subthalamic glutamatergic output [18].

Striatal medium spiny neurons contained dopamine D2 receptors, which are involved in controlling extrapyramidal functions. Haloperidol, an antipsychotic agent, induces catalepsy via selective blocking of dopamine D2 receptor in the striatum [19]. Previous findings indicated that the dopamine system has a modulatory effect on the pain and dopamine D2 receptor agonists attenuate nociceptive behavior initiation in animals and humans. Therefore, striatal dopamine enhancement can attenuate PD pain and catalepsy symptoms. There are a few investigations on the interaction of TG infection with PD pain symptom and behavioral changes; and these results are in paradox; also, most of the study on the relation between TG and PD were done according to a serological study in human and there is not any study on the brain. Therefore, the present investigation was done to study the effects of TG infection on experimental PD induction rat's asymmetric and cataleptic behavior, pain perception, percentage of dopamine depletion, level of striatal BDNF, TAC and MDA levels, and Nissl-body and neuron distribution in striatal neurons.

2. Materials and Methods

2.1. Subjects and Study Design. Fifty Sprague Dawley male rats, weighing 220–300 g in standard condition 12-h light/-dark cycle with food and water ad libitum were used. Animal handling was conducted according to the Ethical Committee for Animal Experiments at Shiraz University. Animals were randomly divided into five groups ($n = 10$ in each group): control group, intact rats; sham group, intrastriatally ACSF-injected rats; PD control group, induction of PD in rats by intrastriatal injection of 6OHDA; TG control group, rats were infected by TG; and PD-infected group, the infection by TG was done on the third week after the induction of PD..

RH strain TG tachyzoites were obtained from the Razi Vaccine and Serum Research Institute, Shiraz, Iran. For infection induction, rats received intraperitoneal (IP) injection of 200 μl normal saline containing 10^5 tachyzoites (counted by a hemocytometer). At the end of the experiment, for the confirmation of tissue cyst formation, the brain smears were prepared and stained by Giemsa (Figure 1(a)).

2.2. Behavioral Testing. Rats were subjected to elevated body swing test by the method of Roghani et al. [20]. Catalepsy was evaluated by the bar test. In brief, the forepaws of each rat were located in a half-rearing position on a horizontal metal bar, which was set at 9 cm above the base in a parallel form. The time was recorded until the rats removed one paw from the bar (descent latency time). Descent latency cutoff time was 180 sec for the bar test [21]. The PD-infected design of the behavioral tests was performed in four steps: first, one week before the surgery; second and third, two and three weeks after surgery, respectively; and forth, eight weeks after TG infection (Figure 1(b)).

2.3. Formalin Test. Pain behavior was examined by the formalin test eight weeks after the infection as follows: the rats were located in the $32 \times 32 \times 32$ cm Plexiglas boxes and a mirror was mounted at a 45″ angle, beneath the floor to the view of the rats' paws. 50 μl of 2.5% formalin was injected by 27G needle into the foot plantar surface of the hind paw contralateral to the 6-OHDA injection site. The pain behavior was scored in 15 sec intervals and continued for 60 min [22]. After behavioral testing, the animals were decapitated and the striatum was dissected and stored at -80 C°.

2.4. Stereotaxic Surgery. Animal was anesthetized by IP injection of ketamine (100 mg/kg) and xylazine (8 mg/kg). PD induction was done by a unilateral and single injection of

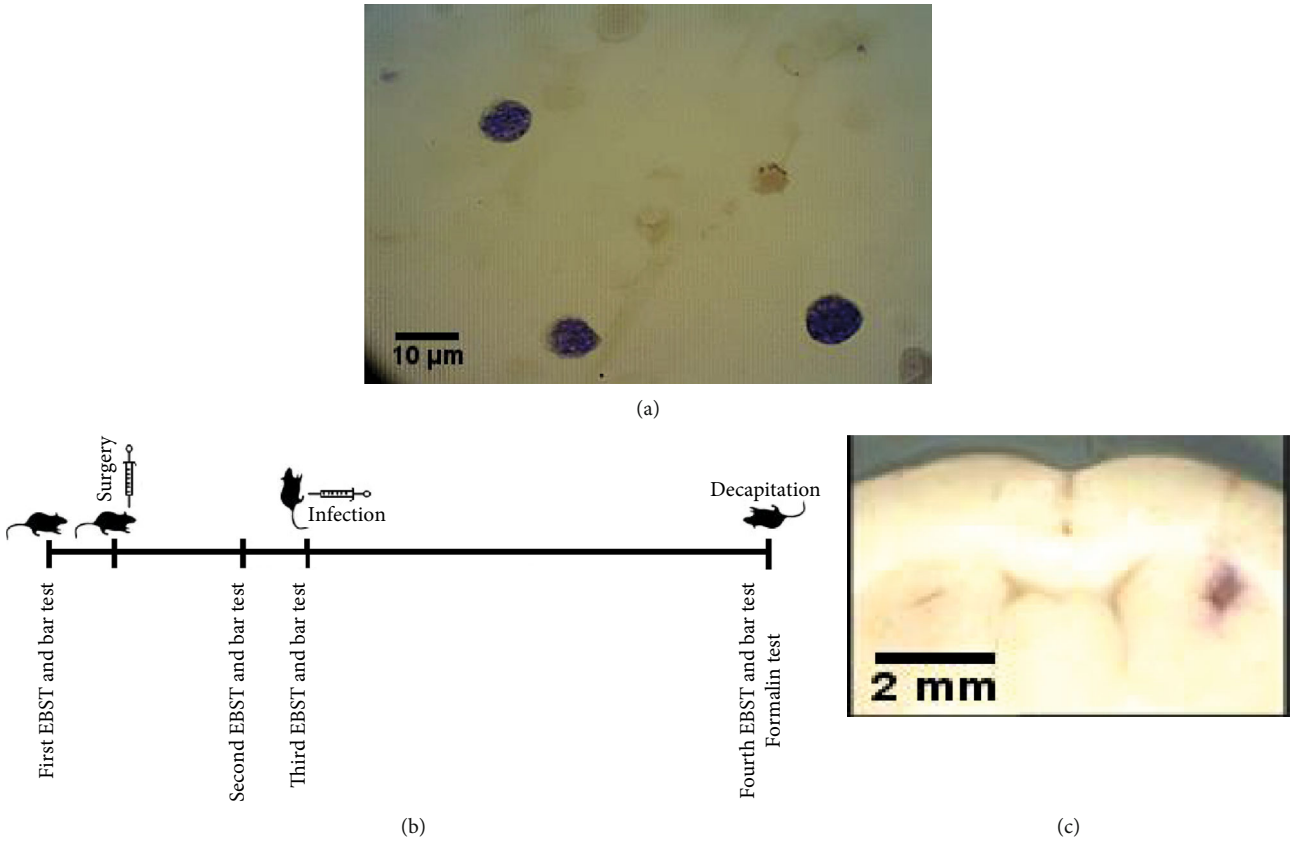

Figure 1: (a) Photomicrograph showing *Toxoplasma gondii* cysts (Giemsa stained) in a brain smear of infected rats. (b) The overall design of the study and the scheduling of behavioral tests. (c) Photomicrograph shows the rat brain section in the striatum region confirming the injection site.

20 μg of 6-OHDA (in 4 μl saline with 0.2 mg/ml of ascorbic acid) into the striatum (0.7 mm anterior to the bregma, 3 mm lateral to the midline, and 5 mm ventral to the dura).

The accuracy of the injection site location was determined by the microinjection of 4 μl methylene blue into the striatum at the end of each experiment. In decapitated rats, the brains were removed and then were fixed in 10% of phosphate-buffered formalin for 24 hours. The striatum injection site was confirmed by comparing it with the atlas of Paxinos and Watson (Figure 1(c)).

2.5. Nissl Body and Neuron Distribution in the Striatum. At the end of the experiments, the rats were deeply anesthetized and sacrificed. For Nissl-body and neuron distribution measuring, after brain tissue fixation by 10% formalin, automatic tissue processor prepared paraffin blocks; then, 5 μ coronal section of the brain blocks in the region of striatum neurons was prepared. In all sections, Nissl-body counting in six cells and cell counting in six parts of each slide section of the striatum in all of the groups by Cresyl violet and hematoxylin eosin staining were done.

2.6. Dopamine, BDNF, TAC, and MDA Measurement. Dopamine concentration was measured using an ELISA kit (RE59161, IBL, Hamburg, Germany) in 50 μg of homogenized striatal tissues based on Mabandla et al.'s modification [23]. The percentage of dopamine relative to the control group was determined according to following formula:

$$\frac{\text{dopamine concentration of group } x}{\text{dopamine concentration of control group}} \times 100 \quad (1)$$

A rat ELISA kit (MyBioSource, USA, catalog # MBS824814) according to the manufacturer's instructions measured striatal BDNF. An ELISA standard kit was used to evaluate striatal TAC (ZB-TAC-96A, Zell Bio Germany) and MDA (ZB-MDA-96A, Zell Bio Germany).

2.7. Statistical Analysis. SPSS version 22 was used for data analysis. The Kolmogorov–Smirnov test was used for verifying the normalization of data. One-way ANOVA and Tukey's test, as the post hoc test, were used, and the significant level was considered $P < 0.05$.

3. Result

Catalepsy, via the bar test, revealed a significant increase in the descent latency time at the second, third, and fourth steps in the PD control group compared to the control and sham groups ($P < 0.001$). In addition, the PD-infected group showed a significant ($P < 0.001$) increase in the descent latency time at the second and third steps, but not at the

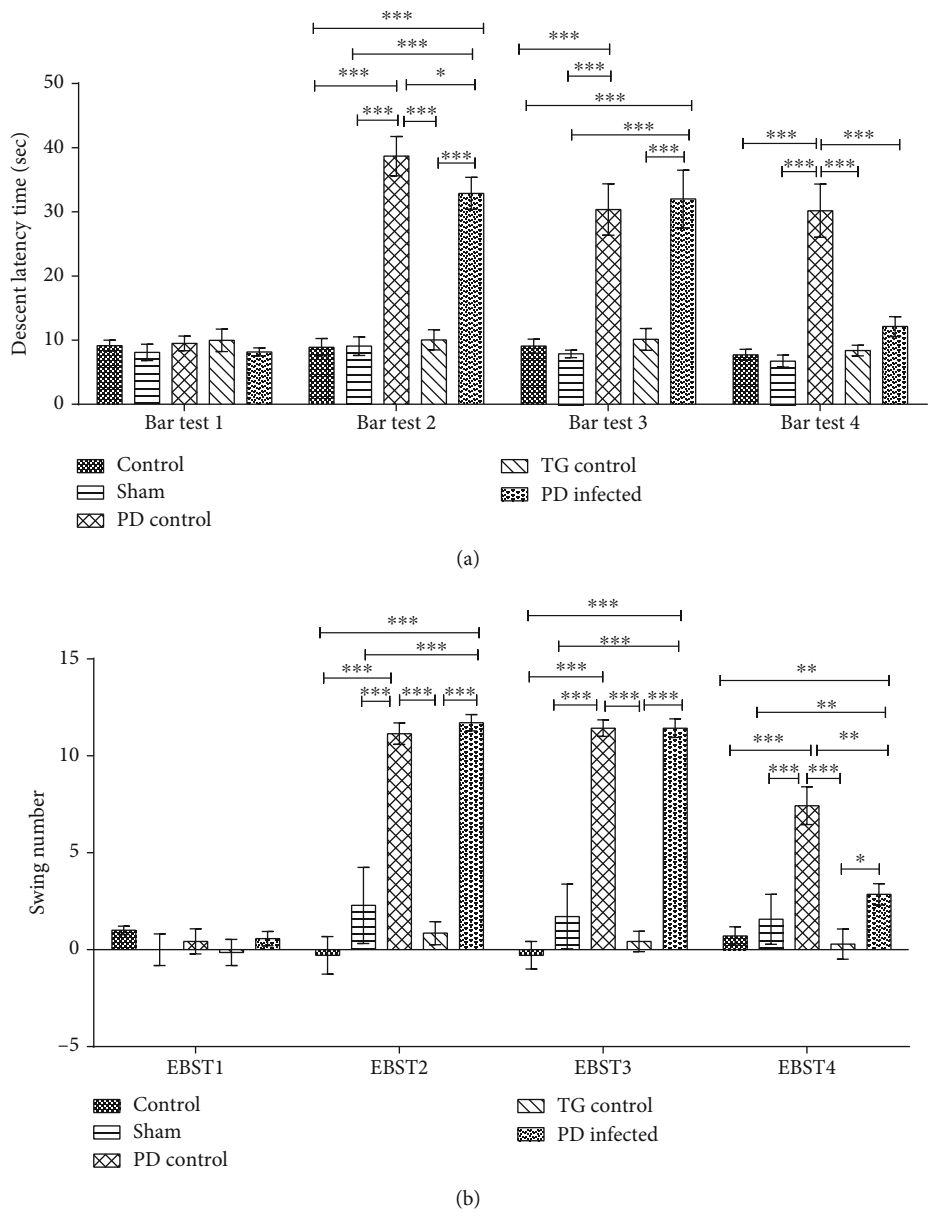

Figure 2: Two behavioral tests for PD induction confirmation. (a) Bar test (sec) and (b) EBST test in all groups. $^{*}P < 0.05$, $^{**}P < 0.01$, and $^{***}P < 0.001$ significant differences. Data are shown as means ± SEM.

fourth step. The TG control group had no significant difference in descent latency time in all steps in comparison with the control and sham groups ($P > 0.05$) (Figure 2(a)).

The elevated body swing test (EBST) confirmed asymmetric behavior representation and success of PD induction. It was performed at four steps of behavioral investigation as EBST1, EBST2, EBST3, and EBST4 (Figure 2(b)). As shown in Figure 2(b), the PD control and PD-infected groups showed a significant ($P < 0.001$) increase in the number of swinging in comparison to the control, sham, and TG control groups in EBST2 and EBST3. In EBST4, the PD-infected group revealed a significant reduction in the biased swing in comparison with the PD control group, whereas it had no significant difference with the control, sham, and TG control groups. However, the PD control group exhibited a significant increase in the biased swing compared with other groups.

As shown in Figure 3(a), after formalin injection into the hind paw, the PD control group showed a significant increase in the nociceptive scores in the early phase compared to the control and sham ($P < 0.05$) and TG control groups ($P < 0.001$). The PD-infected group had lower formalin-induced nociceptive scores in the early phase of the formalin test in comparison with the control and sham ($P < 0.05$) and PD control groups ($P < 0.01$). In the interphase of the formalin test, the PD control group showed a significant ($P < 0.01$) increase in the nociceptive scores in comparison to another groups, but there were no significant differences among the other groups (Figure 3(b)). As illustrated in Figure 3(c), the PD control group had a significant increase in the nociceptive

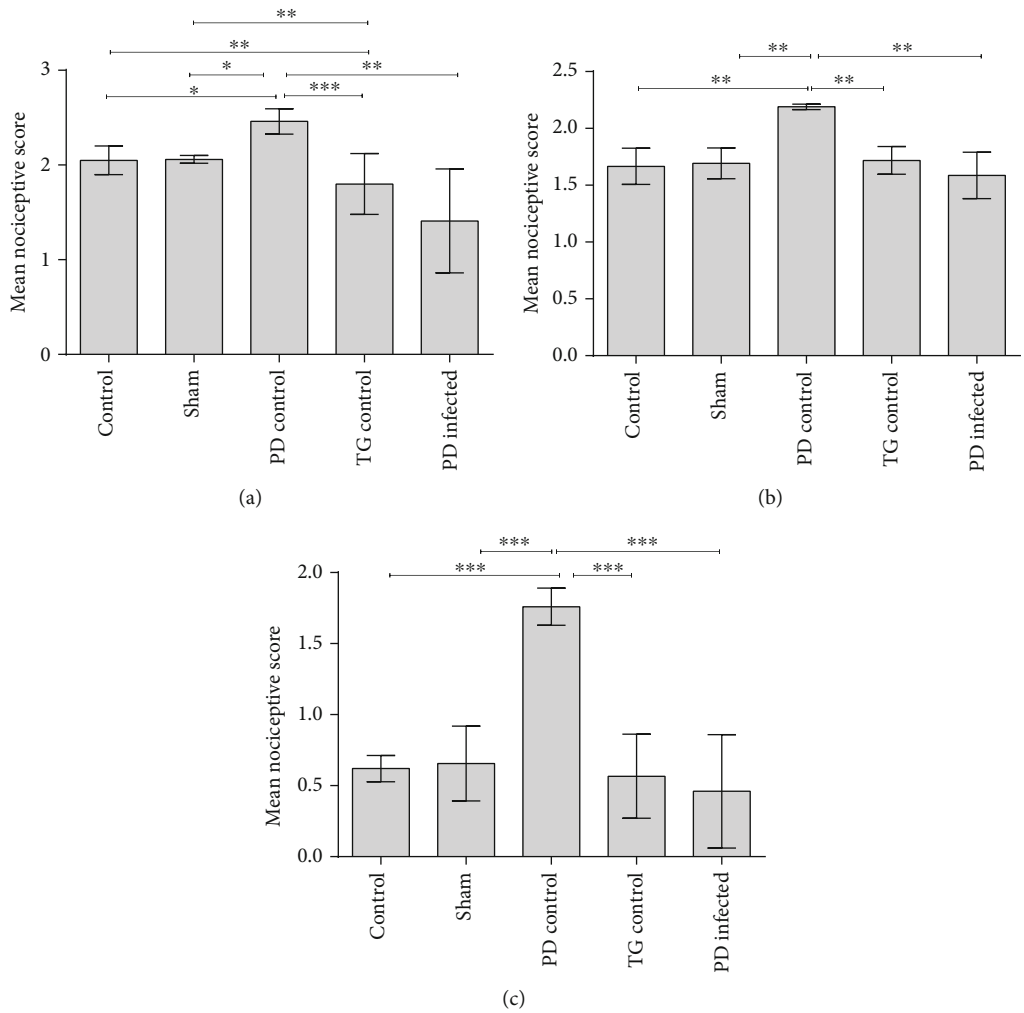

Figure 3: Nociceptive score in the PD-infected rats. (a) The mean of nociceptive score in the early phase of the formalin test. (b) The mean of the nociceptive score in the interphase of the formalin test. (c) The mean of the nociceptive score in the late phase of the formalin test. $^{*}P < 0.05$, $^{**}P < 0.01$, and $^{***}P < 0.001$ significant differences. Data are shown as means ± SEM.

scores in the late phase of formalin test compared to the other groups ($P < 0.05$).

As shown in Figure 4, a significant loss of Nissl-body in the striatal cells was evident in the PD control group compared with other groups ($P < 0.001$). Nevertheless, the PD-infected group significantly recovered from the Nissl-body loss in the striatal cells in comparison with the PD control group ($P < 0.001$). Meanwhile, no significant difference was found between the PD-infected and control, sham, and TG control groups ($P > 0.05$).

According to Figure 5 the number of neuron in striatum was significantly lower compared with other groups ($P < 0.01$). The PD-infected group significantly recovered from the neuron loss in the striatal cells in comparison with the PD control group ($P < 0.001$). Meanwhile, no significant difference was found between the PD-infected and control and sham groups ($P > 0.05$).

Table 1 shows that the percentage of dopamine in striatum neurons of the PD group is lower than that of the control; however, this reduction in the PD control was higher than that of the PD-infected group. Additionally, TG

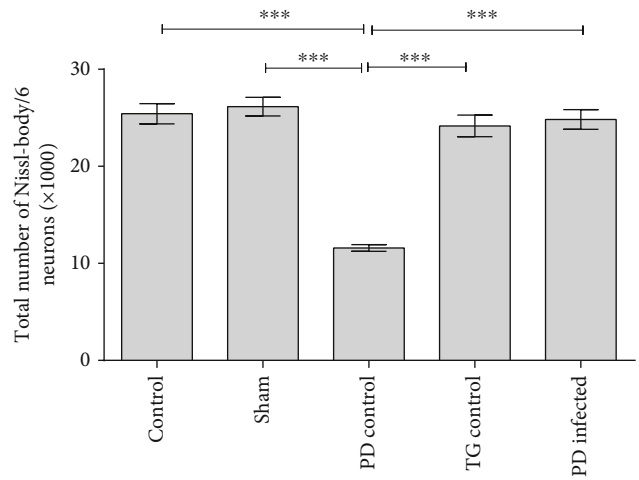

Figure 4: The total number of Nissl-bodies in rat striatum cells. $^{***}P < 0.001$ significant difference. Data are shown as means ± SEM.

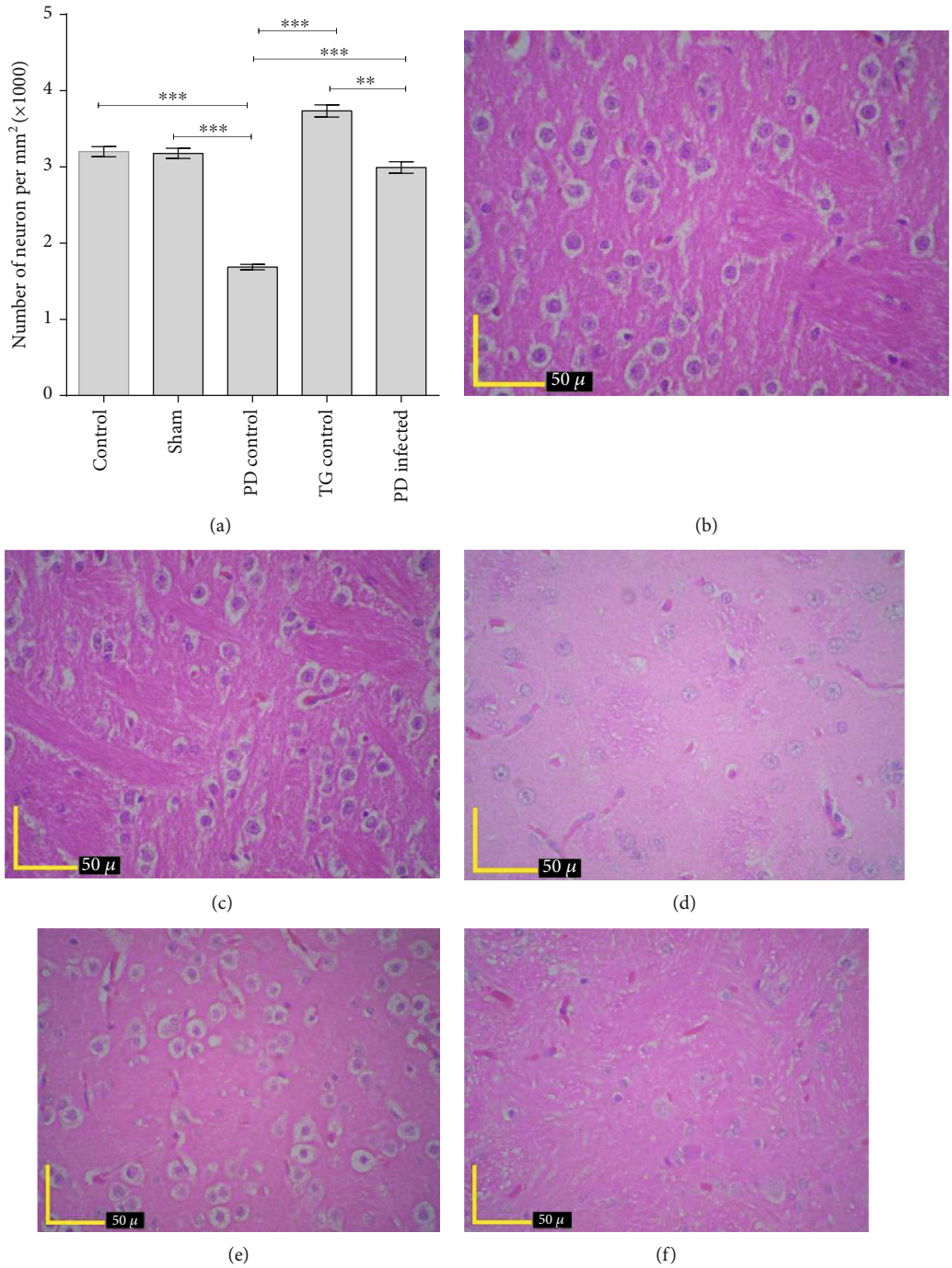

Figure 5: The number of neurons in the striatum (a). Photomicrograph of striatum neuron staining by hematoxylin eosin in the control group (b), sham group (c), PD control group (d), TG control group (e), and PD-infected group (f). $^{**}P < 0.01$; $^{***}P < 0.001$ significant differences. Data are shown as means ± SEM.

infection led to an increase in the mean of the dopamine concentration to 25.24% more than that of the control group.

BDNF of the striatum had a significant reduction ($P < 0.001$) in the PD control group compared to all the other groups (Figure 6(a)). The TG control group showed a significantly higher level of BDNF compared to the PD infected ($P < 0.01$), but PD infected had no significant differences with the control and sham groups ($P > 0.05$).

Figure 6(b) showed that the PD control group significantly decrease the TAC levels compared to the control and sham groups ($P < 0.05$), whereas the PD-infected and TG control groups showed no significant decrease in TAC levels vs. the control and sham groups ($P > 0.05$).

Figure 6(c) showed that the PD control group significantly increased the MDA levels compared to the control and sham groups ($P < 0.001$) whereas the PD-infected and

Table 1: Percentage of dopamine reduction relative to the control group.

Groups	Percentage of dopamine relative to control group
Control	100%
Sham	97%
PD control	15.45%
TG control	+125.24%
PD infected	63.73%

TG control groups showed no significant increases in MDA levels vs. the control and sham groups ($P > 0.05$).

4. Discussion

The aim of the present study was to investigate the effect of the cataleptic and analgesic behaviors of the rat model of PD and how they may be affected by TG infection. Catalepsy is an extrapyramidal dysfunction that is explained as a disability to improve the external abnormal forced positions [24]. In addition to motor symptoms, pain is one of the most troublesome nonmotor symptoms of PD with a high prevalence that impairs patients' quality of life.

In our experiment, no significant asymmetry and descent latency time were observed among groups in the first step of the behavioral test. Following progressive dopaminergic nigrostriatal degeneration and decrease in the ipsilateral dopamine level, this imbalance resulted in a functional asymmetry [25]. In agreement with the previous studies, the results of this study indicated that PD induction significantly increase the biased swings in the second and third steps of the behavioral test compared with the other groups [20, 25–27]. In the PD-infected group, a significant decrease in the biased swing was observed in the fourth step of the behavioral test compared to the PD control group. TG was able to encode an enzyme with TH activity, a tyrosine to L-DOPA converter, which, in turn, is the rate-limiting step of the dopamine synthesis [28]. As shown in the results, the PD control group caused dopamine depletion by 84.53% in the striatum tissue. The degree of striatum DA reduction in PD-infected rats was 36.27%; as a result, TG infection has prevented severe dopamine decrease in the striatum. Additionally, the TG control group showed 25.24% of dopamine amplification in the striatum. In agreement with our finding, an increase for dopamine in the different regions of infected mouse brains including the striatum has been reported [11]. Decreasing dopamine in the lesioned striatum has been known as the primary factor of cataleptic behavior with concomitant descent latency [29]. Induction of PD causes damage to the nigrostriatal dopaminergic neurons, resulting in the abnormal firing of the basal ganglia circuits, manifested as muscle rigidity and catalepsy. Our results were consistent with those of other studies and showed that the descent latency time increased in the 6-OHDA-lesioned rats compared with other groups [30, 31]. However, PD-infected rats showed a significant decrease in descent latency.

Similar to the previous studies, in our experiment, in the PD control group, dopamine depletion increased formalin-induced pain behaviors in all three phases of the formalin test compared with the other groups [3, 5]. Hence, it can be concluded that the nigrostriatal dopaminergic system plays an important role in the processing of pain behavior. Previous studies have shown that the intrastriatal injection of dopamine D2 receptor agonists inhibits pain responses [32]. Present results were in agreement with a report that brain dopamine levels increased by TG infection [33]. TG infection improved PD-induced hyperalgesia and rats exhibited less pain behavior compared to the control, sham, and PD control groups in the early phase, interphase, and late phase of the formalin test.

Diminution of the asymmetric behavior following TG infection probably indicates its potency in increasing the striatal dopamine at a level that attenuates motor bias. It has been shown that the increase in the dopaminergic neuron activity and dopamine release could attenuate the catalepsy induced by PD [30]. Striatal medium spiny neurons, in addition to dopaminergic projections from the substantia nigra (inhibitory pathway), receive the glutamatergic input (excitatory pathway) from the motor cortex [34]. Previous research have indicated that the decrease in the function of glutamatergic neurons or NMDA-selective glutamate receptor within the striatum could lead to a reduction in the catalepsy of PD patients [35]. Hama et al. found that NMDA agonist receptors involved in the maintenance of hyperalgesia and NMDA antagonists have analgesic effects on the management of hyperalgesia [36]. Kynurenic acid is an endogenous NMDA-receptor antagonist with antiexcitotoxicity activity in the brain. Schwarcz and Hunter showed that TG infection could increase the synthesis of kynurenic acid in the brain via an immune process [16]. The effectiveness of kynurenic acid in the relief of pain has been confirmed in recent studies [37]. It could be a possible explanation for our observations, where in the fourth step of behavioral test, the PD-infected rats revealed a significant attenuated cataleptic and pain behavior. In the present study, it seems that TG via increasing striatal dopamine and decreasing glutamate through NMDA receptor exerts anticataleptic and analgesic effects on PD rats.

Meanwhile, in present study, the Nissl-body and neuron distribution in the ipsilateral striatum to the site of 6-OHDA injection have shown significant reduction in the Nissl-body of striatum neurons in the PD control group compared to the other groups; whereas, no significant differences were observed between the PD-infected, control, and sham groups. Therefore, TG could compensate for the decrease in the Nissl-body and neuron numbers induced by PD in the rats' striatum neurons.

Brain-derived neurotrophic factor (BDNF) is a member of the nerve growth factor (NGF) with a critical role in neuronal development, survival, and plasticity that is reduced in PD's brain [38]. Previous studies have demonstrated that BDNF could play a primary role in the protection of dopaminergic neurons against neurotoxins [39]. Present results revealed that TG infection could increase striatal BDNF level in PD-infected rats in comparison with the PD control rats. Therefore, TG recovered neurons against the neurotoxicity of 6-OHDA, probably due to improving striatal BDNF level.

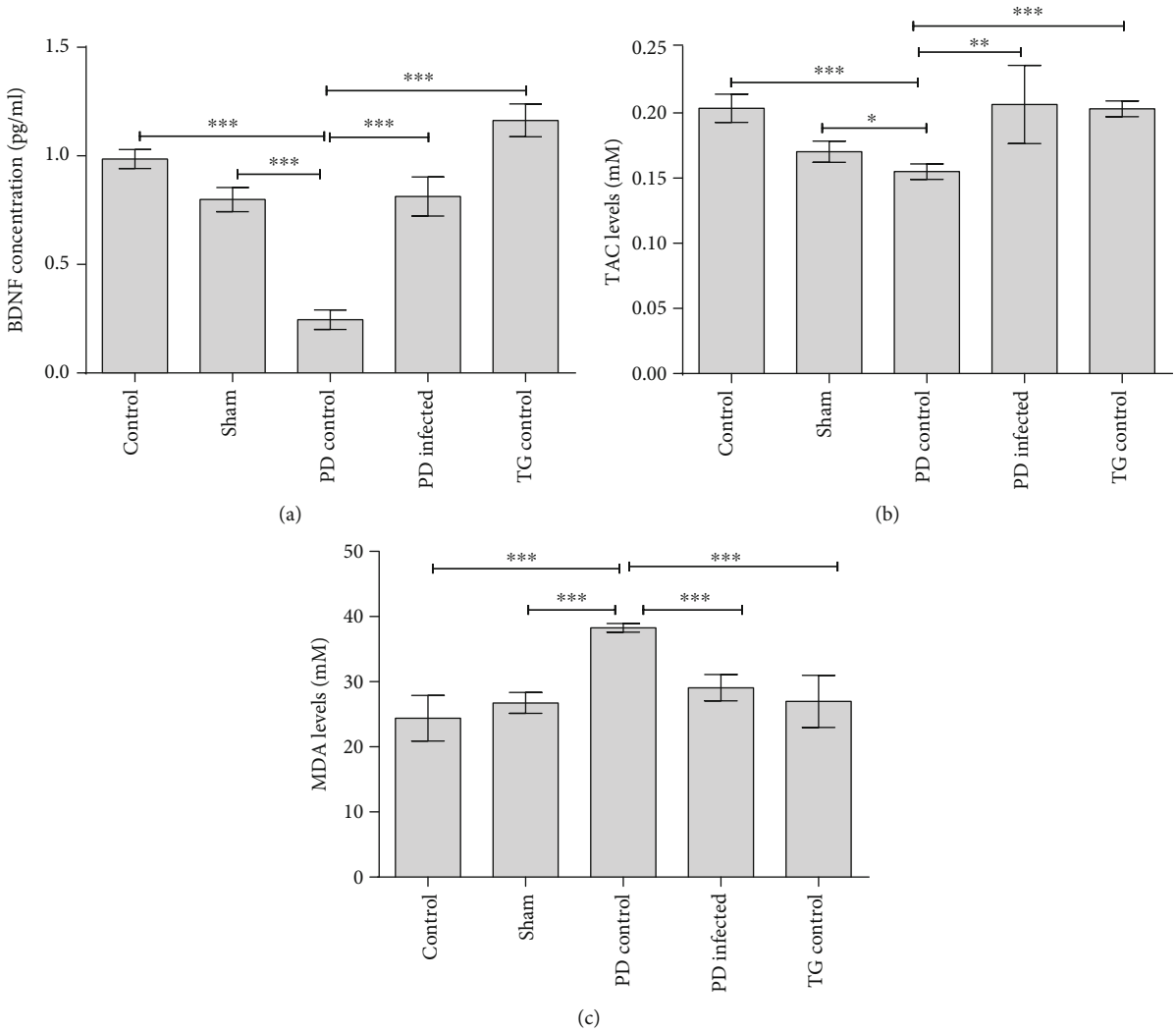

Figure 6: (a) Brain-derived neurotrophic factor (BDNF) protein concentration of striatum tissue. (b) Total antioxidant capacity (TAC) of striatum tissue. (c) Malondialdehyde (MDA) levels of striatum tissue. $^{*}P < 0.05$, $^{**}P < 0.01$, and $^{***}P < 0.001$ significant differences. Data are shown as means ± SEM.

Consistent with our results, Xiao et al. reported that TG could increase the BDNF levels in infected mouse striatum tissue. They also demonstrated microRNA- (miR-) 132 high expression in the striatum of infected mice [11]. Transcription of miR-132 in neuronal cells is upregulated by BDNF; it seems that miR-132 mediated the effects of BDNF on the brain [40]. Therefore, miR-132 plays important roles in neurogenesis, synaptic plasticity and neuronal differentiation, neuronal outgrowth, and sprouting [41]. It regulates the differentiation of dopamine neurons from mouse embryonic stem cells [42]. Consequently, it seems that BDNF protects dopaminergic neurons against oxidative stress and prevents cell death [39]. It seems that TG protects cells against oxidative stress via increasing the BDNF levels.

Present findings showed a significant increase in the levels of striatal MDA and decrease in the TAC levels in the PD control group rats compared with the control and sham groups. TG is able to express an antioxidant system, including superoxide dismutase, catalase, at least one peroxiredoxin and complete thioredoxin, and glutathione-based antioxidant systems, that could protect cells against reactive oxygen species (ROS) [43]. An in vitro study by Zhou et al. showed that *TG* infection caused a significant reduction of NADPH oxidase 4 (Nox4) mRNA and protein level and intracellular reactive oxygen species (ROS) level of the host. These results suggest that Nox4 is the main target for *TG* in reducing host intracellular ROS level, and PI3K/Akt signaling pathway is responsible for the suppression of Nox4 expression. The results are consistent with our in vivo results in oxidative stress [44].

5. Conclusion

Present investigation revealed that TG infection might repair cataleptic, asymmetric, and pain behaviors in the PD control rats by the following ways: (1) enhancing the release of dopamine in the striatum, (2) inhibiting the NMDA-selective glutamate receptor within the striatum by increasing the

synthesis of kynurenic acid and improving the striatal BDNF level of the rescued neurons against 6-OHDA, and (3) enhancing the TAC levels and decreasing the MDA levels. Further studies are required for a deeper understanding of the proposed pathways responsible for the anticataleptic, antiasymmetric, antinociceptive, and biochemical changes, which are associated with the TG infection in the PD rats. The results of the present study can be used for the development of new drugs or vaccine for the treatment of Parkinson's disease.

Data Availability

The data used to support the findings of this study are available from the corresponding author upon request.

Ethical Approval

The animal handling was conducted according to the Ethical Committee for Animal Experiments at Shiraz University.

Conflicts of Interest

The authors declare that they have no conflicts of interest.

Acknowledgments

All the people who helped to do this study were included as authors. This study was financially supported by Shiraz University (grant#: 94GCU4M1755).

References

[1] P. Redgrave, N. Vautrelle, and J. N. Reynolds, "Functional properties of the basal ganglia's re-entrant loop architecture: selection and reinforcement," *Neuroscience*, vol. 198, pp. 138–151, 2011.

[2] D. W. Dickson, "Parkinson's disease and parkinsonism: neuropathology," *Cold Spring Harbor Perspectives in Medicine*, vol. 2, no. 8, 2012.

[3] H. Maegawa, Y. Morimoto, C. Kudo et al., "Neural mechanism underlying hyperalgesic response to orofacial pain in Parkinson's disease model rats," *Neuroscience Research*, vol. 96, pp. 59–68, 2015.

[4] I. D. Ionov, I. I. Pushinskaya, L. A. Roslavtseva, and N. N. Severtsev, "Brain sites mediating cyclosomatostatin-induced catalepsy in Wistar rats: a specific role for the nigrostriatal system and locus coeruleus," *Brain Research*, vol. 1691, pp. 26–33, 2018.

[5] M. Dolatshahi, Y. Farbood, A. Sarkaki, S. M. Mansouri, and A. Khodadadi, "Ellagic acid improves hyperalgesia and cognitive deficiency in 6-hydroxidopamine induced rat model of Parkinson's disease," *Iranian Journal of Basic Medical Sciences*, vol. 18, no. 1, pp. 38–46, 2015.

[6] M. Wang, J. Zhu, Y. Pan et al., "Hydrogen sulfide functions as a neuromodulator to regulate striatal neurotransmission in a mouse model of Parkinson's disease," *Journal of Neuroscience Research*, vol. 93, no. 3, pp. 487–494, 2015.

[7] W. Zhang, H. An, F. Zhang et al., "Triptolide protects dopaminergic neurons from 6-OHDA lesion in a rat model of Parkinson's disease," *International Journal of Pharmacology*, vol. 11, no. 1, pp. 10–18, 2015.

[8] D. E. Hill and J. Dubey, "Toxoplasma gondii," in *Foodborne Parasites*, Y. Ortega and C. Sterling, Eds., pp. 119–138, Springer, 2018.

[9] N. Mammari, M. A. Halabi, S. Yaacoub, H. Chlala, M. L. Darde, and B. Courtioux, "*Toxoplasma gondii* modulates the host cell responses: an overview of apoptosis pathways," *BioMed Research International*, vol. 2019, Article ID 6152489, 10 pages, 2019.

[10] M. Ding, C. Clayton, and D. Soldati, "Toxoplasma gondii catalase: are there peroxisomes in toxoplasma?," *Journal of Cell Science*, vol. 113, pp. 2409–2419, 2000.

[11] J. Xiao, Y. Li, E. Prandovszky et al., "MicroRNA-132 dysregulation in *Toxoplasma gondii* infection has implications for dopamine signaling pathway," *Neuroscience*, vol. 268, pp. 128–138, 2014.

[12] E. Prandovszky, E. Gaskell, H. Martin, J. P. Dubey, J. P. Webster, and G. A. McConkey, "The neurotropic parasite Toxoplasma gondii increases dopamine metabolism,," *PLoS One*, vol. 6, no. 9, article e23866, 2011.

[13] L. Kim and E. Y. Denkers, "*Toxoplasma gondii* triggers Gi-dependent PI 3-kinase signaling required for inhibition of host cell apoptosis," *Journal of Cell Science*, vol. 119, no. 10, pp. 2119–2126, 2006.

[14] G. A. McConkey, H. L. Martin, G. C. Bristow, and J. P. Webster, "*Toxoplasma gondii* infection and behaviour–location, location, location?," *Journal of Experimental Biology*, vol. 216, no. 1, pp. 113–119, 2012.

[15] L. Torres, S. A. Robinson, D. G. Kim, A. Yan, T. A. Cleland, and M. S. Bynoe, "*Toxoplasma gondii* alters NMDAR signaling and induces signs of Alzheimer's disease in wild-type, C57BL/6 mice," *Journal of Neuroinflammation*, vol. 15, no. 1, p. 57, 2018.

[16] R. Schwarcz and C. A. Hunter, "*Toxoplasma gondii* and schizophrenia: linkage through astrocyte-derived kynurenic acid?," *Schizophrenia Bulletin*, vol. 33, no. 3, pp. 652-653, 2007.

[17] M. D. Neely, D. E. Schmidt, and A. Y. Deutch, "Cortical regulation of dopamine depletion-induced dendritic spine loss in striatal medium spiny neurons," *Neuroscience*, vol. 149, no. 2, pp. 457–464, 2007.

[18] N. A. Moore, A. Blackman, S. Awere, and J. D. Leander, "NMDA receptor antagonists inhibit catalepsy induced by either dopamine D1 or D2 receptor antagonists," *European Journal of Pharmacology*, vol. 237, no. 1, pp. 1–7, 1993.

[19] K. Hattori, S. Uchino, T. Isosaka et al., "Fyn is required for haloperidol-induced catalepsy in mice," *Journal of Biological Chemistry*, vol. 281, no. 11, pp. 7129–7135, 2006.

[20] M. Roghani, G. Behzadi, and T. Baluchnejadmojarad, "Efficacy of elevated body swing test in the early model of Parkinson's disease in rat," *Physiology & Behavior*, vol. 76, no. 4-5, pp. 507–510, 2002.

[21] N. Xiong, J. Xiong, G. Khare et al., "Edaravone guards dopamine neurons in a rotenone model for Parkinson's disease," *PLoS One*, vol. 6, no. 6, article e20677, 2011.

[22] M. J. Morgan and K. B. Franklin, "6-Hydroxydopamine lesions of the ventral tegmentum abolish D-amphetamine and morphine analgesia in the formalin test but not in the tail flick test," *Brain Research*, vol. 519, no. 1-2, pp. 144–149, 1990.

[23] M. V. Mabandla, M. Nyoka, and W. M. U. Daniels, "Early use of oleanolic acid provides protection against 6-hydroxydopamine

induced dopamine neurodegeneration," *Brain Research*, vol. 1622, pp. 64–71, 2015.

[24] L. A. Baez, N. K. Eskridge, and R. Schein, "Postnatal development of dopaminergic and cholinergic catalepsy in the rat," *European Journal of Pharmacology*, vol. 36, no. 1, pp. 155–162, 1976.

[25] R. K. Schwarting and J. P. Huston, "Behavioral and neurochemical dynamics of neurotoxic meso-striatal dopamine lesions," *Neurotoxicology*, vol. 18, no. 3, pp. 689–708, 1997.

[26] C. V. Borlongan and P. R. Sanberg, "Elevated body swing test: a new behavioral parameter for rats with 6-hydroxydopamine-induced hemiparkinsonism," *Journal of Neuroscience*, vol. 15, no. 7, pp. 5372–5378, 1995.

[27] H. Yuan, S. Sarre, G. Ebinger, and Y. Michotte, "Histological, behavioural and neurochemical evaluation of medial forebrain bundle and striatal 6-OHDA lesions as rat models of Parkinson's disease," *Journal of Neuroscience Methods*, vol. 144, no. 1, pp. 35–45, 2005.

[28] H. L. Martin, I. Alsaady, G. Howell et al., "Effect of parasitic infection on dopamine biosynthesis in dopaminergic cells," *Neuroscience*, vol. 306, pp. 50–62, 2015.

[29] A. Klein and W. J. Schmidt, "Catalepsy intensifies context-dependently irrespective of whether it is induced by intermittent or chronic dopamine deficiency," *Behavioural Pharmacology*, vol. 14, no. 1, pp. 49–53, 2003.

[30] A. M. Nayebi, S. R. Rad, M. Saberian, S. Azimzadeh, and M. Samini, "Buspirone improves 6-hydroxydopamine-induced catalepsy through stimulation of nigral 5-HT(1A) receptors in rats," *Pharmacological Reports*, vol. 62, no. 2, pp. 258–264, 2010.

[31] S. K. Prajapati, D. Garabadu, and S. Krishnamurthy, "Coenzyme Q10 prevents mitochondrial dysfunction and facilitates pharmacological activity of atorvastatin in 6-OHDA induced dopaminergic toxicity in rats," *Neurotoxicity Research*, vol. 31, no. 4, pp. 478–492, 2017.

[32] N. Hagelberg, I. K. Martikainen, H. Mansikka et al., "Dopamine D2 receptor binding in the human brain is associated with the response to painful stimulation and pain modulatory capacity," *Pain*, vol. 99, no. 1-2, pp. 273–279, 2002.

[33] J. Gatkowska, M. Wieczorek, B. Dziadek, K. Dzitko, and H. Dlugonska, "Sex-dependent neurotransmitter level changes in brains of *Toxoplasma gondii* infected mice," *Experimental Parasitology*, vol. 133, no. 1, pp. 1–7, 2013.

[34] D. J. Surmeier, J. Ding, M. Day, Z. Wang, and W. Shen, "D1 and D2 dopamine-receptor modulation of striatal glutamatergic signaling in striatal medium spiny neurons," *Trends in Neurosciences*, vol. 30, no. 5, pp. 228–235, 2007.

[35] J. T. Greenamyre and C. F. O'Brien, "N-methyl-D-aspartate antagonists in the treatment of Parkinson's disease," *Archives of Neurology*, vol. 48, no. 9, pp. 977–981, 1991.

[36] A. Hama, J. Woon Lee, and J. Sagen, "Differential efficacy of intrathecal NMDA receptor antagonists on inflammatory mechanical and thermal hyperalgesia in rats," *European Journal of Pharmacology*, vol. 459, no. 1, pp. 49–58, 2003.

[37] G. Veres, A. Fejes-Szabó, D. Zádori et al., "A comparative assessment of two kynurenic acid analogs in the formalin model of trigeminal activation: a behavioral, immunohistochemical and pharmacokinetic study," *Journal of Neural Transmission*, vol. 124, no. 1, pp. 99–112, 2017.

[38] K. Parain, M. G. Murer, Q. Yan et al., "Reduced expression of brain-derived neurotrophic factor protein in Parkinson's disease substantia nigra," *Neuroreport*, vol. 10, no. 3, pp. 557–561, 1999.

[39] M. B. Spina, S. P. Squinto, J. Miller, R. M. Lindsay, and C. Hyman, "Brain-derived neurotrophic factor protects dopamine neurons against 6-hydroxydopamine and N-methyl-4-phenylpyridinium ion toxicity: involvement of the glutathione system," *Journal of Neurochemistry*, vol. 59, no. 1, pp. 99–106, 1992.

[40] J. Remenyi, C. J. Hunter, C. Cole et al., "Regulation of the miR-212/132 locus by MSK1 and CREB in response to neurotrophins," *Biochemical Journal*, vol. 428, no. 2, pp. 281–291, 2010.

[41] S. Impey, M. Davare, A. Lasiek et al., "An activity-induced microRNA controls dendritic spine formation by regulating Rac1-PAK signaling," *Molecular and Cellular Neuroscience*, vol. 43, no. 1, pp. 146–156, 2010.

[42] D. Yang, T. Li, Y. Wang et al., "miR-132 regulates the differentiation of dopamine neurons by directly targeting Nurr1 expression," *Journal of Cell Science*, vol. 125, no. 7, pp. 1673–1682, 2012.

[43] E. S. Son, K. J. Song, J. C. Shin, and H. W. Nam, "Molecular cloning and characterization of peroxiredoxin from *Toxoplasma gondii*," *The Korean Journal of Parasitology*, vol. 39, no. 2, pp. 133–141, 2001.

[44] W. Zhou, J. H. Quan, Y. H. Lee, D. W. Shin, and G. H. Cha, "*Toxoplasma gondii* proliferation require down-regulation of host Nox4 expression via activation of PI3 kinase/Akt signaling pathway," *PLoS One*, vol. 8, no. 6, article e66306, 2013.

Hindawi
BioMed Research International
Volume 2020, Article ID 1295492, 11 pages
https://doi.org/10.1155/2020/1295492

Research Article

Dunaliella salina Attenuates Diabetic Neuropathy Induced by STZ in Rats: Involvement of Thioredoxin

Farouk K. El-Baz,[1] Abeer Salama,[2] and Rania A. A. Salama[3]

[1]*Plant Biochemistry Department, National Research Centre (NRC), 33 El Bohouth St. (Former El-Tahrir St.), 12622 Dokki, Giza, Egypt*
[2]*Pharmacology Department, National Research Centre (NRC), 33 El Bohouth St. (Former El-Tahrir St.), 12622 Dokki, Giza, Egypt*
[3]*Toxicology and Narcotics Department, National Research Centre (NRC), 33 El Bohouth St. (Former El-Tahrir St.), 12622 Dokki, Giza, Egypt*

Correspondence should be addressed to Abeer Salama; berrotec@yahoo.com

Received 11 October 2019; Accepted 10 December 2019; Published 8 January 2020

Guest Editor: Moustafa Gabr

Diabetic neuropathy (DN) is a widespread disabling disorder including peripheral nerves' damage. The aim of the current study was to estimate the potential ameliorative effect of *Dunaliella salina (D. salina)* on DN and the involvement of the thioredoxin. Diabetes was induced by streptozotocin (STZ; 50 mg/kg; i.p). Glimepiride (0.5 mg/kg) or *D. salina* powder (100 or 200 mg/kg) were given orally, after 2 days of STZ injection for 4 weeks. Glucose, total antioxidant capacity (TAC), superoxide dismutase (SOD), and catalase (CAT) serum levels as well as brain contents of thioredoxin (Trx), tumor necrosis factor-alpha (TNF-α), and interleukin-6 (IL-6) were measured with the histopathological study. STZ-induced DN resulted in a significant ($P < 0.05$) rise in glucose blood level and brain contents of TNF-α and IL-6 and produced a reduction in serum TAC, SOD, CAT, and brain Trx levels with irregular islets of Langerhans cells and loss of brain Purkinje cells. Treatment with glimepiride or both doses of *D. salina* alleviated these biochemical and histological parameters as compared to the STZ group. *D. salina* has a neurotherapeutic effect against DN via its inhibitory effect on inflammatory mediators and oxidative stress molecules with its upregulation of Trx activity.

1. Introduction

Diabetic neuropathy (DN) is the most common diabetes complication and its prevalence ranges from 40% to 50% of patients with diabetes. DN induced foot ulcer pain, disability, and recurrent hospitalizations. There is no treatment for DN other than glycemic control [1]. Epidemiology of DN involves poor glycemic control that is a major risk factor for its development and other factors as hyperlipidemia, hypertension, obesity, cigarette smoking, and consumption of alcohol. Diabetes mellitus is associated with neurodegenerative disorders [2]. Hyperglycemia is considered a central key to DN pathogenesis and induces the formation of reactive oxygen species (ROS) damaging the nerves [3, 4] and provokes sensory symptoms that start in the toes then affect the upper limbs by time which is diagnosed by loss of pain sensation [5] using thermal hot plate test [6]. Glucose is necessary to supply central nervous system with energy [7] and hyperglycemia in diabetes can induce also a variety of complications such as nephropathy, retinopathy, and increased risk of cardiovascular disease [8] that are induced by an injection of streptozotocin (STZ) that selectively destructs insulin-producing β-cells of the pancreas experimentally and leads to brain injury [9].

Oxidative stress contributes to diabetes and DN, through the dysfunction of pancreatic β-cell, in which β-cells express low levels of catalase, glutathione peroxidases, and antioxidant enzymes and slowly detoxify ROS [10]. In the DN process, superoxide ($O_2\cdot^-$) is the most common ROS and induces other ROS as it is converted to hydrogen peroxide (H_2O_2) that is detoxified by superoxide dismutase (SOD) and catalase [1]. Another key antioxidant system in DN is

thioredoxin (Trx) which is localized in the mitochondria and the cytoplasm, protects cells from oxidative stress through its disulfide reductase activity, and has as a reciprocal role in disease pathogenesis: autoimmune diseases and cancer [11]. Experimental diabetes impaired Trx in the brain [12].

Antioxidant therapy suppressed oxidative stress in DN. *Dunaliella salina* (*D. salina*) is a natural source of carotenoids and is considered as an antioxidant therapy improving diabetes associated with oxidative stress [13]. Antioxidant defense pathway against oxidative stress and inflammation in DN is an essential task within the brain. Therefore, the present study aimed to evaluate the ameliorative efficacy of *D. salina* against oxidative stress and inflammation in DN induced by STZ in rats through the upregulation of Trx.

2. Materials and Methods

2.1. Cultivation of D. salina in the Vertical Photobioreactor. Algal species *D. salina* isolated from a salt pond in Al-Fayoum are grown by using bold media for algal isolation and purification [14]. After growing *D. salina* for 10 days under lab conditions, they are then transferred to a vertical photobioreactor with a capacity of 4000 L. Reservoir (1000 L) tank associated pipe work proprietary in line pigging systems was used for removal of all biofilms. In addition 10 L basket centrifuge for harvesting connected to the system was used. Alga Connect Data Acquisition System was used for online measurements.

Tap water is used for the cultivation of algae in the PBR. Water is sterilized using hypochlorite; after that sodium thiosulphate is added. Chlorine test is done to ensure no residual chlorine is present. A nutrient solution of bold was used for growing *D. salina*. One millilitre of micronutrient solution was added to the culture medium. To ensure the purity of the culture, samples are taken regularly and examined microscopically. The culture is left to grow until the biomass is reached the maximum (2–2.5 gm/L). Algal biomass is harvested using basket centrifuge at 2000 rpm and dried in a sun dryer where the temperature reached approximately 45°C and then grounded into a homogeneous fine powder.

2.2. Drugs, Chemicals, and Kits. Glimepiride was obtained from Sanofi-Aventis, Egypt. STZ, diethyl ether, sodium citrate, and formaldehyde were obtained from Sigma Aldrich Chemical Co., USA. Total antioxidant capacity (TAC), Superoxide dismutase (SOD), and catalase were purchased from Biodiagnostic, Egypt. Thioredoxin (Trx), tumor necrosis factor-alpha (TNF-α), and interleukin-6 (IL-6) were purchased from NOVA, Beijing, China, Eliza kits.

2.3. Animals. Adult male albino Wister rats weighing 150–200 gm were obtained from the animal house at the National Research Centre (Giza, Egypt) and were fed a standard laboratory diet and tap water ad libitum. Experimental animals were housed in an air-conditioned room at 22–25°C with a 12 h light/dark cycle. All animals received human care and the study protocols were carried out according to the ethical guidelines for care and use of experimental animals approved by the Ethical Committee of the National Research Centre.

2.4. Experimental Design. DN was induced by a single intraperitoneal injection of STZ (50 mg/kg) dissolved in 0.1 M citrate buffer (pH 4.5) [15, 16]. Fifty adult male albino Wister rats were allowed to drink a 5% glucose solution overnight to overcome the drug-induced hypoglycemia. Blood samples were taken 48 h after injection of STZ to ensure that diabetes has been induced and fasting plasma glucose levels of rats were determined using glucose strips (One Touch SureStep Meter, LifeScan, Calif, USA). Rats with plasma glucose concentration $>$300 mg/dl were considered diabetic and included in the experiment [17]. Rats were assigned randomly into five groups. Group 1: normal control rats were treated with the same volume citrate buffer only without STZ for 30 days. Group 2: diabetic control rats (STZ). Group 3: diabetic rats received glimepiride reference drug (0.5 mg/kg; p.o.) [18] for 30 days. Groups 4 and 5: diabetic rats received *D. salina* powder (100 & 200 mg/kg) [19, 20] for 30 days.

2.5. Effects of D. salina on Pain Perception (Hot Plate Test). A hot plate test was conducted using an electronically controlled hot plate (Ugo Basile, Italy) adjusted at 52 ± 0.1°C, and the time elapsed until either paw licking or jumping occurs is recorded [21].

2.6. Preparation of Blood Samples and Determination of Serum Levels of TAC, SOD, and Catalase. At the end of the 30 days of treatment, rats were anesthetized with pentobarbital sodium and blood samples were collected for biochemical analyses. Three ml blood was withdrawn from the retro-orbital plexus vein of each rat for biochemical assays. Blood samples were left to clot at room temperature then centrifuged at 1500 rpm for 10 min for serum separation, and serum samples were stored at −20°C in order to determine TAC, SOD, and catalase serum levels.

2.7. Preparation of Tissue Homogenate and Determination of Brain Contents of Trx, TNF-α, and IL-6. The brains were then excised and washed with saline. Brains were placed in ice-cold phosphate buffer (pH 7.4) to prepare the 20% homogenate that was used for the estimation of brain contents of Trx, TNF-α, and IL-6.

Brain contents of Trx, TNF-α, and IL-6 were determined using ELISA (Enzyme-Linked Immunosorbent Assay) kit. We followed the manufacturer's instructions of NOVA kit, Beijing, China, for calculating the results. Standards and samples were pipetted into wells with immobilized antibodies specific for rat Trx, TNF-α, and IL-6 and then were incubated 30 min at 37°C. After incubation and washing, horseradish peroxidase-conjugated streptavidin was pipetted into the wells and incubated 30 min at 37°C, which was washed once again. Chromogens A & B were added to the wells and incubated 15 min at 37°C; color developed

proportionally to the amount of Trx, TNF-α, and IL-6 bound. Color development was discontinued (Stop Solution) and after 10 min color intensity was measured at 450 nm.

2.8. Histological Examination. The parts of the brain were fixed in 10% formalin solution then dehydrated in ascending grades of alcohol and embedded in paraffin. Four sections/group, at 4 μm thickness, were taken and stained with hematoxylin and eosin (H & E).

2.9. Statistical Analysis. All the values are presented as means ± standard error of the means (SE). Data were evaluated by one-way analysis of variance followed by Tukey's multiple comparisons test. Graph pad Prism software, version 5 (Inc., San Diego, USA) was used to carry out these statistical tests. The difference was considered significant when $P < 0.05$.

3. Results

3.1. Effects of D. salina on Pain Perception (Hot Plate Test). The results indicated, in diabetic rats, a significant loss of pain perception as indicated by elevated withdrawal time in hot plate, while the treatment with *D. salina* powder (100 & 200 mg/kg) reduced the withdrawal time in hot plate as compared to the STZ group. In addition, *D. salina* (200 mg/kg) was more effective by 20% than the standard drug, glimepiride (Table 1).

3.2. Effects of D. salina on Blood Glucose Levels. Animals injected with STZ exhibited a significant elevation in glucose blood levels after 30 days by 2.7-fold, when compared to normal animals. Treatment with glimepiride reduced glucose blood levels after 30 days by 72% when compared to STZ animals. Treatment with *D. salina* powder (100 & 200 mg/kg) reduced blood glucose levels after 30 days by 46% and 69%, respectively, as compared to the STZ group (Figure 1).

3.3. Effects of D. salina on Serum Oxidative Stress Biomarkers. A reduction in serum levels of SOD, CAT, and TAC was observed in the STZ group by 45%, 32%, and 51% respectively, as compared to normal control values. Treatment with glimepiride increased serum levels of SOD, CAT, and TAC by 47%, 30%, and 87%, respectively, as compared to the STZ group. Also, treatment with *D. salina* powder (100 mg/kg) revealed an elevation in serum levels of SOD and TAC only by 49%, and 82%, respectively, as compared to the STZ group, while treatment with *D. salina* powder (200 mg/kg) increased serum levels of SOD, CAT, and TAC by 76%, 31%, and 93%, respectively, as compared to the STZ group (Table 2).

3.4. Effects of D. salina on Brain Content of Trx. STZ injection, after 4 weeks, reduced a brain content of Trx by 97%, as compared with normal values. Treatment with glimepiride elevated a brain content of Trx by 13-fold as compared to the STZ group. Also, treatment with *D. salina* powder (100 mg/kg) produced a rise in brain content of Trx by 24-fold, treatment with *D. salina* powder (200 mg/kg) increased brain content of Trx by 28-fold as compared to STZ group. In addition, *D. salina* (200 mg/kg) has a higher Trx by 46% than the standard drug glimepiride (Figure 2).

3.5. Effects of D. salina on Brain Contents of Inflammatory Biomarkers. Inflammation in the brain was induced by STZ that was evidenced by significant increases in brain contents of TNF-α and IL-6 by 1.3-fold and 3.1-fold, respectively, as compared to normal control values. Treatment with glimepiride decreased brain contents of TNF-α and IL-6 by 42% and 65%, respectively, as compared to the STZ group. Also, treatment with *D. salina* powder (100 mg/kg) showed a reduction in brain contents of TNF-α and IL-6 by 49% and 59%, respectively. Treatment with *D. salina* powder (200 mg/kg) decreased brain contents of TNF-α and IL-6 by 53% and 73%, respectively, as compared to STZ group. In addition, *D. salina* (200 mg/kg) decreased IL-6 by 22% as compared with the standard drug glimepiride (Figure 3).

3.6. Histopathological Results. The pancreatic section from the normal control group showed regular and normal islets of Langerhans (black arrows) and normal acini tissues (yellow arrows), and duct (blue arrow) (Figure 4(a)). The pancreatic section from the STZ group showed irregular islets of Langerhans cells (black arrows) and necrosis of cells (red arrow) (B). The pancreatic section from glimepiride showed almost regular and normal islets of Langerhans (black arrows) and normal acini tissues (red arrows) (C). Pancreatic section from *D. salina* powder (100 mg/kg) group showed near regular and almost normal islets of Langerhans (black arrows) and normal acini tissues (red arrows) (D). Pancreatic section from *D. salina* powder (200 mg/kg) group showed almost regularly and almost normal islets of Langerhans (black arrows) and normal acini tissues (red arrows) (E). (H & E, x400).

Brain section of the normal control group showed normal cerebellum histological features, a well-defined molecular (black arrow), granular layer (red arrow) and Purkinje layers (large Purkinje cells) (yellow arrow) (Figure 5(a)), with normal structure of neuronal cells of the frontal cortex (green arrow) (B). Brain section of the (STZ) control group, showed cerebellum edematous molecular layer (black arrow), disorganized and thin granular layer (red arrow), and Purkinje layers showing moderate loss of Purkinje cells (yellow arrow) (C), with neuronal cells of the frontal cortex, perineuronal edema (blue arrow), widespread edema (blackhead arrow), and proliferation of oligodendroglia "satellitosis" (white arrow) (D). Brain section of the glimepiride group showed the cerebellum molecular layer (black arrow), granular layer (red arrow), and loss of some Purkinje cells (yellow arrow) (E), with normal neuronal cells of the frontal cortex (green arrow), perineuronal edema (blue arrow), and few oligodendroglia "satellitosis" (white arrow) (F). Brain section of the *D. salina* powder (100 mg/kg) group showed the cerebellum molecular

Table 1: Effects of *D. salina* on pain perception (hot plate test).

	Normal control	STZ (50 mg/kg)	Glimepiride (0.5 mg/kg)	*Dunaliella salina* powder (100 mg/kg)	*Dunaliella salina powder* (200 mg/kg)
Withdrawal time (sec)	16.20 ± 0.51	56.80 ± 1.71[a]	31.00 ± 0.45[ab]	32.50 ± 1.12[ab]	24.80 ± 1.06[abc]

Data are presented as the mean ± S.E. ($n = 8$). Statistical analysis was performed by one-way analysis of variance followed by Tukey's multiple comparisons test. [a]significant from the normal group. [b]significant from the STZ group. [c]significant from glimepiride group at $P < 0.05$.

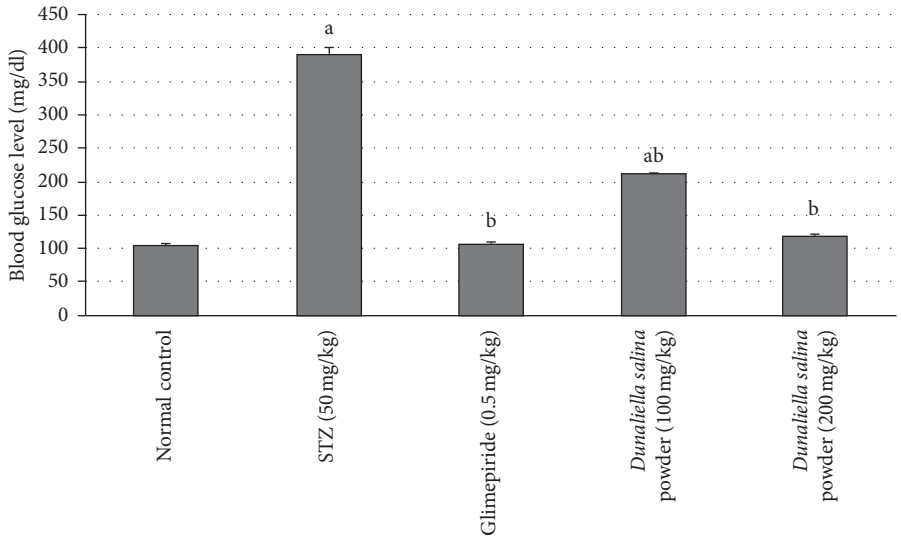

Figure 1: Effects of *D. salina* on blood glucose level. Data are presented as the mean ± S.E. ($n = 8$). Statistical analysis was performed by one-way analysis of variance followed by Tukey's multiple comparisons test. [a]significant from the normal group. [b]significant from the STZ group at $P < 0.05$.

Table 2: Effects of *D. salina* on serum oxidative stress biomarkers.

	Normal control	STZ (50 mg/kg)	Glimepiride (0.5 mg/kg)	*Dunaliella salina* powder (100 mg/kg)	*Dunaliella salina powder* (200 mg/kg)
TAC (mM/L)	0.62 ± 0.04	0.30 ± 0.05[a]	0.57 ± 0.03[b]	0.55 ± 0.07[b]	0.59 ± 0.03[b]
SOD (U/ml)	334.13 ± 5.45	182.66 ± 12.68[a]	268.65 ± 11.96[b]	272.90 ± 22.44[b]	320.65 ± 29.71[b]
Catalase (U/L)	618 ± 3.99	421.31 ± 25.01[a]	546.66 ± 16.79[b]	497.33 ± 1.63[a]	553 ± 33.48[b]

Data are presented as the mean ± S.E. (n=8). Statistical analysis was performed by one-way analysis of variance followed by Tukey's multiple comparisons test. [a]significant from the normal group. [b]significant from the STZ group at $P < 0.05$.

(black arrow), granular layer (red arrow), widespread necrosis, and moderate loss of Purkinje cells (yellow arrow) (G), with almost normal neuronal cells of the frontal cortex (green arrow), perineuronal edema (blue arrow), and proliferation of oligodendroglia "satellitosis" (white arrow) (H). Brain section of the *D. salina* powder (200 mg/kg) group showed the cerebellum almost normal molecular layer (black arrow), granular layer (red arrow), and Purkinje cells (yellow arrow) (I), with almost normal neuronal cells of the frontal cortex (green arrow) and perineuronal edema (blue arrow) (J). (H & E stain, x400).

4. Discussion

Diabetes, in developed countries, is the main reason for neuropathic pain and it is considered the greatest cause of morbidity and mortality in diabetes patients. Diabetic conditions showed a loss of pain perception resulting from neurodegeneration and the development of DN [22]. In the present study, STZ-induced DN. It produced a hyperglycemic effect that was associated with pain perception loss due to nerve damage, while glimepiride or both doses *D. salina* regulated neuropathy progression in STZ-induced diabetic rats that was evidenced by decreasing the time of withdrawal latency that was evaluated by the hot plate method. *D. salina* in high dose decreased the time of withdrawal latency than glimepiride. Moreover, intraperitoneal injection of STZ exerted a necrotic effect on insulin-producing pancreatic β-cells leading to hyperglycemia and a significant decrease in insulin secretion within 48 after its injection. These results are associated with irregular islets of Langerhans cells and necrosis of cells in our

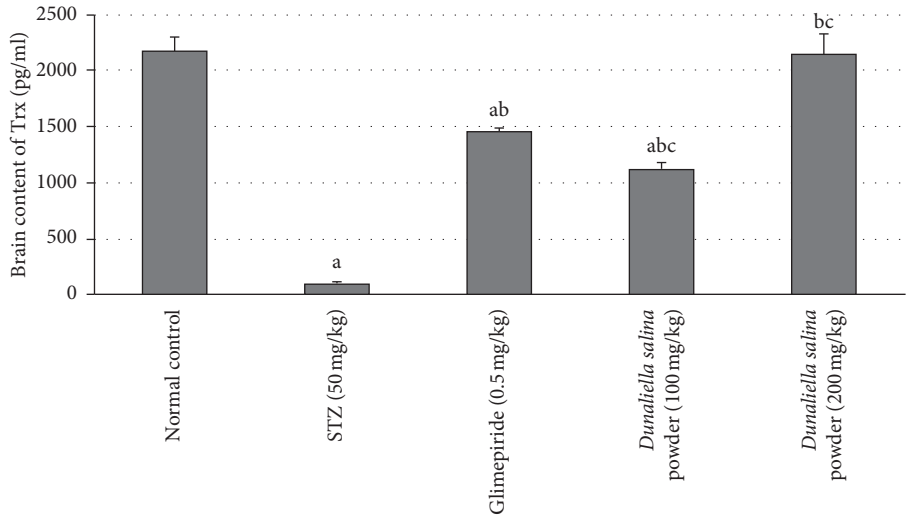

Figure 2: Effects of *D. salina* on brain contents of thioredoxin (Trx). Data are presented as the mean ± S.E. ($n = 8$). Statistical analysis was performed by one-way analysis of variance followed by Tukey's multiple comparisons test. [a]significant from the normal group. [b]significant from the STZ group. [c]significant from glimepride group at $P < 0.05$.

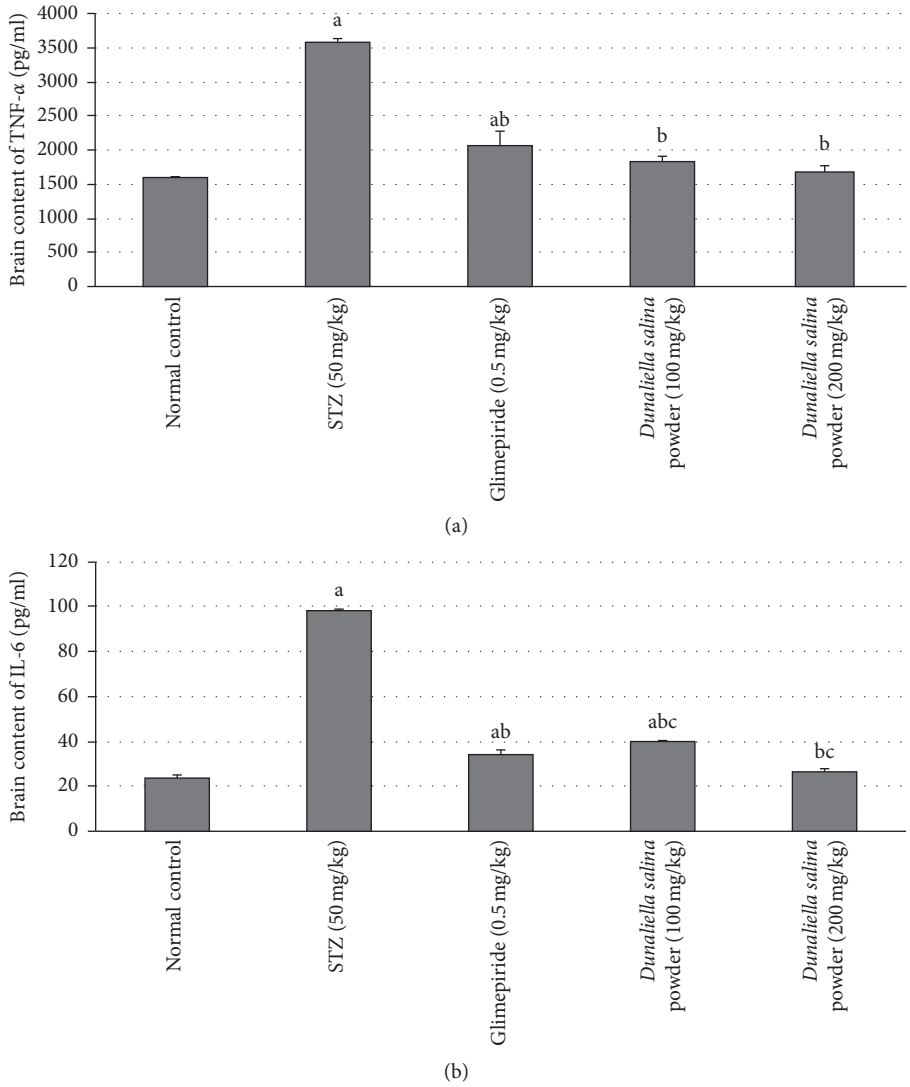

Figure 3: Effects of *D. salina* on brain contents of (a) TNF-α and (b) IL-6. Data are presented as the mean ± S.E. ($n = 8$). Statistical analysis was performed by one-way analysis of variance followed by Tukey's multiple comparisons test. [a]significant from the normal group. [b]significant from the STZ group. [c]significant from glimepride group at $P < 0.05$.

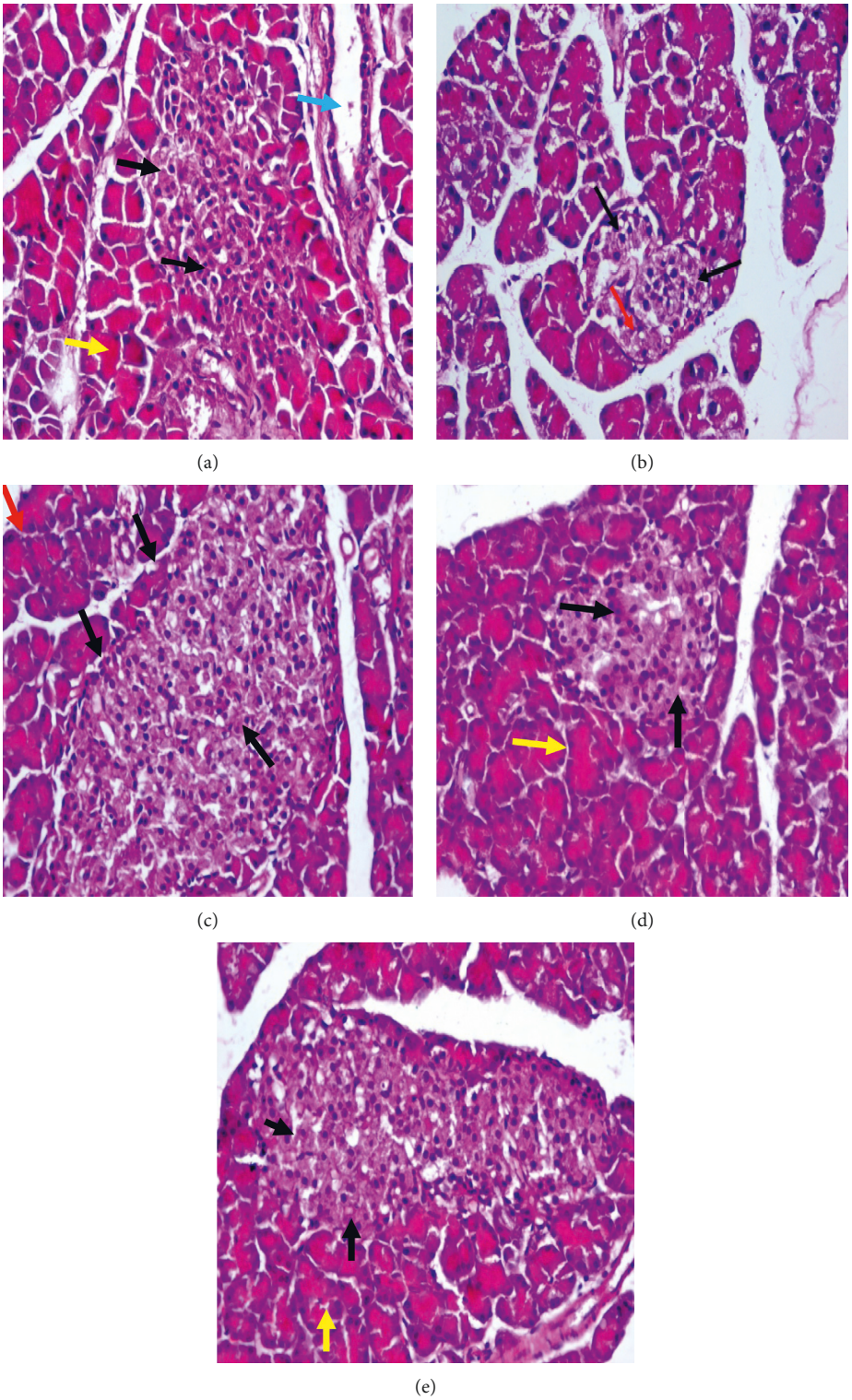

Figure 4: Pancreatic section from the normal control group showed pancreatic islets were shaped regularly and arranged evenly, with normal islets of Langerhans (black arrows) and normal acini tissues (yellow arrows) and duct (blue arrow) (a). Pancreatic section from (STZ) control group showed pancreatic islets with irregular islets of Langerhans cells, not well defined (black arrows), necrosis of cells (red arrow) (b). Pancreatic section from the glimepiride group showed pancreatic islets were shaped almost regularly and arranged evenly, with normal islets of Langerhans (black arrows) and normal acini tissues (red arrows) (c). Pancreatic section from *D. salina* powder 100 mg/kg group showed pancreatic islets were shaped near regularly and arranged evenly, with almost normal islets of Langerhans (black arrows) and normal acini tissues (red arrows) (d). Pancreatic section from *D. salina* powder 200 mg/kg group showed pancreatic islets were shaped almost regularly and arranged evenly, with almost normal islets of Langerhans (black arrows) and normal acini tissues (red arrows) (e). (H&E, x400).

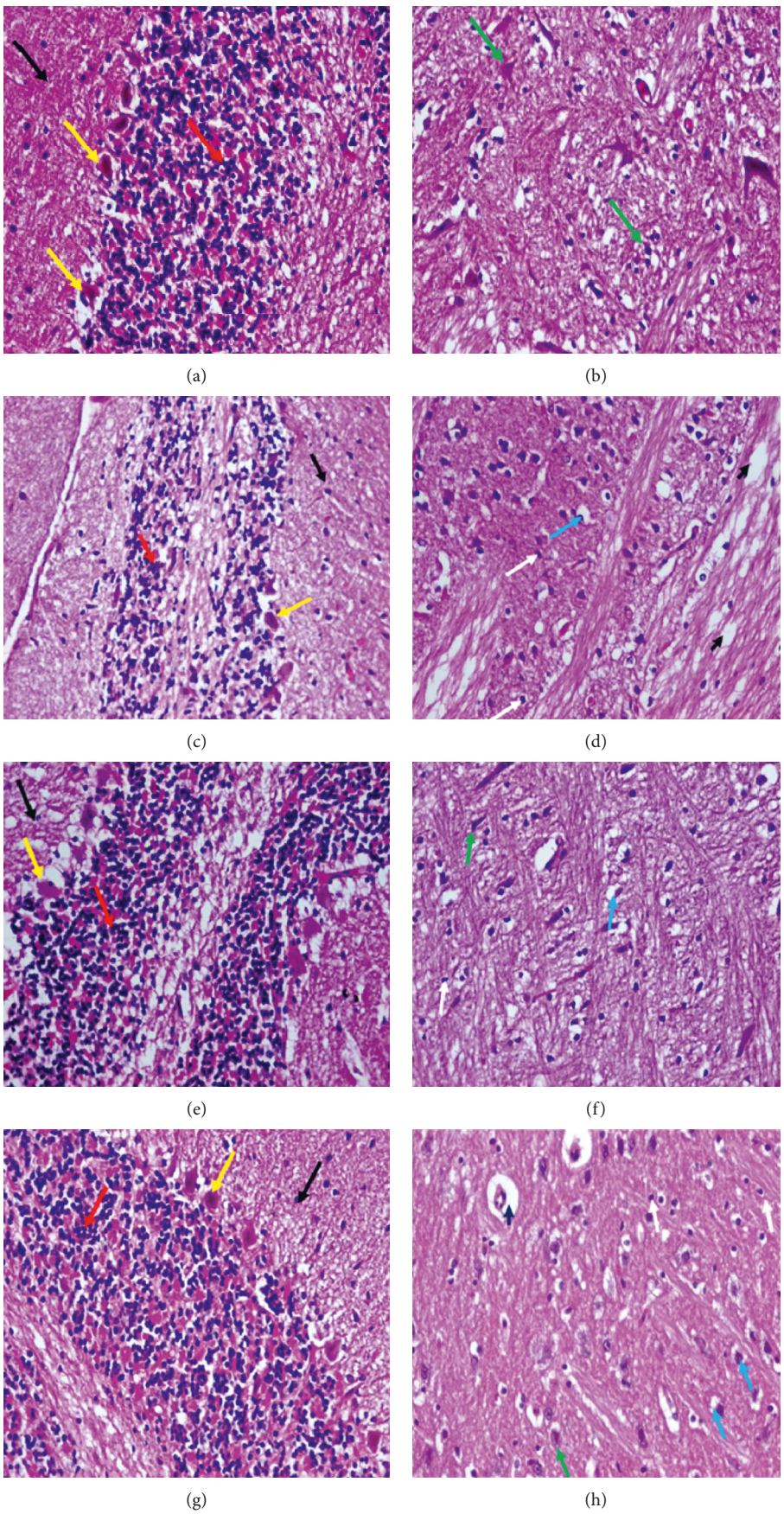

Figure 5: Continued.

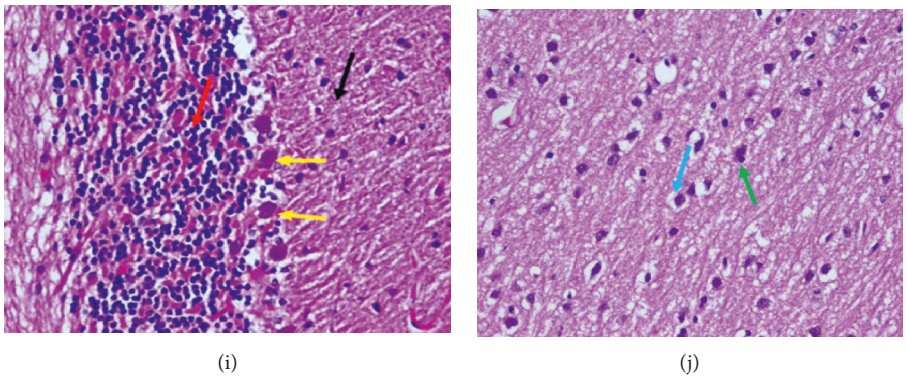

Figure 5: Brain section of normal control group showed the cerebellum showed normal histological features, a well-defined molecular (black arrow), granular (presence of numerous closely packed small cells in the granular layer) (red arrow), and Purkinje layers (large Purkinje cells) (yellow arrow) (a), with normal structure of neuronal cells of the frontal cortex (green arrow) (b). Brain section of the (STZ) control group showed the cerebellum edematous molecular (black arrow), disorganized and thin granular (presence of numerous closely packed small cells in the granular layer) (red arrow), and Purkinje layers showing moderate loss of Purkinje cells (yellow arrow) (c), neuronal cells of the frontal cortex showing perineuronal edema (blue arrow), showing widespread edema (blackhead arrow) and proliferation of oligodendroglia "satellitosis" (white arrow) (d). Brain section of the glimepiride group showed the cerebellum molecular layer (black arrow), granular (presence of numerous closely packed small cells in the granular layer) (red arrow), and loss of some Purkinje cells (yellow arrow) (e), with normal neuronal cells of the frontal cortex (green arrow), perineuronal edema (blue arrow), and few oligodendroglia "satellitosis" (white arrow) (f). Brain section of the *D. Salina* powder 100 mg/kg group showed the cerebellum molecular (black arrow), granular (presence of numerous closely packed small cells in the granular layer) (red arrow), and widespread necrosis and moderate loss of Purkinje cells (yellow arrow) (g), almost normal neuronal cells of the frontal cortex (green arrow), showing perineuronal edema (blue arrow), proliferation of oligodendroglia "satellitosis" (white arrow) (h). Brain section of the *D. Salina* powder 200 mg/kg group showed the cerebellum almost normal molecular layer (black arrow), granular (presence of numerous closely packed small cells in the granular layer) (red arrow), and Purkinje cells (yellow arrow) (i), with almost normal neuronal cells of the frontal cortex (green arrow) and perineuronal edema (blue arrow) (j). (H & E stain, x400).

histopathological study. Several investigations showed that STZ enters the pancreatic β-cells by glucose protein-2 transporter and disrupts the balance between antioxidant and oxidant systems damaging the insulin-producing islet β-cells and inducing the progression of diabetes [23, 24]. Another study showed STZ produced islet β-cells injury, which in turn elevated glucose level and decreased insulin level [25].

The results of the current study indicated that the administration of glimepiride or both doses *D. Salina* significantly alleviated the adverse effects of STZ-induced diabetes. *D. Salina* treatment decreased glucose blood level and increased insulin level with normal islets of Langerhans when compared with rats treated with STZ alone. Previous work showed a decreased level of glucose after *D. salina* administration in STZ diabetic rats [26].

DN progressed in the STZ-treated rats due to the induction of oxidative stress, and this is evidenced by decreased serum levels of TAC, SOD, and catalase and is associated with moderate loss of Purkinje cells and neuronal cells of the frontal cortex showing perineuronal edema. Previous findings showed that STZ enhanced the oxidative stress susceptibility inducing diabetes [23]. Although diabetic complications pathophysiology is multifactorial, animal studies suggest oxidative stress role through elevated levels of ROS that affect many organs [27–30]. In uncontrolled diabetes, oxidative stress is the main feature [31, 32] in which the reduction of antioxidant enzymes activity occurred with elevated blood glucose levels [33]. Moreover, diabetes provoked pathological changes in the central nervous system and damaged mitochondria in the neurons releasing ROS that produced diabetic brain complications [34].

Treatment with glimepiride or *D. saline* ameliorated oxidative stress indices through an elevation in antioxidant contents of TAC, SOD, and catalase and showed normal Purkinje cells and normal neuronal cells of the frontal cortex. These results may be due to *D. saline* high content of carotenoids. Natural products as carotenoids have benefits on diabetes and protect from oxidative damage caused by ROS [35]. Raposo et al. [36] showed the effect of b- carotene on the glutathione regeneration in human trail slowing the complication of diabetes mellitus. Microalgae containing carotenoids have survival mechanisms that scavenge ROS [36]. The previous study exhibited that *D. saline* has an antioxidant effect and recovered the decreased GSH levels in rats [37].

Thioredoxin (Trx) and glutathione are antioxidant thiol-reductase systems that scavenge ROS protecting cells from oxidative stress [38] and regulate redox balance in the brain [39]. Trx is regulated by a thioredoxin-interacting protein (Trxip) [40, 41] which decreases Trx activity inducing oxidative stres and inhibiting cell growth [42]. Trxip links oxidative/glucose stress, inflammation, and cellular injury through a central signaling hub that makes it a promising new target for brain therapy [43]. Trxip decreases the binding of Trx with apoptosis signal-regulating kinase 1 (ASK1) stimulating an ASK1 apoptosis

mediated pathway [44]. In this study, hyperglycemia induced by STZ inhibited the thioredoxin antioxidative role, while glimepiride or both doses of *D. saline* treatment elicited upregulation of Trx activity in rat brain compared with the STZ group. Another study indicated that STZ produced its deleterious metabolic effect in diabetes through the downregulation of the thioredoxin activity [45] and enhanced the levels of Trxip mRNA in diabetic rat brains [12]. Trxip expression after middle cerebral artery occlusion is elevated in hyperglycemic-ischemic mice brains with inflammatory mediators release [46]. Oxidative stress upregulated inflammatory molecules, TNF-α and IL-6, production [47, 48]. TNF-α alters insulin receptor substrate phosphorylation inhibiting the insulin signaling pathway [49]. In the present DN experimental model, STZ injection produced a significant increase in TNF-α and Il-6. Hyperglycemia may trigger inflammatory process elevating proinflammatory cytokines, IL-6 and TNF-α, expression, possibly due to ROS production [50] or reduction of antioxidant defense systems [51, 52]. Glimepiride or both doses *D. salina* administration after STZ treatment resulted in lower serum levels of IL-6 and TNF-α when compared with the diabetic group. *D. saline* administration recovered increased TNF-α and IL-6 levels in previous work [53]. Finally, *D. saline* treatment in high dose level has higher Trx and lower IL-6 than the standard drug glimepiride.

5. Conclusion

D. salina ameliorates DN through stimulation of the two thiol-reductase antioxidant systems, GSH and Trx, and other antioxidant enzymes and inhibition of inflammatory molecules, so it protects the neurons of the brain from oxidative stress and inflammation induced by STZ in rats.

Data Availability

The data used to support the findings of this study are available upon request to the corresponding author.

Conflicts of Interest

The authors declare no conflicts of interest.

Authors' Contributions

Farouk El-Baz and Abeer Salama designed the study. Farouk El-Baz provided the materials. Abeer salama and Rania salama performed the experimental part and biochemical analysis and drafted the manuscript. Abeer Salama analysed and interpreted the data and wrote the final draft of the article. Farouk El-Baz revised the final draft of the written article.

References

[1] C. Figueroa-Romero, M. Sadidi, and E. L. Feldman, "Mechanisms of disease: the oxidative stress theory of diabetic neuropathy," *Reviews in Endocrine and Metabolic Disorders*, vol. 9, no. 4, pp. 301–314, 2008.

[2] M. Ristow, "Neurodegenerative disorders associated with diabetes mellitus," *Journal of Molecular Medicine*, vol. 82, no. 8, pp. 510–529, 2004.

[3] S. Kaur, P. Pandhi, and P. Dutta, "Painful diabetic neuropathy: an update," *Annals of Neurosciences*, vol. 18, no. 4, pp. 168–175, 2011.

[4] A. Grisold, B. C. Callaghan, and E. L. Feldman, "Mediators of diabetic neuropathy: is hyperglycemia the only culprit?," *Current Opinion in Endocrinology & Diabetes and Obesity*, vol. 24, no. 2, pp. 103–111, 2017.

[5] S. Tesfaye and D. Selvarajah, "Advances in the epidemiology, pathogenesis and management of diabetic peripheral neuropathy," *Diabetes/Metabolism Research and Reviews*, vol. 28, no. Suppl 1, pp. 8–14, 2012.

[6] A. W. Bannon and A. B. Malmberg, "Models of nociception: hot-plate, tail-flick, and formalin tests in rodents," *Current Protocols in Neuroscience*, vol. 6, no. 1, 2007.

[7] A. Paoli, A. Bianco, E. Damiani, and G. Bosco, "Ketogenic diet in neuromuscular and neurodegenerative diseases," *BioMed Research International*, vol. 2014, Article ID 474296, 10 pages, 2014.

[8] D. Huang, M. Refaat, K. Mohammedi, A. Jayyousi, J. Al Suwaidi, and C. Abi Khalil, "Macrovascular complications in patients with diabetes and prediabetes," *BioMed Research International*, vol. 2017, Article ID 7839101, 9 pages, 2017.

[9] J. E. Emordi, E. O. Agbaje, I. A. Oreagba, and O. I. Iribhogbe, "Antidiabetic and hypolipidemic activities of hydroethanolic root extract of Uvaria chamae in streptozotocin induced diabetic albino rats," *BMC Complementary and Alternative Medicine*, vol. 16, no. 1, p. 468, 2016.

[10] J. Lu and A. Holmgren, "The thioredoxin antioxidant system," *Free Radical Biology and Medicine*, vol. 66, pp. 75–87, 2014.

[11] E. Yoshihara, Z. Chen, Y. Matsuo, H. Masutani, and J. Yodoi, "Thiol redox transitions by thioredoxin and thioredoxin-binding protein-2 in cell signaling," *Methods in Enzymology*, vol. 474, pp. 67–82, 2010.

[12] Z. Lappalainen, J. Lappalainen, N. K. Oksala et al., "Diabetes impairs exercise training-associated thioredoxin response and glutathione status in rat brain," *Journal of Applied Physiology*, vol. 106, no. 2, pp. 461–467, 2009.

[13] F. K. El-Baz, W. K. Khalil, H. F. Booles, H. F. Aly, and G. H. Ali, "Dunaliella salina suppress oxidative stress, alterations in the expression of pro-apoptosis and inflammation related genes induced by STZ in diabetic rats," *International Journal of Pharmaceutical Sciences Review and Research*, vol. 38, pp. 219–226, 2016.

[14] J. E. Stein, *Handbook of Phycological Methods. Culture Methods and Growth Measurements*, Cambridge University Press, Cambridge, UK, 1975.

[15] A. A. A. Salama, B. M. M. Ibrahim, N. A. Yassin, S. S. Mahmoud, A. A. Gamal El-Din, and N. A. Shaffie, "Regulatory effects of morus alba aqueous leaf extract in streptozotocin-induced diabetic nephropathy," *Der Pharma Chemica*, vol. 9, pp. 46–52, 2017.

[16] E. A. M. Abdel Rasheed, M. I. Attallah, D. A. Ibrahim, and O. G. Shaker, "Doxycycline as anti-inflammatory in rodent model of diabetic neuropathy," *Current Science International*, vol. 7, pp. 493–507, 2018.

[17] A. A. Kassem, S. H. Abd El-Alim, M. Basha, and A. Salama, "Phospholipid complex enriched micelles: a novel drug delivery approach for promoting the antidiabetic effect of

repaglinide," *European Journal of Pharmaceutical Sciences*, vol. 99, pp. 75–84, 2017.

[18] A. A. A. Salama and N. N. Yassen, "A cytoprotectant effect of morus alba against streptozotocin-induced diabetic damage in rat brains," *Der Pharma Chemica*, vol. 9, pp. 24–30, 2017.

[19] F. K. El-Baz, H. F. Aly, and A. A. A. Salama, "Toxicity assessment of the green *Dunaliella salina* microalgae," *Toxicology Reports*, vol. 6, pp. 850–861, 2019.

[20] F. K. El-Baz, A. Salama, and R. A. A. Salama, "Therapeutic effect of *Dunaliella salina* microalgae on thioacetamide-(TAA-) induced hepatic liver fibrosis in rats: role of TGF-$\beta$and MMP9," *BioMed Research International*, vol. 2019, Article ID 7028314, 9 pages, 2019.

[21] W. M. El Kady, A. A. A. Salama, S. Y. Desoukey, E. G. Hagag, S. M. El-Shenawy, and M. A. El-Shanawany, "Comparative DNA profiling, botanical identification and biological evaluation of *Gazania longiscapa* DC and *Gazania rigens* L," *Bulletin of Faculty of Pharmacy, Cairo University*, vol. 53, no. 2, pp. 129–145, 2015.

[22] I. Raz, D. Hasdai, Z. Seltzer, and R. N. Melmed, "Effect of hyperglycemia on pain perception and on efficacy of morphine analgesia in rats," *Diabetes*, vol. 37, no. 9, pp. 1253–1259, 1988.

[23] S. Samarghandian, A. Borji, and S. H. Tabasi, "Effects of Cichorium intybus linn on blood glucose, lipid constituents and selected oxidative stress parameters in streptozotocin-induced diabetic rats," *Cardiovascular & Hematological Disorders-Drug Targets*, vol. 13, no. 3, pp. 231–236, 2013.

[24] P. Strugala, O. Dzydzan, I. Brodyak et al., "Antidiabetic and antioxidative potential of the blue Congo variety of purple potato extract in streptozotocin-induced diabetic rats," *Molecules*, vol. 24, no. 17, p. 3126, 2019.

[25] R. Kumar, V. Arora, V. Ram, A. Bhandari, and P. Vyas, "Hypoglycemic and hypolipidemic effect of allopolyherbal formulations in streptozotocin induced diabetes mellitus in rats," *International Journal of Diabetes Mellitus*, vol. 3, no. 1, pp. 40–45, 2015.

[26] F. K. El-Baz, W. K. Khalil, H. F. Booles, H. F. Aly, and G. H. Ali, "Dunaliella salina suppress oxidative stress, alterations in the expression of pro-apoptosis and inflammation related genes induced by STZ in diabetic rats," *International Journal of Pharmaceutical Sciences and Research*, vol. 38, pp. 219–226, 2016.

[27] P. A. Low and K. K. Nickander, "Oxygen free radical effects in sciatic nerve in experimental diabetes," *Diabetes*, vol. 40, no. 7, pp. 873–877, 1991.

[28] D. F. Mansour, A. A. A. Salama, R. R. Hegazy, E. A. Omara, and S. A. Nada, "Whey protein isolate protects against cyclophosphamide-induced acute liver and kidney damage in rats," *Journal of Applied Pharmaceutical Science*, vol. 7, no. 6, pp. 111–120, 2017.

[29] R. E. Mostafa, A. A. A. Salama, R. F. Abdel-Rahman, and H. A. Ogaly, "Hepato- and neuro-protective influences of biopropolis on thioacetamide-induced acute hepatic encephalopathy in rats," *Canadian Journal of Physiology and Pharmacology*, vol. 95, no. 5, pp. 539–547, 2017.

[30] O. O. Oguntibeju, "Type 2 diabetes mellitus, oxidative stress and inflammation: examining the links," *International Journal of Physiology, Pathophysiology and Pharmacology*, vol. 11, no. 3, pp. 45–63, 2019.

[31] K. Horie, T. Miyata, K. Maeda et al., "Immunohistochemical colocalization of glycoxidation products and lipid peroxidation products in diabetic renal glomerular lesions. Implication for glycoxidative stress in the pathogenesis of diabetic nephropathy," *Journal of Clinical Investigation*, vol. 100, no. 12, pp. 2995–3004, 1997.

[32] H. Yang, X. Jin, C. W. Kei Lam, and S.-K. Yan, "Oxidative stress and diabetes mellitus," *Clinical Chemistry and Laboratory Medicine*, vol. 49, no. 11, pp. 1773–1782, 2011.

[33] F. A. Matough, S. B. Budin, Z. A. Hamid, N. Alwahaibi, and J. Mohamed, "The role of oxidative stress and antioxidants in diabetic complications," *Sultan Qaboos University Medical Journal*, vol. 12, no. 1, pp. 5–18, 2012.

[34] S. M. A. Sangi and N. A. A. Jalaud, "Prevention and treatment of brain damage in streptozotocin-induced diabetic rats with metformin, nigella sativa, zingiber officinale, and punica granatum," *Biomedical Research and Therapy*, vol. 6, no. 7, pp. 3274–3285, 2019.

[35] N. Arun and D. P. Singh, "A review on pharmacological applications of halophilic alga dunaliella," *Indian Journal of Geo-Marine Science*, vol. 45, pp. 440–447, 2016.

[36] M. Raposo, A. de Morais, and R. de Morais, "Carotenoids from marine microalgae: a valuable natural source for the prevention of chronic diseases," *Marine Drugs*, vol. 13, no. 8, pp. 5128–5155, 2015.

[37] F. F. Madkour and M. M. Abdel-Daim, "Hepatoprotective and antioxidant activity of dunaliella salina in paracetamol-induced acute toxicity in rats," *Indian Journal of Pharmaceutical Sciences*, vol. 75, no. 75, pp. 642–648, 2013.

[38] A. Holmgren, C. Johansson, C. Berndt, M. E. Lönn, C. Hudemann, and C. H. Lillig, "Thiol redox control via thioredoxin and glutaredoxin systems," *Biochemical Society Transactions*, vol. 33, no. 6, pp. 1375–1377, 2005.

[39] X. Ren, L. Zou, X. Zhang et al., "Redox signaling mediated by thioredoxin and glutathione systems in the central nervous system," *Antioxidants & Redox Signaling*, vol. 27, no. 13, pp. 989–1010, 2017.

[40] P. C. Schulze, G. W. De Keulenaer, J. Yoshioka, K. A. Kassik, and R. T. Lee, "Vitamin D3-upregulated protein-1 (VDUP-1) regulates redox-dependent vascular smooth muscle cell proliferation through interaction with thioredoxin," *Circulation Research*, vol. 91, no. 8, pp. 689–695, 2002.

[41] K. Nagaraj, L. Lapkina-Gendler, R. Sarfstein et al., "Identification of thioredoxin-interacting protein (TXNIP) as a downstream target for IGF1 action," *Proceedings of the National Academy of Sciences*, vol. 115, no. 5, pp. 1045–1050, 2018.

[42] J. A. Morrison, L. A. Pike, S. B. Sams et al., "Thioredoxin interacting protein (TXNIP) is a novel tumor suppressor in thyroid cancer," *Molecular Cancer*, vol. 13, no. 1, p. 62, 2014.

[43] J. M. Abais, M. Xia, Y. Zhang, K. M. Boini, and P.-L. Li, "Redox regulation of NLRP3 inflammasomes: ROS as trigger or effector?," *Antioxidants & Redox Signaling*, vol. 22, no. 13, pp. 1111–1129, 2015.

[44] S. Nasoohi, S. Ismael, and T. Ishrat, "Thioredoxin-interacting protein (TXNIP) in cerebrovascular and neurodegenerative diseases: regulation and implication," *Molecular Neurobiology*, vol. 55, no. 10, pp. 7900–7920, 2018.

[45] B. I. Ogunyinka, B. E. Oyinloye, F. O. Osunsanmi, A. R. Opoku, and A. P. Kappo, "Proteomic analysis of differentially-expressed proteins in the liver of streptozotocin-induced diabetic rats treated with parkia biglobosa protein isolate," *Molecules*, vol. 23, no. 2, p. 156, 2018.

[46] D. Silva-Adaya, M. E. Gonsebatt, and J. Guevara, "Thioredoxin system regulation in the central nervous system: experimental models and clinical evidence," *Oxidative Medicine and Cellular Longevity*, vol. 2014, Article ID 590808, 13 pages, 2014.

[47] E. Shahady, "Hyperlipidemia in diabetes—etiology, consequences, and treatment," *Circulation*, vol. 91, pp. 2844–2850, 1995.

[48] J. Colado-Velazquez III, P. Mailloux-Salinas, J. M. L. Medina-Contreras, D. Cruz-Robles, and G. Bravo, "Effect of serenoa repens on oxidative stress, inflammatory and growth factors in obese wistar rats with benign prostatic hyperplasia," *Phytotherapy Research*, vol. 29, no. 10, pp. 1525–1531, 2015.

[49] H. S. El-Abhar and M. F. Schaalan, "Topiramate-induced modulation of hepatic molecular mechanisms: an aspect for its anti-insulin resistant effect," *PLoS One*, vol. 7, no. 5, Article ID e37757, 2012.

[50] A. Ceriello, L. Quagliaro, L. Piconi et al., "Effect of postprandial hypertriglyceridemia and hyperglycemia on circulating adhesion molecules and oxidative stress generation and the possible role of simvastatin treatment," *Diabetes*, vol. 53, no. 3, pp. 701–710, 2004.

[51] A. C. Carr, B.-Z. Zhu, and B. Frei, "Potential antiatherogenic mechanisms of ascorbate (vitamin C) and α-tocopherol (vitamin E)," *Circulation Research*, vol. 87, no. 5, pp. 349–354, 2000.

[52] E. Emara and M. Elsawy, "The impact of ghrelin on oxidative stress and inflammatory markers on the liver of diabetic rats," *Tanta Medical Journal*, vol. 44, no. 4, pp. 163–169, 2016.

[53] D. Obistioiu, R. T. Cristina, I. Schmerold et al., "Chemical characterization by GC-MS and in vitro activity against *Candida albicans* of volatile fractions prepared from *Artemisia dracunculus*, *Artemisia abrotanum*, *Artemisia absinthium* and *Artemisia vulgaris*," *Chemistry Central Journal*, vol. 8, no. 1, p. 6, 2014.

Hindawi
BioMed Research International
Volume 2019, Article ID 2072635, 6 pages
https://doi.org/10.1155/2019/2072635

Research Article

Cell Ratio Differences in Peripheral Blood between Early- and Late-Onset Parkinson's Disease: A Case-Control Study

Sen Jiang,[1] Yuling Wang,[1,2] Hua Gao,[1,3] Qin Luo,[4] Dan Wang,[1] Yanxia Li,[5] Yuxuan Yong,[1] and Xinling Yang[1]

[1]*Department of Neurology, Second Affiliated Hospital of Xinjiang Medical University, No. 38, Nanhudonglu Road, Urumqi 830054, China*
[2]*Medicine VIP, First Affiliated Hospital of Xinjiang Medical University, No. 137, Liyushanlu Road, Urumqi 830011, China*
[3]*Department of Neurology, Fifth Affiliated Hospital of Xinjiang Medical University, No. 118, Henanxilu Road, Urumqi 830000, China*
[4]*Department of Medicine, Tumor Hospital Affiliated of Xinjiang Medical University, No. 789, Suzhoudongjie Road, Urumqi 830000, China*
[5]*Department of Rehabilitation, Second Affiliated Hospital of Xinjiang Medical University, No. 38, Nanhudonglu Road, Urumqi 830054, China*

Correspondence should be addressed to Xinling Yang; yangxinling2014@163.com

Received 16 July 2019; Accepted 5 September 2019; Published 7 November 2019

Guest Editor: Mohamed Benchekroun

Objectives. To explore the differences of immune disorders in peripheral blood between patients with early-onset Parkinson's disease (EOPD) and late-onset Parkinson's disease (LOPD). *Methods*. We retrospectively reviewed medical records of Parkinson's disease (PD) patients and healthy controls between June 2002 and July 2017. At last, we included 117 PD patients who were divided into EOPD and LOPD according to whether onset age of PD was after 50 and 99 controls divided into E-Control (match for EOPD) and L-Control (match for LOPD) according to whether their age was after 53 which was onset age plus median of disease duration. We compared the ratios of cells between multiple groups and performed the multinominal logistic regression analysis to explore the relationship between ratios and subtypes of PD. We also carried out the receiver operating characteristic (ROC) curve analysis to estimate the diagnostic value of the variable. *Results*. Lymphocyte-red blood cell ratio (LRR) was lower in LOPD compared with that in EOPD or L-Control. LRR was also negatively associated with LOPD (OR: 0.623; 95% CI: 0.397–0.980; $P = 0.040$). The ROC curve analysis showed the optimal cutoff value of 4.53 ($\times 10^{-4}$) of LRR for discrimination of LOPD versus L-Control (sensitivity: 0.596, specificity: 0.764). The area under curve (AUC) was 0.721. As for LOPD versus EOPD, the optimal threshold of LRR was 4.10 ($\times 10^{-4}$) (sensitivity: 0.516, specificity: 0.745). AUC was 0.641. *Conclusions*. Peripheral immune disorders might play an important part in the pathological progression of LOPD. Also, LRR has potential diagnostic value.

1. Introduction

Parkinson's disease (PD) is a neurodegenerative disorder with the pathological change of degeneration of substantia nigra and clinical characteristics of bradykinesia, rigidity, and resting tremor. The onset age of PD is usually after 50. However, it is often found in clinical practice that some patients show symptoms of PD at a young age. These patients have relatively unique clinical features, such as tremor with small amplitude and fast frequency with relatively good response to drug treatment, yet rarely pill-rolling tremor [1]. Therefore, researchers could classify PD into early-onset PD (EOPD) and late-onset PD (LOPD) based on the patient's onset age.

However, there is some controversy regarding the onset age for discriminate EOPD versus LOPD. Not all researchers accept age 50, and some still define the age 40 or 45 as the dividing line. However, a study with large sample of twins in

1999 showed that genetic factors play an important role in the pathological progression of PD with onset before age 50 but have no effects on that with onset after age 50 [2]. Then, subsequent research suggested that effects of genetic factors on LOPD are smaller than those on EOPD [3]. Therefore, it is reasonable to define age of 50 years as the dividing line between EOPD and LOPD based on the effects of genetic factors.

Recently, some studies showed the evidence for the role of immune disorders in the pathological progression of PD, which gets more and more attention. For example, microglia in Central Nervous System (CNS) gets activated [4] and releases the inflammatory factors [5]; lymphocyte regulates the inflammatory response in CNS [6]; some peripheral immune cells change their numbers during the progression of PD [7]; and neutrophil-lymphocyte ratio (NLR) decreases in PD patients [8]. However, no studies have ever reported the relationship between immune factor and EOPD or LOPD.

Peripheral blood cells that involve neutrophil (NEU), lymphocyte (LY), monocyte (MO), eosinophil (EO), basophil (BA), red blood cell (RBC), and platelet (PLT) have certain immune capabilities. Based on the counts of the cells, we can calculate some ratios that reflect information from two different cells at the same time to indicate the disorders of peripheral immune function, such as NLR, which usually plays a prognostic role in cancer [9]. In this study, we compared the ratios in EOPD patients with those in LOPD patients and used the multinominal logistic regression analysis to explore the association of peripheral immune disorders with EOPD and LOPD. We also performed receiver operating characteristic (ROC) curve analysis to estimate the potential diagnostic value of significant indicator.

2. Methods

2.1. Participants. We retrospectively reviewed the medical records of subjects who sought for health checkup or treatment for PD in First Affiliated Hospital of Xinjiang Medical University between June 2002 and July 2017. Their medical records included the patients' information, such as age, gender, duration of disease, smoking history, symptoms and signs at admission, results of auxiliary examination, and diagnosis at discharge. The severity of PD was quantified by the modified Hoehn–Yahr (HY) Scale.

Two neurologists asked patients who sought for treatment for PD about their history of present illness and past history, performed the physical examination on them, and decided which auxiliary examinations are needed, such as Blood Routine (BR) Examination and Magnetic Resonance Imaging. At last, the two neurologists made the diagnosis following the United Kingdom Parkinson's Disease Society Brain Bank Clinical Diagnostic Criteria [10].

PD group inclusive criteria were diagnosis of PD, normal nutritional status, and no diarrhea.

Control group inclusive criteria were healthy individuals matched to PD patients on age, gender, and smoking history; normal nutritional status; and no diarrhea.

Exclusive criteria were as follows: be vaccinated within 3 months; use of immunosuppressant or immune booster within 3 months; chronic neurodegenerative disease other than PD; cancer; infectious disease; chronic inflammation; and systemic disease.

At last, we did not get enough controls to apply 1 : 1 match and included a total of 117 PD patients and 99 controls into this study. The dividing line for onset age was age 50 [2]. Of the 117 PD patients, 62 were EOPD and 55 were LOPD. The median of disease duration of all patients was 3 years. So we divided the controls according to age of 53 years which was onset age plus disease duration. Of 99 controls, 42 were matched to EOPD patients (E-Control) and 57 were matched to LOPD patients (L-Control).

When the participants were admitted to the hospital, they signed an informed consent to declare to agree on sharing their medical information for research. The study was carried out in accordance with the Helsinki Declaration. The protocol was approved by the Ethics Committee of the First Affiliated Hospital of Xinjiang Medical University.

2.2. Ratios of Cells. The nurse took the blood sample from the vein in the antecubital fossa of patients with an empty stomach on the second day after admission. An automated hematology analyzer (SYSMEX 2000; Sysmex Corp., Kobe, Japan) analyzed the blood sample. The result provided the counts of 7 kinds of cells, NEU, LY, MO, EO, BA, RBC, and PLT. We can calculate the different ratios by dividing any two numbers of cells, including NLR, neutrophil-monocyte ratio (NMR), basophil-neutrophil ratio (BNR), eosinophil-neutrophil ratio (ENR), lymphocyte-monocyte ratio (LMR), eosinophil-lymphocyte ratio (ELR), basophil-lymphocyte ratio (BLR), eosinophil-monocyte ratio (EMR), basophil-monocyte ratio (BMR), basophil-eosinophil ratio (BER), neutrophil-platelet ratio (NPR), lymphocyte-platelet ratio (LPR), monocyte-platelet ratio (MPR), eosinophil-platelet ratio (EPR), basophil-platelet ratio (BPR), neutrophil-red blood cell ratio (NRR), lymphocyte-red blood cell ratio (LRR), monocyte-red blood cell ratio (MRR), eosinophil-red blood cell ratio (ERR), basophil-red blood cell ratio (BRR), and platelet-red blood cell ratio (PRR).

2.3. Statistical Analysis. We used SPSS 22.0 software (SPSS Inc., Chicago, IL, USA) for statistical analysis and entered all data into the software. The qualitative variables were assessed by Pearson's Chi-squared test or Fisher's exact test. The normality of quantitative data was detected by analytic methods (e.g., Kolmogorov–Smirnov test or Shapiro–Wilk test). When the variable was compliant with normal distribution, it was presented as mean (standard deviations (SD)). We used one way analysis of variance (one-way ANOVA) to compare means between multiple groups. When the variable was not normally distributed, it was presented as median (interquartile (IQR)). We used the Mann–Whitney U test for comparison between two groups and the Kruskal–Wallis test between multiple groups.

In addition, we used the multinominal logistic regression analysis of significant variables with EOPD or LOPD to

explore the association of ratios of cells with subtypes of PD. Then we performed ROC curve analysis to estimate the diagnostic value of the variable. The value with the largest Youden index was the optimal cutoff point. We also calculated area under curve (AUC).

If the missing data was less than 5% of the sample, we would not carry out any process. All tests were 2-sided. $P < 0.05$ was statistically significant.

3. Results

3.1. Comparison of Characteristics between Groups. Table 1 shows the comparisons of baseline characteristics. EOPD group included 62 patients; LOPD included 55; E-Control included 42; and L-Control included 57. The median onset age in EOPD was significantly lower than that in LOPD. There were differences of age between any two groups except for EOPD versus E-Control or LOPD versus L-Control ($P > 0.999$). Also, there were no differences of duration of PD and HY scales between EOPD and LOPD and no smoking history and gender differences between any two groups.

3.2. Comparison of Ratios between Groups. We compared different ratios between multiple groups (Table 2). We excluded 2 patients because of their incomplete data, which was the error occurred randomly in the transition from paper medical records to electronic medical records. There were increment of NLR and decrement of LMR, LPR, and LRR in LOPD relative to L-Control ($P = 0.003$, $P = 0.017$, $P = 0.018$, and $P < 0.001$). LRR also decreased in LOPD relative to EOPD or E-Control ($P = 0.018$, $P = 0.003$). As for E-Control versus L-Control, only BER was higher in E-Control ($P = 0.014$). When we compared EOPD with L-Control, LPR and LRR decreased in EOPD ($P = 0.004$, $P = 0.037$), while BER increased ($P = 0.024$).

3.3. Multinominal Logistic Regression Analysis of Significant Variables. We included 61 EOPD patients, 54 LOPD patients, 42 E-Controls, and 57 L-Controls in the model. The group was dependent variable (EOPD = 1, LOPD = 2, E-Control = 3, and L-Control = 4). We also included age, sex, and smoking history to adjust the model and NLR, LMR, BER, LPR, and LRR as independent variables, the variance inflation factors of which were all smaller than 2 (data not shown), indicating no existence of multi-collinearity. The reference category was L-Control. The results are shown in Table 3. LRR was negatively associated with LOPD.

3.4. ROC Curve Analysis of LRR. We performed ROC curve analysis to estimate the diagnostic value of LRR (Figures 1 and 2). The data of 61 EOPD patients, 54 LOPD patients, and 57 L-Controls were available. The optimal cutoff value for discriminate LOPD versus L-Control was 4.53 ($\times 10^{-4}$) when the largest Youden index was 0.360 (sensitivity: 0.596, specificity: 0.764). And, the AUC was 0.721 (Table 4). We also obtained an optimal cutoff value 4.10 ($\times 10^{-4}$) with the largest youden index of 0.262 to differentiate LOPD versus EOPD (sensitivity: 0.516; specificity: 0.745). And, the AUC was 0.641 (Table 4).

4. Discussion

We found the decrement of LRR in LOPD compared with that in EOPD or L-Control. Besides, between LOPD and L-Control, we also found the increment of NLR and decrement of LMR and LPR in LOPD. After multinominal logistic regression analysis, we observed the association of LRR with LOPD. The ROC curve analysis also showed the LRR has diagnostic value for discriminate LOPD versus L-Control or LOPD versus EOPD. According to our search in the database, it is the first study to explore the differences of peripheral immune disorders between EOPD and LOPD patients.

The previous researches regarding EOPD and LOPD focused on the genetic factor, which has more effects on the pathological progression of EOPD [3], whereas, in our research, we studied the immune factor which is associated with LOPD. Some studies also have reported the relationship between ratios of blood cells and PD. As the commonly used indicator for systemic inflammation, some studies suggested the increment of NLR in PD patients. In addition, researchers found the NLR is not only higher in PD patients [8], but also positively associated with severity of PD [11]. Nevertheless, not all results are consistent. Someone compared NLR between patients with different clinical manifestations and observed no differences [12]. In this study, it was found that NLR was higher in LOPD patients compared with that in L-Control. However, based on our findings, LRR might play an more important role than the NLR in the pathological progression of LOPD.

There have been some evidence suggested that LY and RBC take their effects on the pathological progression of PD, such as the accumulation of T lymphocytes in CNS in animal model [13] and PD patients [14]. Whether lymphocyte activates the microglia or microglia leads to the accumulation of T lymphocytes in CNS is still not clear. However, the procession plays an important role in the inflammatory response in the CNS of PD patients. After being activated, microglia will release some inflammatory factors [5] to regulate the inflammatory response. On the other hand, the cellular immune response leads to death of dopamine (DA) neurons via CD4+ T lymphocytes-dependent Fas/Fasl [6]. Besides, someone also observed the decrement of CD3+ T lymphocytes [7] in peripheral blood of PD patients. It is still not clear how inflammatory response in CNS affects the peripheral immune cell. Because of lack of evidence, it is only an assumption that neuron-immune network has an effect on the progression.

One of the characteristic pathological manifestations of PD is the accumulation of Lewy bodies in neurons of CNS, which is composed of alpha-synuclein (α-syn) with rich content in CNS [15]. The α-syn oligomer in cerebrospinal fluid with more toxicity than α-syn monomer [16] can be used as the indicator for the diagnosis of Parkinson's disease [17]. In addition, α-syn can penetrate the blood-brain barrier

Table 1: Characteristics of the included population.

	EOPD ($n = 62$)	E-Control ($n = 42$)	LOPD ($n = 55$)	L-control ($n = 57$)	P
Onset age, median (IQR), y	44.00 (8.00)	—	57.00 (6.83)	—	<0.001a*
Age, median (IQR), y	48.00 (7.00)	46.50 (5.00)	60.00 (6.00)	61.00 (9.00)	<0.001b*
Duration, median (IQR), y	3.00 (3.50)	—	2.00 (3.00)	—	0.05[a]
HY, median (IQR)	2.00 (2.00)	—	2.00 (0.50)	—	0.602[a]
Sex					
Female (%)	29 (46.8)	26 (61.9)	29 (52.7)	34 (59.6)	0.376[c]
Male (%)	33 (53.2)	16 (38.1)	26 (47.3)	23 (40.4)	
Smoking					
No	52 (83.9)	37 (88.1)	46 (83.6)	45 (78.9)	0.684[c]
Yes	10 (16.1)	5 (11.9)	9 (16.4)	12 (21.1)	

[a]Mann–Whitney U test. [b]Kruskal–Wallis test. [c]Pearson's Chi-squared test. *$P < 0.001$.

Table 2: Intergroup comparison of cell ratios.

	EOPD ($n = 61$)	E-Control ($n = 42$)	LOPD ($n = 54$)	L-control ($n = 57$)	P
NLR, median (IQR)	1.733 (0.715)	1.888 (1.037)	2.039 (1.289)	1.539 (0.694)	0.008a*
NMR, median (IQR)	8.194 (3.772)	8.663 (4.211)	9.370 (4.217)	9.027 (4.265)	0.275[a]
BNR, median (IQR), $\times 10^{-2}$	0.631 (0.717)	0.634 (0.764)	0.460 (0.459)	0.465 (0.723)	0.109[a]
ENR, median (IQR), $\times 10^{-2}$	3.543 (2.837)	3.322 (2.904)	3.301 (3.237)	3.721 (5.107)	0.315[a]
LMR, median (IQR),	5.042 (2.678)	5.283 (2.678)	4.274 (3.103)	5.405 (3.185)	0.011a*
ELR, median (IQR), $\times 10^{-2}$	6.122 (4.300)	5.580 (5.153)	6.790 (6.975)	5.983 (6.442)	0.851[a]
BLR, median (IQR), $\times 10^{-2}$	1.020 (1.350)	1.105 (0.991)	0.833 (1.293)	0.823 (0.885)	0.066[a]
EMR, median (IQR),	0.290 (0.272)	0.309 (0.220)	0.288 (0.269)	0.388 (0.381)	0.139[a]
BMR, median (IQR), $\times 10^{-2}$	5.556 (7.438)	6.667 (5.978)	4.226 (4.298)	5.000 (6.388)	0.129[a]
BER, median (IQR),	0.188 (0.259)	0.200 (0.229)	0.155 (0.188)	0.125 (0.183)	0.035a*
NPR, median (IQR), $\times 10^{-2}$	1.525 (0.675)	1.729 (1.046)	1.694 (0.990)	1.861 (0.999)	0.300[a]
LPR, median (IQR), $\times 10^{-2}$	0.872 (0.488)	0.873 (0.351)	0.854 (0.541)	1.077 (0.487)	0.003a*
MPR, median (IQR), $\times 10^{-2}$	0.186 (0.089)	0.182 (0.087)	0.199 (0.137)	0.188 (0.112)	0.718[a]
EPR, median (IQR), $\times 10^{-3}$	0.519 (0.458)	0.582 (0.484)	0.510 (0.683)	0.700 (0.733)	0.214[a]
BPR, median (IQR), $\times 10^{-3}$	0.108 (0.131)	0.122 (0.112)	0.074 (0.085)	0.089 (0.104)	0.182[a]
NRR, median (IQR), $\times 10^{-3}$	0.758 (0.268)	0.861 (0.412)	0.798 (0.328)	0.726 (0.327)	0.703[a]
LRR, mean (SD), $\times 10^{-4}$	4.455 (1.166)	4.659 (1.335)	3.880 (1.048)	4.920 (1.404)	<0.001b*
MRR, mean (SD), $\times 10^{-4}$	0.973 (0.291)	0.919 (0.349)	0.889 (0.302)	0.905 (0.322)	0.479[b]
ERR, median (IQR), $\times 10^{-4}$	0.270 (0.213)	0.252 (0.226)	0.261 (0.248)	0.291 (0.304)	0.344[a]
BRR, median (IQR), $\times 10^{-4}$	0.044 (0.067)	0.052 (0.057)	0.031 (0.048)	0.045 (0.053)	0.063[a]
PRR, median (IQR), $\times 10^{-2}$	4.784 (1.689)	4.942 (1.438)	4.538 (2.190)	4.518 (1.763)	0.205[a]

[a]Kruskal–Wallis test. [b]one-way ANOVA. *$P < 0.05$.

to the peripheral blood. 99% of α-syn entered the blood accumulate in the RBC, and 0.1% are present in plasma [18]. High concentration of free iron in RBC might be the reason of aggregation of α-syn oligomers in these cells [19]. Furthermore, there is a paper showing the relationship between homocysteine (HCY) and PD [20], which reflects the oxidative stress in CNS. The metabolism of HCY requires vitamin B12 as coenzyme. Some studies also found the decrement of vitamin B12 in PD patients [21] that can lead to the megaloblastic anemia. Through above two routes, RBC plays an important part in the peripheral immune disorders of PD.

Moreover, it has been reported that RBC activates the immune function of T lymphocytes by interaction between CD58, CD59 on the surface of RBC, and CD2 on the surface of T helper cell [22]. RBC can also promote proliferation and differentiation of B lymphocytes to produce immunoglobulins [22]. Variation of LRR might reflect the information of the interaction between lymphocyte and RBC. Thus, we could make an assumption that interaction also has its effect on the pathological progression of LOPD.

This study is limited. First, doctors have recorded the accurate drug history in patients' medical records since only a few years ago. Unfortunately, drug history is not detailed enough before that. Because of the lack of these data, we cannot exclude confounding factors that the drugs individuals used in this study. Second, this is a hospital-based study. The selection of study subjects is not random. Thus, biases are certainly existent. Last, genetic factors have been proved to be related with EOPD [3]. However, because our research is a retrospective study, we cannot obtain the subjects' genetic information to analyze the interaction between immune and gene in PD patients.

Table 3: Multinominal logistic regression analysis of ratios of cells.

	P	OR	95% Confidence Interval for OR	
			Lower bound	Upper bound
EOPD				
Age	<0.001*	0.548	0.455	0.661
NLR	0.567	0.748	0.277	2.019
LMR	0.280	0.863	0.660	1.128
BER	0.481	3.082	0.135	70.490
LPR	0.730	0.720	0.112	4.644
LRR	0.382	0.738	0.374	1.458
Sex				
Female	0.280	0.425	0.090	2.006
Smoking				
No	0.178	3.420	0.572	20.446
LOPD				
Age	0.348	0.964	0.892	1.041
NLR	0.328	1.383	0.723	2.644
LMR	0.480	1.008	0.986	1.030
BER	0.890	1.173	0.122	11.305
LPR	0.352	0.531	0.140	2.014
LRR	0.040*	0.623	0.397	0.980
Sex				
Female	0.193	0.490	0.167	1.434
Smoking				
No	0.231	2.168	0.612	7.680
E-Control				
Age	<0.001*	0.520	0.428	0.632
NLR	0.743	0.845	0.308	2.313
LMR	0.903	1.005	0.921	1.098
BER	0.588	2.411	0.100	58.033
LPR	0.680	0.650	0.084	5.020
LRR	0.455	0.764	0.377	1.549
Sex				
Female	0.765	0.778	0.149	4.057
Smoking				
No	0.203	3.639	0.497	26.648

*$P < 0.05$.

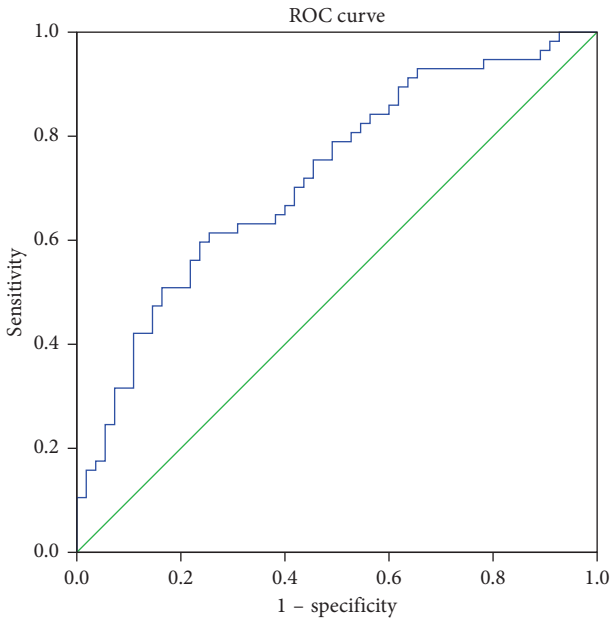

Figure 1: ROC curve for discrimination of LOPD versus L-Control.

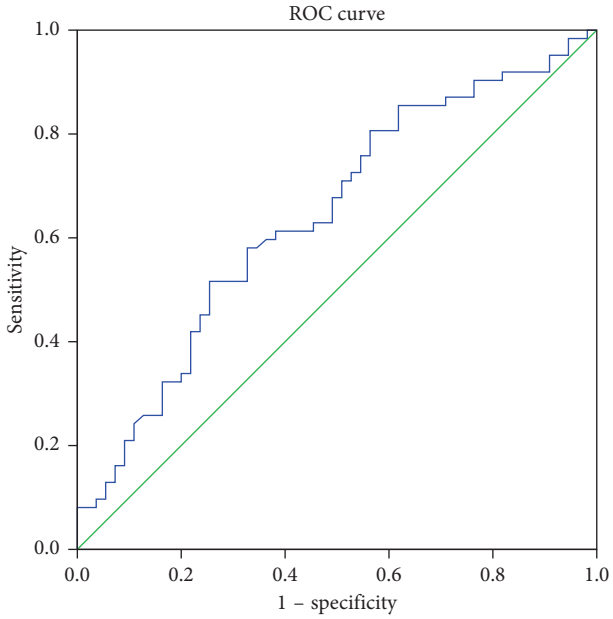

Figure 2: ROC curve for discrimination of LOPD versus EOPD.

Table 4: ROC analysis of LRR.

	P	Area	95% confidence interval	
			Lower bound	Upper bound
L-control vs. LOPD	<0.001*	0.721	0.627	0.814
EOPD vs. LOPD	0.008*	0.641	0.541	0.742

*$P < 0.05$.

In summary, not only do genetic factors differ between EOPD and LOPD, but also immune factors differ between these two kinds of PDs. LRR which showed potential diagnostic value was associated with LOPD, suggesting that there might be differences of inflammatory responses between EOPD and LOPD. The peripheral immune disorders are more serious in LOPD patients. However, the detailed mechanism is still unclear and only speculation could be made. More fundamental researches are needed.

Data Availability

The data that support the findings of this study are available on request from the corresponding author. The data are not publicly available due to privacy restrictions.

Disclosure

The funding source had no involvement in study design; in the collection, analysis and interpretation of data; in the writing of the report; and in the decision to submit the article for publication.

Conflicts of Interest

The authors declare that they have no conflicts of interest.

Authors' Contributions

SJ, YW, HG, and QL contributed equally to this work. SJ, YW, HG, and QL conceived the study. SJ, YW, HG, QL, DW, YL, YY, and XY acquired, analyzed, or interpreted the data. SJ drafted the manuscript. SJ, YW, HG, QL, DW, YL, YY, and XY revised the paper for intellectual content. SJ, YW, HG, and QL performed statistical analysis. XY obtained funding and supervised the study as well. SJ, YW, HG, QL, DW, YL, YY, and XY approved the final version to be submitted.

Acknowledgments

We thank First Affiliated Hospital of Xinjiang Medical University for sharing the data. This work was supported by the National Natural Science Foundation of China (Grant No. U1503222).

References

[1] G. G. Arevalo, R. Jorge, S. Garcia, O. Scipioni, and O. Gershanik, "Clinical and pharmacological differences in early-versus late-onset Parkinson's disease," *Movement Disorders*, vol. 12, no. 3, pp. 277–284, 1997.

[2] C. M. Tanner, R. Ottman, S. M. Goldman et al., "Parkinson disease in twins: an etiologic study," *JAMA*, vol. 281, no. 4, pp. 341–346, 1999.

[3] H. Payami, S. Zareparsi, D. James, and J. Nutt, "Familial aggregation of Parkinson disease: a comparative study of early-onset and late-onset disease," *Archives of Neurology*, vol. 59, no. 5, p. 848, 2002.

[4] C. F. Orr, D. B. Rowe, Y. Mizuno, H. Mori, and G. M. Halliday, "A possible role for humoral immunity in the pathogenesis of Parkinson's disease," *Brain A Journal of Neurology*, vol. 128, no. 11, p. 2665, 2005.

[5] A. Roy, Y. K. Fung, X. Liu, and K. Pahan, "Up-regulation of microglial CD11b expression by nitric oxide," *Journal of Biological Chemistry*, vol. 281, no. 21, pp. 14971–14980, 2006.

[6] L. Chin, S. E. Artandi, Q. Shen et al., "p53 deficiency rescues the adverse effects of telomere loss and cooperates with telomere dysfunction to accelerate carcinogenesis," *Cell*, vol. 97, no. 4, pp. 527–538, 1999.

[7] S. Jiang, H. Gao, Q. Luo, P. Wang, and X. Yang, "The correlation of lymphocyte subsets, natural killer cell, and Parkinson's disease: a meta-analysis," *Neurological Sciences*, vol. 38, no. 8, pp. 1373–1380, 2017.

[8] E. Akil, A. Bulut, İ. Kaplan, H. H. Özdemir, D. Arslan, and M. U. Aluçlu, "The increase of carcinoembryonic antigen (CEA), high-sensitivity C-reactive protein, and neutrophil/lymphocyte ratio in Parkinson's disease," *Neurological Sciences*, vol. 36, no. 3, pp. 423–428, 2015.

[9] L. B. Xue, Y. H. Liu, B. Zhang et al., "Prognostic role of high neutrophil-to-lymphocyte ratio in breast cancer patients receiving neoadjuvant chemotherapy: meta-analysis," *Medicine*, vol. 98, no. 1, Article ID e13842, 2019.

[10] A. J. Hughes, S. E. Daniel, L. Kilford, and A. J. Lees, "Accuracy of clinical diagnosis of idiopathic Parkinson's disease: a clinico-pathological study of 100 cases," *Journal of Neurology, Neurosurgery & Psychiatry*, vol. 55, no. 3, pp. 181–184, 1992.

[11] H. S. Moghaddam, F. G. Sherbaf, M. M. Zadeh, A. Ashraf-Ganjouei, and M. H. Aarabi, "Association between peripheral inflammation and DATSCAN data of the striatal nuclei in different motor subtypes of Parkinson disease," *Frontiers in Neurology*, vol. 9, p. 234, 2018.

[12] C. A. Uçar, B. G. Çokal, H. A. Ü Artık, L. E. İnan, and T. K. Yoldaş, "Comparison of neutrophil–lymphocyte ratio (NLR) in Parkinson's disease subtypes," *Neurological Sciences*, vol. 38, no. 2, pp. 287–293, 2017.

[13] M. Orre, W. Kamphuis, S. Dooves et al., "Reactive glia show increased immunoproteasome activity in Alzheimer's disease," *Brain*, vol. 136, no. 5, pp. 1415–1431, 2013.

[14] E. J. Benner, R. Banerjee, A. D. Reynolds et al., "Nitrated alpha-synuclein immunity accelerates degeneration of nigral dopaminergic neurons," *PLoS One*, vol. 3, no. 1, Article ID e1376, 2008.

[15] D. F. Clayton and J. M. George, "Synucleins in synaptic plasticity and neurodegenerative disorders," *Journal of Neuroscience Research*, vol. 58, pp. 120–129, 1999.

[16] O. Kenjiro and Y. Masahito, "Alpha-Synuclein in blood and cerebrospinal fluid of patients with alpha-synucleinopathy," *Rinsho Byori*, vol. 62, no. 3, pp. 241–245, 2014.

[17] B. Mollenhauer, "Quantification of α-synuclein in cerebrospinal fluid: how ideal is this biomarker for Parkinson's disease?," *Parkinsonism & Related Disorders*, vol. 20, pp. S76–S79, 2014.

[18] R. Barbour, K. Kling, J. P. Anderson et al., "Red blood cells are the major source of alpha-synuclein in blood," *Neurodegenerative Diseases*, vol. 5, no. 2, pp. 55–59, 2008.

[19] E. M. Haacke, N. Y. C. Cheng, M. J. House et al., "Imaging iron stores in the brain using magnetic resonance imaging," *Magnetic Resonance Imaging*, vol. 23, no. 1, pp. 1–25, 2005.

[20] F. Blandini, R. Fancellu, E. Martignoni et al., "Plasma homocysteine and l-dopa metabolism in patients with Parkinson disease," *Clinical Chemistry*, vol. 47, no. 6, pp. 1102–1104, 2001.

[21] G. Madenci, S. Bilen, B. Arli, M. Saka, and F. Ak, "Serum iron, vitamin B12 and folic acid levels in Parkinson's disease," *Neurochemical Research*, vol. 37, no. 7, pp. 1436–1441, 2012.

[22] F. Arosa, C. Pereira, and A. Fonseca, "Red blood cells as modulators of T cell growth and survival," *Current Pharmaceutical Design*, vol. 10, no. 2, pp. 191–201, 2004.